Pacific Northwest
NATIONAL LABORATORY

PNNL-37762, Rev. 0
EWG-RPT-053, Rev. 0

Glass Property-Composition Models Update for use in Direct Feed High-Level Waste Flowsheet Development: EWG2.6

July 2025

John D Vienna
Xiaonan Lu
Pavel Ferkl
Dongsang Kim
José Marcial
Jincheng Bai
Jarrod V Crum
Nicholas A Lumetta

U.S. DEPARTMENT of ENERGY

Prepared for the U.S. Department of Energy
under Contract DE-AC05-76RL01830

DISCLAIMER

PACIFIC NORTHWEST NATIONAL LABORATORY
operated by
BATTELLE
for the
UNITED STATES DEPARTMENT OF ENERGY
under Contract DE-AC05-76RL01830

Printed in the United States of America

Available to DOE and DOE contractors from
the Office of Scientific and Technical Information,
P.O. Box 62, Oak Ridge, TN 37831-0062
www.osti.gov
ph: (865) 576-8401
fox: (865) 576-5728
email: reports@osti.gov

Available to the public from the National Technical Information Service
5301 Shawnee Rd., Alexandria, VA 22312
ph: (800) 553-NTIS (6847)
or (703) 605-6000
email: info@ntis.gov
Online ordering: http://www.ntis.gov

PNNL-37762, Rev. 0
EWG-RPT-053, Rev. 0

Glass Property-Composition Models Update for use in Direct Feed High-Level Waste Flowsheet Development: EWG2.6

July 2025

John D Vienna
Xiaonan Lu
Pavel Ferkl
Dongsang Kim
José Marcial
Jincheng Bai
Jarrod V Crum
Nicholas A Lumetta

Prepared for
the U.S. Department of Energy
under Contract DE-AC05-76RL01830

Pacific Northwest National Laboratory
Richland, Washington 99354

Abstract

A set of preliminary glass property models and constraints were developed and augmented by models from literature for use in design of Direct Feed High-Level Waste glasses for flowsheet evaluation, testing, and design of the High-Level Waste Facility at the Hanford Waste Treatment and Immobilization Plant. These models and constraints are meant to be used as a placeholder while glass property-composition data gaps are filled and final plant operating models are developed. This report describes the motivation and intended use of the models, the compilation of data, model fitting and selection, methods to apply the models and constraints in glass design, and offers example calculations demonstrating their intended use.

Quality Assurance

This work was performed in accordance with the Pacific Northwest National Laboratory (PNNL) Nuclear Quality Assurance Program (NQAP). The NQAP complies with DOE Order 414.1D, *Quality Assurance*, and 10 CFR 830, *Nuclear Safety Management*, Subpart A, *Quality Assurance Requirements*. The NQAP uses NQA-1-2012, *Quality Assurance Requirements for Nuclear Facility Application*, as its consensus standard and NQA-1-2012, Subpart 4.2.1, as the basis for its graded approach to quality.

The NQAP works in conjunction with PNNL's laboratory-level Quality Management Program, which is based on the requirements as defined in DOE Order 414.1D and 10 CFR 830 Subpart A.

The work of this report was performed to a technology readiness level of 6 and is appropriate for nuclear facility design activities within the constraints identified in the report.

Acknowledgments

The authors gratefully acknowledge the financial support provided by the U.S. Department of Energy Hanford Field Office, Waste Treatment and Immobilization Plant Project, with technical oversight by Albert Kruger. The following Pacific Northwest National Laboratory staff members are acknowledged for their contributions: Dewei Wang for technical review of the report; Matthew Willburn for technical editing of the report; David MacPherson, Aaron Sachs, Chrissy Charron, and Cassie Martin for quality assurance and programmatic support during the conduct of this work; Renee Russell, Vivianaluxa Gervasio, and Will Eaton for project management. We thank Daniel Bauer, Steve Barnes, Rich Peters, and Bharthwaj Anantharaman from Bechtel National Inc., and Glenn Smith and Alec Schubick from Hanford Tank Waste Operations & Closure for helpful discussions.

Acronyms and Abbreviations

3TS	three times saturation (method)
Alt-18	(Analysis of Alternatives) alternative #18
APPS	Aspen Process Performance Simulation (WTP steady-state flowsheet model)
AMPS	Advanced Modular Pretreatment System
BOF	balance of facilities
CCC	canister centerline cooling
CCP	Calculation Control Package
CI	confidence interval
DFHLW	Direct Feed High-Level Waste
DOE	U.S. Department of Energy
DWPF	Defense Waste Processing Facility
EC	electrical conductivity
ELG	enhanced LAW glass
EWG	enhanced waste glass
EWG2	second iteration of enhanced waste glass
GFC	glass-forming chemical
HFO	Hanford Field Office
HLW	high-level waste
INEEL	Idaho National Engineering and Environmental Laboratory
INL	Idaho National Laboratory
LAB	WTP Laboratory
LAW	low-activity waste
MdAE	median average error
MV	model validity
NL	normalized loss by 7-day PCT
NQAP	Nuclear Quality Assurance Program
PCT	product consistency test
PNNL	Pacific Northwest National Laboratory
PQM	partial quadratic mixture
PT	pretreatment
PTHLW	pretreated high-level waste
RMSE	root mean squared error
SRNL	Savannah River National Laboratory
SUCI	simultaneous upper confidence interval
TCLP	toxicity characteristic leaching procedure
TSCR	Tank Side Cesium Removal

V	viscosity
VFT	Vogel-Fulcher-Tammann (viscosity-temperature equation)
VSL	Vitreous State Laboratory
WTP	Waste Treatment and Immobilization Plant

Symbols

A	preexponential term in VFT viscosity- or EC-temperature equation
B	temperature effect term in VFT viscosity- or EC-temperature equation
B_i	temperature effect coefficient for i^{th} component viscosity or EC model
c_α	concentration of element α in PCT test solution (α = B, Na, Li)
f_α	concentration of element α in glass (α = B, Na, Li)
g_i	concentration of i^{th} component in glass, mass basis
k_{1208}	K-3 refractory neck corrosion at 1208°C
k_{bubb}	K-3 refractory neck corrosion at 1208°C using bubbled method
k_i	ith component coefficient for K-3 refractory neck corrosion model
k_s	an offset for k_{stat} data compared to k_{bubb} data
k_{stat}	K-3 refractory neck corrosion at 1200°C using static method
n	number of datapoints used to fit a model
N_{ALK}	normalized alkali content in glass = g_{Na2O} + 0.66 g_{K2O} + 2.07 g_{Li2O}
N_{NaLi}	normalized soda and lithia content in glass = g_{Na2O} + 2.07 g_{Li2O}
N_{SiAl}	normalized silica-alumina content in glass = g_{SiO2} + 1.697 g_{Al2O3}
NL_α	normalized loss of component α during 7-day PCT (α = B, Na, Li)
p	distance from nepheline formation boundary line
p	number terms in a model
p_i	i^{th} component model coefficient
p_{ii}	i^{th} component quadratic term model coefficient
p_{ij}	i^{th} and j^{th} components cross-product term model coefficient
R^2	coefficient of determination
q	number of normalized PCT responses for a given glass
S	glass surface area in PCT
$S_{0/1}$	a static method counter (= 1 for k_{stat}, = 0 for k_{bubb})
T	temperature
T_0	infinite viscosity or EC temperature value in VFT equation
$T_{1\%}$	temperature at 1 vol% spinel
$T_{2\%}$	temperature at 2 vol% spinel
T_M	melting temperature
T_L	liquidus temperature (temperature at 0 vol% crystal)
T_L-Zr	liquidus temperature for zirconium-containing phases
U_{pred}	prediction uncertainty
V	PCT solution volume
w_i	ith component w_{SO3} model coefficient
wt%	weight percent

w_{SO3}	sulfur solubility
$w_{SO3\text{-}MT}$	sulfur solubility by melter tolerance method
$w_{SO3\text{-}bub}$	sulfur solubility by bubbling method
$w_{SO3\text{-}sat}$	sulfur solubility by (one time) saturation method
$w_{SO3\text{-}3TS}$	sulfur solubility by three times saturation method
x_i	normalized concentration of *i*th component in glass, mole basis
ε	electrical conductivity
ε_{1100}	electrical conductivity at 1100°C
ε_{1150}	electrical conductivity at 1150°C
ε_{1200}	electrical conductivity at 1200°C
η_{1100}	viscosity at 1100°C
η_{1150}	viscosity at 1150°C
η_T	viscosity at temperature, T
ρ	density at room temperature

Contents

Abstract ii
Quality Assurance iii
Acknowledgments iv
Acronyms and Abbreviations v
Symbols vii
1.0 Introduction 1.1
2.0 Property Models 2.1
2.1 Viscosity and Electrical Conductivity 2.1
2.1.1 Database 2.2
2.1.2 Model 2.3
2.2 Melter SO_3 Tolerance 2.9
2.2.1 Database 2.9
2.2.2 Model 2.10
2.3 K-3 Refractory Corrosion Neck Loss 2.13
2.3.1 Database 2.13
2.3.2 Model 2.14
2.4 P_2O_5-Bearing Phases Liquidus Temperature 2.17
2.4.1 Database 2.17
2.4.2 Model 2.18
2.5 ZrO_2-Bearing Phases Liquidus Temperature 2.21
2.5.1 Database 2.21
2.5.2 Model 2.22
2.6 Spinel $T_{1\%}$ 2.25
2.6.1 Database 2.25
2.6.2 Model 2.26
3.0 Formulation Methods and Constraints 3.1
3.1 Property Constraints 3.1
3.2 Model Validity Constraints 3.2
3.3 Optimization Criteria 3.4
3.4 Example Calculations 3.4
3.5 Model Recommendations 3.9
4.0 Conclusions 4.1
5.0 References 5.1
Appendix A – Variance-Covariance Matrices A.1
Appendix B – Waste Compositions B.1
Appendix C – Glass-Forming Chemical Compositions C.1

Figures

Figure 2.1. Measured vs. predicted ln(η_{1150}) of APPS2 glasses from Russell et al. (2025). 2.1
Figure 2.2. Measured vs. predicted ln(ε_{1150}) of APPS2 glasses from Russell et al. (2025). 2.2
Figure 2.3. Measured (a) logarithm viscosity and (b) logarithm electrical conductivity vs. inverse temperature. 2.3
Figure 2.4. Measured vs. estimated (a) viscosity and (b) electrical conductivity. The notches display the 95% prediction intervals 2.5
Figure 2.5. Component effect on log(η_{1150}, Pa·s) (For Information Only). 2.7
Figure 2.6. Component effect on log(ε_{1150}, S/m) (For Information Only) 2.8
Figure 2.7. Predicted vs. measured w_{SO3} of APPS2 glasses using 3TS method from Russell et al. (2025). 2.9
Figure 2.8. Predicted vs. measured $w_{SO3\text{-}3TS}$ in wt%. Blue circles represent the APPS and APPS2 glasses, red crosses represent outliers that have been removed from the fit, and gray/red circles represent the other data. Red line is the 1:1 line to guide the eye. 2.12
Figure 2.9. Component effects on $w_{SO3\text{-}3TS}$ (For Information Only). 2.12
Figure 2.10. Measured vs. predicted K-3 neck corrosion by static test at 1200°C from Russell et al. 2025. ..... 2.13
Figure 2.11. Predicted vs. measured ln[*k*, inch]. Blue circles represent the APPS and APPS2 glass data, red crosses represent outliers, and gray circles represent the remainder of the data. 2.16
Figure 2.12. Component effects on ln[*k*, inch] (For Information Only). 2.16
Figure 2.13. Predicted vs. measured T_L-P. Blue circles represent the PNNL glass data, black circles represent VSL glass data, and green/red circles represent INEEL glass data. 2.19
Figure 2.14. Component effects on T_L-P model (For Information Only). 2.20
Figure 2.15. Predicted vs. measured T_L-Zr °C. Black circles represent the remainder of the data, and the red ones are outliers. 2.23
Figure 2.16. Component effects on T_L-Zr model (For Information Only). 2.24
Figure 2.17. Predicted vs. measured $T_{1\%}$-Sp, °C. Red circles represent outliers and black circles represent the remainder of the data 2.27
Figure 2.18. Component effects on $T_{1\%}$-Sp model (For Information Only). 2.28

Tables

Table 1.1. Summary of reports for DFHLW glass formulation algorithm, process rate evaluation and experimental validation. 1.2
Table 1.2. Summary of the timeline, objectives, data used, and additions for DFHLW glass formulation algorithms. 1.2
Table 1.3. Summary of EWG2.5 model performance and recommendation of future property model developments (EWG2.6 and EWG3). 1.4
Table 2.1. Range of viscosity and electrical conductivity data used in model development, normalized mass fraction. 2.3
Table 2.2. Metrics of viscosity (V) and electrical conductivity (EC) models. 2.6
Table 2.3. Viscosity and electrical conductivity model parameters. 2.7
Table 2.4. Summary of $w_{SO3\text{-}3TS}$ model data. 2.9
Table 2.5. Range of $w_{SO3\text{-}3TS}$ and composition data used in model development, normalized mass fraction. 2.10
Table 2.6. 3TS SO_3 solubility model coefficients and summary statistics, composition in normalized mass fractions (before applying retention factors) and w_{SO3} in wt%. 2.11
Table 2.7. K-3 corrosion data summary. 2.14
Table 2.8. Component concentration ranges in ln[k] dataset, mass fractions. 2.14
Table 2.9. Coefficients and summary statistics for ln[k, inch] model with composition in normalized mass fractions. 2.15
Table 2.10. Phosphate T_L data summary. 2.17
Table 2.11. Component range in glass (mass fraction) and T_L-P (°C) range for data used in model development. 2.18
Table 2.12. Model coefficient for the T_L-P model. 2.19
Table 2.13. T_L-Zr data summary. 2.21
Table 2.14. Range of glass data used in the T_L-Zr model development, mass fraction. 2.21
Table 2.15. Model coefficient for the T_L-Zr model. 2.23
Table 2.16. $T_{1\%}$-Sp data summary. 2.25
Table 2.17. Range of glass data used in the $T_{1\%}$-Sp model development, mass fraction. 2.25
Table 2.18. Model coefficient for the $T_{1\%}$-Sp model. 2.28
Table 3.1. List of property constraints for DFHLW glass composition estimation 3.1
Table 3.2. Model validity constraints in mass fractions. 3.3
Table 3.3. Composition (mass fraction of oxides and halogen) of the five wastes used in example calculations. Compositions in mg/L element can be found in Appendix B. 3.4
Table 3.4. Formulation of example glasses (mass fraction of component oxide in glass). 3.6
Table 3.5. Target glass composition (after applying retention factors) in mass fraction of oxides and halogen. 3.6

Table 3.6. Predicted glass properties, limiting values are bold 3.8
Table 3.7. Models and constraints recommendations for treating DFHLW, pretreated HLW, LAW (TSCR), and LAW (AMPS). 3.10
Table 3.8. Modal validity ranges for HLW and LAW glass formulation algorithms. 3.11
Table 3.9. GFCs used (labeled as Y) in DFHLW, pretreated HLW, LAW (TSCR) and LAW (AMPS) glass formulation algorithms. 3.12

1.0 Introduction

The U.S. Department of Energy (DOE) Hanford Field Office (HFO) is responsible for the safe storage, treatment, and immobilization of nuclear wastes stored in underground tanks at the Hanford Site. The Waste Treatment and Immobilization Plant (WTP) is the cornerstone of the tank waste cleanup strategy at Hanford. This plant includes, as primary components, the Low-Activity Waste (LAW) Facility, the High-Level Waste (HLW) Facility, the Pretreatment (PT) Facility, the Laboratory (LAB), and the balance of facilities (BOF). The current strategy is to stage the startup of the LAW, HLW, and PT facilities (DOE 2013; Bernards et al. 2020). The startup of the LAW Facility along with the needed components of the LAB and the BOF is underway. To facilitate the startup of the LAW Facility prior to the PT Facility, a Tank Side Cesium Removal (TSCR) system was constructed to remove solids and cesium-137 (^{137}Cs) from the tank waste supernate, thereby removing much of the radioactivity of the supernatant liquid to feed to the LAW Facility (Westesen et al. 2022). The TSCR began operations on January 26, 2022, and completed the first campaign of LAW on December 20, 2023.[1]

An analysis of alternatives for startup and operations of the PT and HLW facilities was conducted to identify the most likely alternatives along with the upper-level implications (Parsons 2023). Seventeen alternatives were considered, including concurrent startup of the HLW and PT facilities and HLW Facility operations without the PT Facility. Based on the results of these options, HFO requested an 18th alternative (Alt-18), in which the annual budget for Hanford was constrained (Bernards et al. 2021). This scenario includes a Waste Transfer Vault that couples the HLW Facility with tank farms using a waste feed transfer vessel and an effluent collection vessel.

HFO empowered a team of experts from the WTP contractor (Bechtel National Inc.), Tank Farm Contractor (currently Hanford Tank Waste Operations & Closure), Pacific Northwest National Laboratory (PNNL), and HFO to develop a more detailed Direct Feed High-Level Waste (DFHLW) flowsheet based on the Alt-18 concept. Through this effort, the team identified the need to formulate glass using the enhanced waste glass (EWG) method, which results in reasonable waste processing rates (Vienna et al. 2023).

To support the DFHLW flowsheet evaluations and ultimately HLW Facility operations, an iterative process for EWG glass development was adopted, including the following steps:

1. Conduct DFHLW glass formulation with existing property modeling and constraints using the latest feed vectors
2. Evaluate the processing rate
3. Select representative glasses (e.g., cluster analysis) to conduct experimental validation
4. Compare measured vs. predicted data
5. Design matrices to systematically cover composition gaps and test glasses
6. Develop property models with additional data and update formulation constraints

[1] The first TSCR campaign processed five batches of waste from Hanford tank AP-107 and was completed in December 2023. However, the receiving tank (AP-106) contained sufficient residual ^{137}Cs to warrant a second round of ion exchange, which commenced in March 2024, and four of five batches were completed in November 2024. The fifth batch will be initiated at an appropriate time for the mission while considering WTP waste consumption rate and TSCR idle time requirements.

Table 1.1 summarizes the iterations performed to date. Table 1.2 lists the timeline, objectives, data used, and additions for DFHLW glass formulation algorithms.

Table 1.1. Summary of reports for DFHLW glass formulation algorithm, process rate evaluation and experimental validation.

Algorithm	Property Models/Formulation	Process Rate Evaluation	Experimental Validation
WTP Baseline	Vienna and Kim 2014 (24590-HLW- RPT-RT-05-001, Rev. 1)	Chapman 2007 (24590-HLW-RPT-PE-07-001)	Kot et al. 2006 (VSL-06R1240-1)
		Vienna et al. 2022a (PNNL-32866, Rev. 1)	Matlack et al. 2008a (VSL-08R1220-1)
EWG1	Vienna et al. 2016 (PNNL-25835, Rev. 0)	Vienna et al. 2022a (PNNL-32866, Rev. 1)	--
EWG2	Lu and Vienna 2023, DFHLW Example Glass Selection Memo (CCN-335241, PNNL-SA-187966)	Lu et al. 2024a, DFHLW Process Control Chemical Limits Memo (PNNL-SA-199714)	Gervasio et al. 2023 (PNNL-35503, Rev. 0)
EWG2.5	Vienna et al. 2024 (PNNL-35884, Rev. 0)	Lu et al. 2024b (PNNL-36196, Rev. 0)	Russell et al. 2025 (PNNL-37506, Rev. 0)
EWG2.6	This report	Future	Not planned
EWG3.0	Future	Future	Future

Table 1.2. Summary of the timeline, objectives, data used, and additions for DFHLW glass formulation algorithms.

Version:	EWG1	EWG2	EWG2.5	EWG3	EWG4	EWG5	GlassApp
Timeline:	2016	2022	2024	2025	2028	2030	2032
Objectives	Mission projections with pretreated HLW (PTHLW)	Mission projections with DFHLW	Initial estimate of DFHLW for flowsheet evaluation	Refined estimate of DFHLW for flowsheet evaluation	Waste qualification report and initial integrated plant version	CX, HX, initial operations [(b)]	Plant operations interface
DFHLW glasses	0	0	15	215	400-500	450-550	No change
Data additions	PTHLW	(a)	+LAW, +Clusters-1	+Clusters-2, +VSLglasses, +EMHQ-Al, +EMHQ-S,+HFO-P	+Clusters-3, +Na10, +S10, +Al10 +EMHQ-Na, +K3M1, +M2 +Melter data, +Gap M	+V&V-crucible, +V&V-melter	None
Plant data	None	None	None	Baseline design	Updated design	+Equip testing	+Plant interfaces

(a) No new models or data were generated under EWG2. LAW and PTHLW models were combined to calculate properties.
(b) CH and HX stand for cold and hot commissioning, respectively.

Table 1.3 summarizes the status and recommendations for the update of EWG models series by property. It is recommended that new property models be developed for EWG3, as a significantly increased amount of data are expected to be collected in pertinent compositional spaces where little or no data were previously available. To enable near-future calculations and formulations for designing DFHLW glasses and estimating processing rates, a formulation algorithm, EWG2.6 (minor modifications on existing property models), is reported here for use while waiting for EWG3 to become available.

Table 1.3. Summary of EWG2.5 model performance and recommendation of future property model developments (EWG2.6 and EWG3).

Property	EWG2.5 (Vienna et al. 2024)	EWG2.6 (this report)	EWG3 objectives
CCC crystallinity	The p threshold was modified to 0.028 from the Lu et al. 2021 model to make the model more conservative. One (APPS2-10) out of the 16 APPS2 glasses formed 8 wt% nepheline after canister centerline cooling (CCC), resulting in this sample failing the product consistency test (PCT) constraints.	Modify the p threshold to avoid glasses such as APPS2-10	New model approach for broader applicability and smaller uncertainty
Isothermal crystallinity	Zirconia-containing phases T_L model and spinel $T_{2\%}$ models from Vienna et al. 2016 successfully limited unacceptably high concentrations of these crystals at 950°C, except APPS2-09, which formed 2.1 vol% total crystals (0.7 vol% spinel and 1.4 vol% $NdPO_4$).	New model for spinel 1 vol% ($T_{1\%}$) ≤ 950°C and new T_L-Zr model incorporating all data since 2009	New model for spinel concentration as functions of composition and temperature to enable sensitivity on spinel constraint New zirconia-containing phase model
Phosphate	APPS2-08 and APPS2-09 formed phosphate crystals (< 2 wt%) after CCC.	New model for phosphate phase T_L	New model that expands to more crystalline phases
Sulfur solubility	Model slightly overpredicted the three times saturation (3TS) SO_3 solubility.	New model	New model to take advantage of broader database
Density	Densities of APPS2 glasses are well predicted by the Vienna et al. 2002 model and slightly overpredicted by Vienna et al. 2009 model.	No change	To be determined after analyses of experimental data.
Viscosity	Viscosities of APPS2 glasses are within constraints, except APPS2-08 (underpredicted), which contained crystals.	New model with combined LAW and HLW glass data	New model to include additional data
Electrical conductivity (EC)	ECs of APPS2 glasses are adequately predicted.	New model with combined LAW and HLW glass data	New model to include additional data
Product consistency test	PCT responses of the quenched glasses are not adequately predicted by the EWG2.5 model, while predictions are better using the Vienna and Crum 2018 model. All the APPS2 quenched glasses passed the constraints. Only APPS2-10 glass failed the limit after CCC due to nepheline formation.	Vienna and Crum 2018 model with prediction uncertainty	New model focused on Hanford glass data only to reduce uncertainties
Toxicity	Toxicity characteristic leaching procedure (TCLP) results for APPS2 glasses are not adequately predicted. Since all the 16 APPS2 glasses passed the constraints, the current model can be used for near-future DFHLW glass formulations.	Kim and Vienna 2004	New model to include additional data
K-3	K-3 neck corrosion by static testing was not well predicted by existing models, and improved models will be needed. Four of the 16 glasses failed the nominal 0.04-inch K-3 neck corrosion limit used during the formulation.	New model with additional data	New model to expand composition range and reduce uncertainty
Composition and process uncertainty	Not applied	Not applied	Will be applied

APPS = Aspen Process Performance Simulation

2.0 Property Models

Each of the EWG2.6 model updates are discussed in this report. Viscosity and EC models are summarized in Section 2.1, the w_{SO3} model is summarized in Section 2.2, the k_{1208} model is summarized in Section 2.3, the P-containing phase liquidus temperature (T_L) model (T_L-P) is summarized in Section 2.4, the Zr-containing phase T_L model (T_L-Zr) is summarized in Section 2.5, and the $T_{1\%}$ spinel model is summarized in Section 2.6. Glass formulation constraints, overall model validity (MV) constraint, optimization criteria, and example calculations are presented in Section 3.0.

2.1 Viscosity and Electrical Conductivity

Figure 2.1 shows the measured viscosity of APPS2 glasses at 1150°C compared to viscosity estimated by the EWG2.5 model. The data are scattered around the unity line with the notable exception of APPS2-08, which had significantly higher measured viscosity than predicted, likely because of magnetite crystallization in that melt.

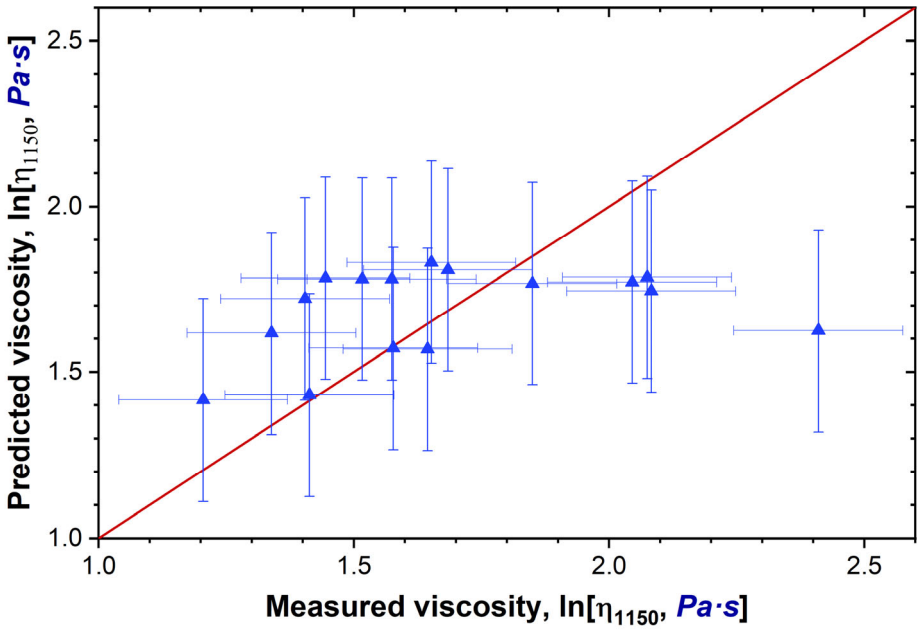

Figure 2.1. Measured vs. predicted ln(η_{1150}) of APPS2 glasses from Russell et al. (2025).

A relatively good agreement was found between the measured and estimated ECs at 1150°C for APPS2 glasses using the EWG2.5 models, as shown in Figure 2.2.

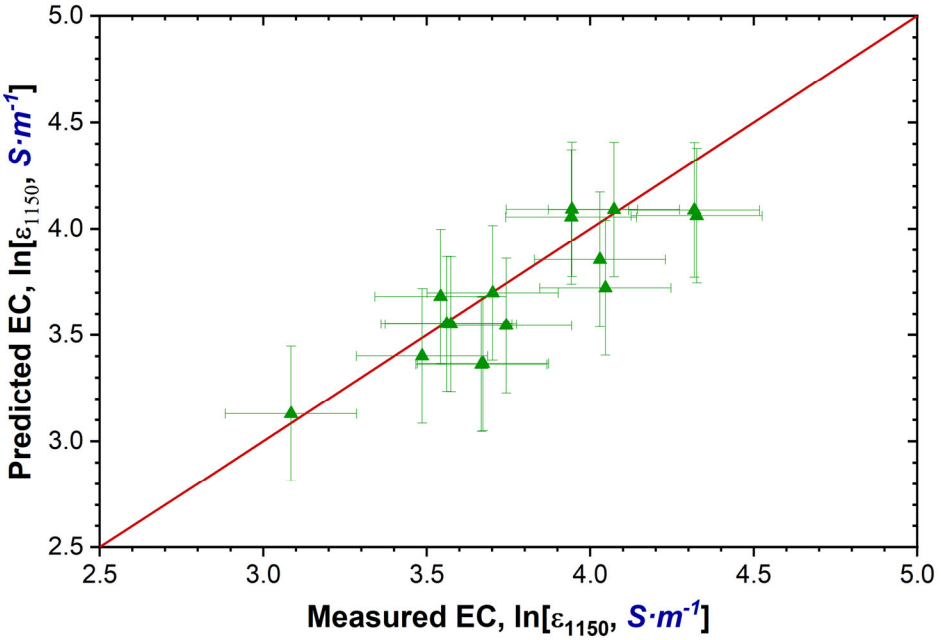

Figure 2.2. Measured vs. predicted ln(ε_{1150}) of APPS2 glasses from Russell et al. (2025).

It was decided to include additional data in the database and reformulate the viscosity and EC models based on the same principles used in EWG2.5 models.

2.1.1 Database

Compared to the EWG2.5 database, which contained 4,487 η points and 4,462 ε points, the EWG2.6 database was considerably larger, containing 9,136 η points and 5,044 ε points. This increase resulted from including recently measured η and ε data for APPS2 glasses, η data for HAL24 glasses, and selected η and ε data from a larger HLW database. For both properties, 80% of glasses were randomly selected for model training and the remaining 20% were left for model testing. Figure 2.3 shows training and testing data vs. inverse temperature. The minimum and maximum mass fractions of model components are given in Table 2.1.

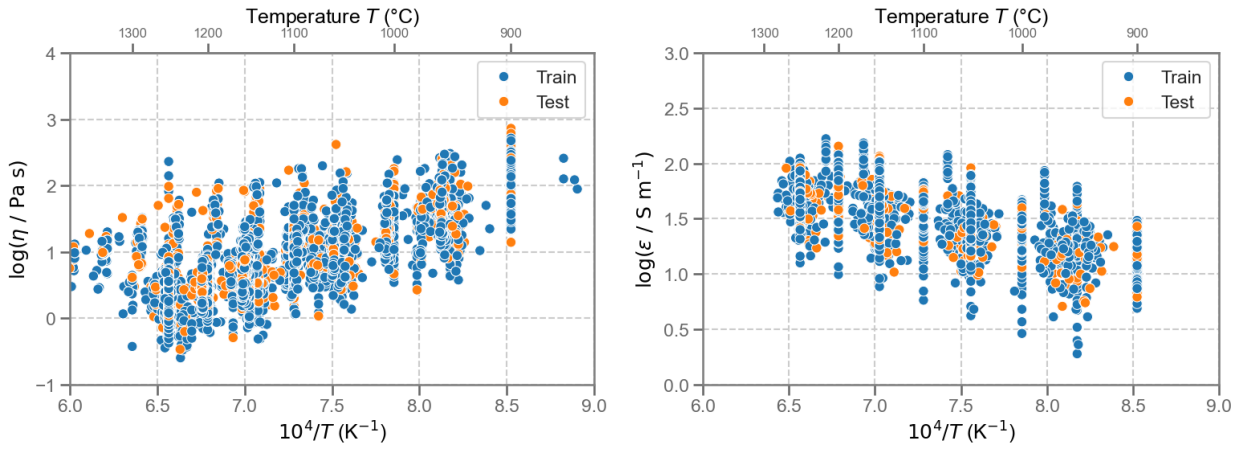

(a) Viscosity

(b) Electrical conductivity

Figure 2.3. Measured (a) logarithm viscosity and (b) logarithm electrical conductivity vs. inverse temperature.

Table 2.1. Range of viscosity and electrical conductivity data used in model development, normalized mass fraction.

	Viscosity		EC	
Component	Min	Max	Min	Max
Al_2O_3	0.0301	0.2711	0.0301	0.2588
B_2O_3	0	0.2392	0	0.2229
CaO	0	0.1276	0	0.1276
Cl	0	0.0117	0	0.0117
Cr_2O_3	0	0.0133	0	0.0143
F	0	0.0453	0	0.0453
Fe_2O_3	0	0.1206	0	0.1206
K_2O	0	0.0752	0	0.0809
Li_2O	0	0.0628	0	0.0633
MgO	0	0.0818	0	0.0502
Na_2O	0.0247	0.2695	0.0337	0.2695
P_2O_5	0	0.0402	0	0.0402
SO_3	0	0.0133	0	0.0133
SiO_2	0.2409	0.5872	0.2701	0.5872
SnO_2	0	0.0501	0	0.0504
TiO_2	0	0.0501	0	0.0501
V_2O_5	0	0.0568	0	0.0568
ZnO	0	0.0964	0	0.0581
ZrO_2	0	0.0932	0	0.0932
Others	0	0.0799	0	0.0799

2.1.2 Model

The temperature- and composition-dependence of viscosity and EC were modeled using the Vogel-Fulcher-Tammann (VFT) equation, which can be written as:

$$\log_{10}(\eta) = A + \frac{B}{T - T_0}$$

where $\log_{10}(\eta)$ is a decadic logarithm of viscosity in Pa·s [replaced by $\log_{10}(\varepsilon)$ for EC in S/m]; T is temperature in K; and A, B, and T_0 are parameters of the VFT equation. Parameters A and T_0 were modeled as constants while a linear model was used for the activation energy parameter as

$$B = \sum_{i=1}^{n} g_i B_i$$

where n is the number of components, g_i is the i^{th} component mass fraction, and B_i is the i^{th} component coefficient. The 20 components listed in Table 2.1 were chosen as model components. Thus, the models have 21 features (one for each component and T) and 22 parameters (one for each component and A and T_0), which were fitted by the least squares method.

Figure 2.4 shows the measured vs. estimated viscosity and EC for several selected DFHLW and LAW groups of glasses as well as the remaining LAW and HLW data. Overall, both models show reasonably good agreement between the measured and estimated values for DFHLW, HLW, and LAW data. Moreover, the similarity of train and test R^2 indicates a good performance of the models on data that were not used for model development. A deeper look into the additional model metrics provided in Table 2.2 reveals that some data categories are estimated with higher errors than others. Relatively higher median average error (MdAE) values were found for the LAWPH3, EMHQ-LBE, and LAWML1 groups for viscosity and the EMHQ-LBE, LP5, and LAWML1 groups for EC. Model parameters are listed in Table 2.3.

Composition effects on a centroid reference glass are shown in Figure 2.5 (η) and Figure 2.6 (ε). The models predict that the viscosity is increased by addition of SiO_2 and Al_2O_3 and decreased by addition of Li_2O, Na_2O, and B_2O_3 or increasing temperature, whereas EC is increased by increasing temperature or by addition of Li_2O and Na_2O and decreased by addition of SiO_2 and Al_2O_3. These effects are consistent with previously measured component effects (e.g., Vienna et al. 2022b; Heredia-Langner et al. 2022).

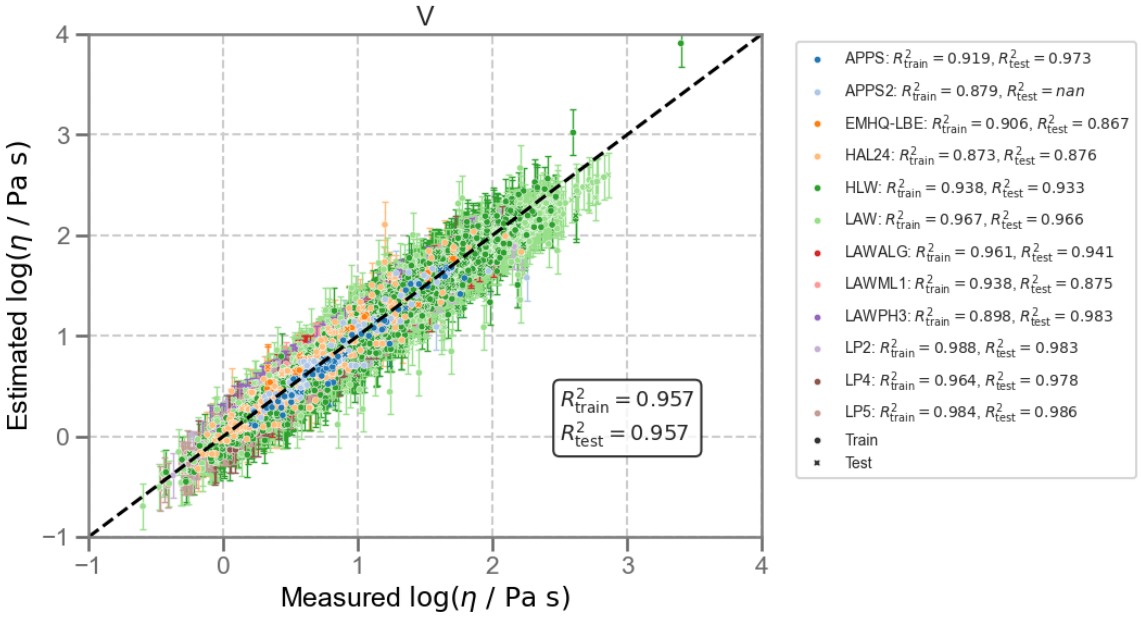

(a) Viscosity

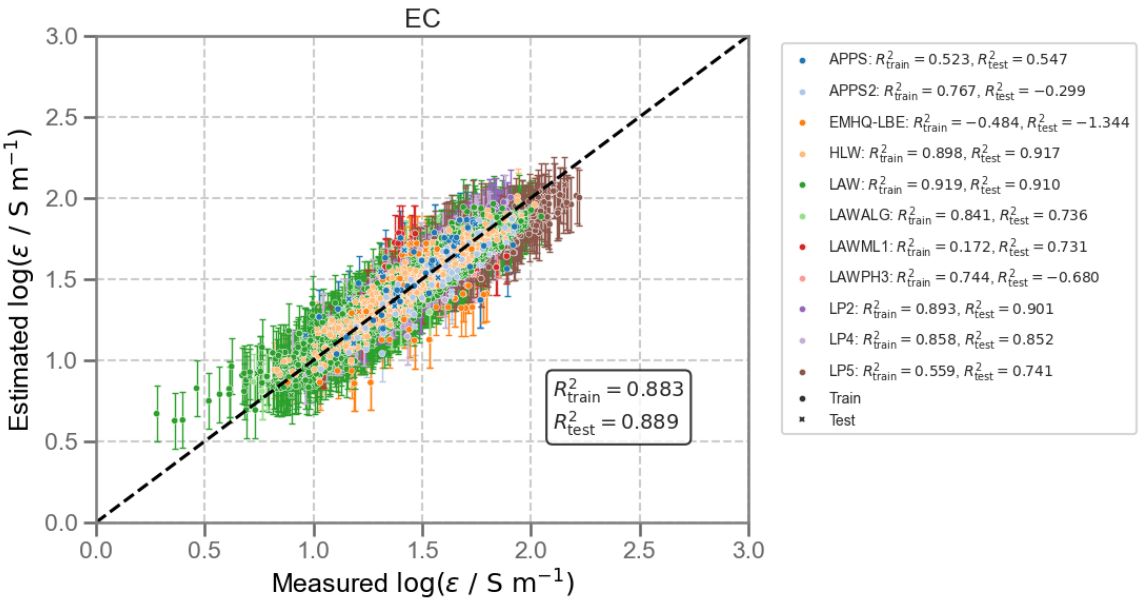

(b) Electrical conductivity

Figure 2.4. Measured vs. estimated (a) viscosity and (b) electrical conductivity. The notches display the 95% prediction intervals.

Table 2.2. Metrics of viscosity (V) and electrical conductivity (EC) models.

Set	Type	R^2, V	R^2, EC	RMSE, V	RMSE, EC	MdAE, V	MdAE, EC
Test	APPS	0.973	0.547	0.064	0.140	0.038	0.073
Test	APPS2	-	-0.299	-	0.159	-	0.157
Test	EMHQ-LBE	0.867	-1.344	0.151	0.158	0.111	0.090
Test	HAL24	0.876	-	0.143	-	0.065	-
Test	HLW	0.933	0.917	0.120	0.068	0.077	0.045
Test	LAW	0.966	0.910	0.110	0.076	0.053	0.047
Test	LAWALG	0.941	0.736	0.111	0.100	0.096	0.110
Test	LAWML1	0.875	0.731	0.160	0.102	0.165	0.074
Test	LAWPH3	0.983	-0.680	0.048	0.126	0.030	0.112
Test	LP2	0.983	0.901	0.066	0.051	0.043	0.028
Test	LP4	0.978	0.852	0.072	0.085	0.048	0.051
Test	LP5	0.986	0.741	0.064	0.116	0.064	0.079
Train	APPS	0.919	0.523	0.112	0.146	0.061	0.095
Train	APPS2	0.879	0.767	0.140	0.095	0.080	0.076
Train	EMHQ-LBE	0.906	-0.484	0.130	0.239	0.099	0.203
Train	HAL24	0.873	-	0.161	-	0.098	-
Train	HLW	0.938	0.898	0.121	0.075	0.073	0.050
Train	LAW	0.967	0.919	0.107	0.072	0.051	0.043
Train	LAWALG	0.961	0.841	0.090	0.092	0.068	0.064
Train	LAWML1	0.938	0.172	0.115	0.198	0.095	0.130
Train	LAWPH3	0.898	0.744	0.138	0.055	0.136	0.046
Train	LP2	0.988	0.893	0.060	0.056	0.041	0.039
Train	LP4	0.964	0.858	0.092	0.081	0.053	0.037
Train	LP5	0.984	0.559	0.060	0.147	0.035	0.132

RMSE = root mean squared error

Table 2.3. Viscosity and electrical conductivity model parameters.

Model	V	EC
A (log(Pa·s or S/m))	-2.9659	2.75163
B Al_2O_3 (K)	8343.46	-1982.57
B B_2O_3 (K)	-602.93	-1126.16
B CaO (K)	-86.56	-1755.05
B Cl (K)	5617.72	-2622.56
B Cr_2O_3 (K)	2400.54	991.29
B F (K)	-3148.99	-2572.47
B Fe_2O_3 (K)	2307.84	-1337.99
B K_2O (K)	690.59	-720.36
B Li_2O (K)	-12518.50	4197.67
B MgO (K)	2200.39	-876.67
B Na_2O (K)	-1585.89	1864.19
B P_2O_5 (K)	5101.18	-2077.61
B SO_3 (K)	4402.92	-2388.89
B SiO_2 (K)	6621.23	-1742.82
B SnO_2 (K)	5332.17	-2344.12
B TiO_2 (K)	2645.25	-902.01
B V_2O_5 (K)	1908.27	-397.10
B ZnO (K)	1676.30	-1323.45
B ZrO_2 (K)	5781.03	-1764.33
B Others (K)	1846.38	-1464.05
T_0 (K)	477.574	608.327

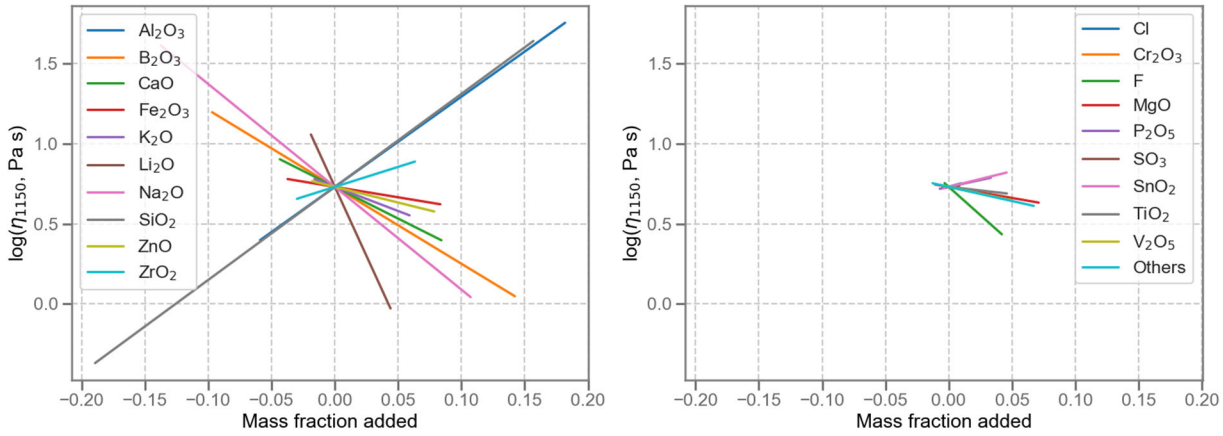

Figure 2.5. Component effect on log(η_{1150}, Pa·s) (For Information Only).

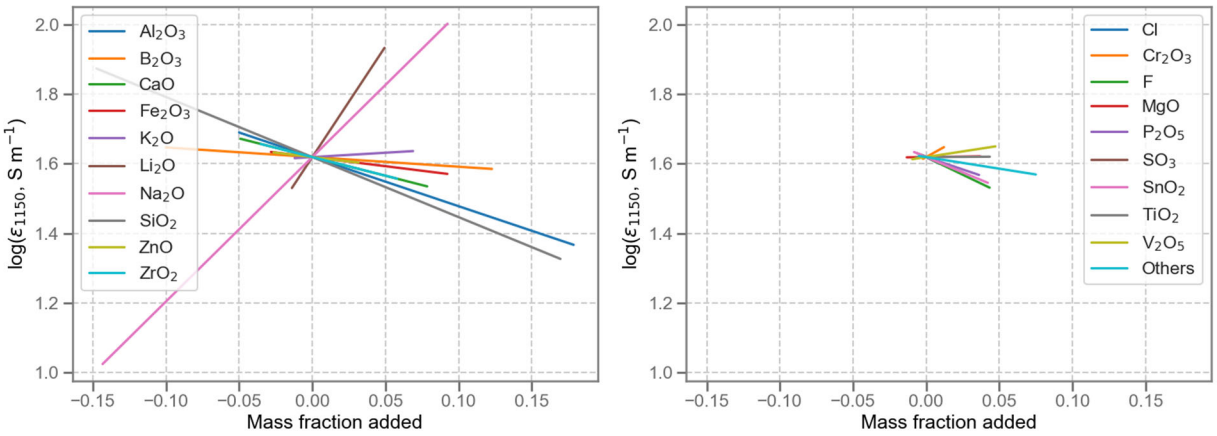

Figure 2.6. Component effect on log(ε_{1150}, S/m) (For Information Only).

2.2 Melter SO_3 Tolerance

The measured $w_{SO3\text{-}3TS}$ values of APPS2 glasses were overpredicted by 0.13 wt% (on average) as shown in Figure 2.7, although all predictions were within the 90% prediction interval. To avoid the overprediction bias, a new model was fitted to the $w_{SO3\text{-}3TS}$ data using the same approach used for the EWG2.5 models (Vienna et al. 2024).

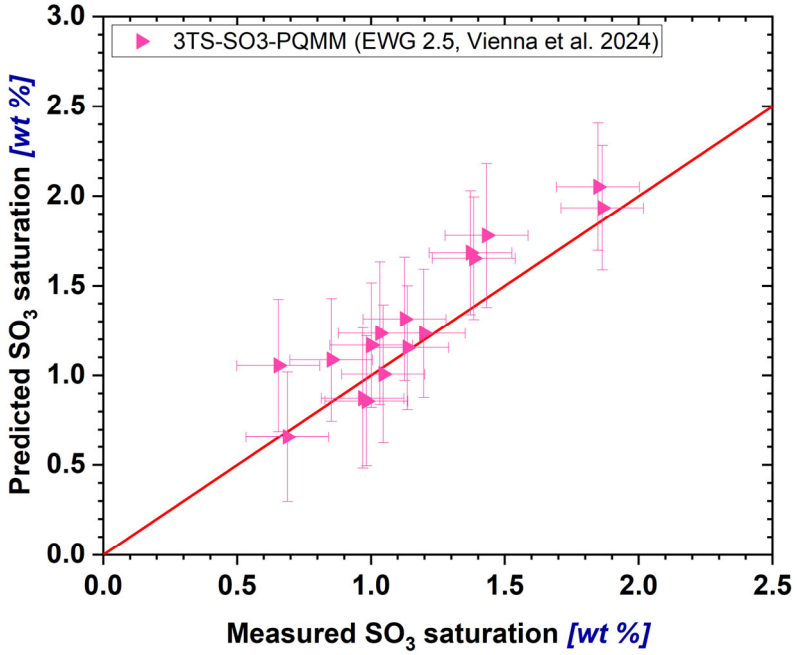

Figure 2.7. Predicted vs. measured w_{SO3} of APPS2 glasses using 3TS method from Russell et al. (2025).

2.2.1 Database

The $w_{SO3\text{-}3TS}$ data were compiled from the data used in the EWG2.5 development with four additional matrices data, as summarized in Table 2.4. The ranges of measured $w_{SO3\text{-}3TS}$ values and component concentrations are listed in Table 2.5. The glass composition used in $w_{SO3\text{-}3TS}$ modeling was renormalized after removing the target g_{SO3}.

Table 2.4. Summary of $w_{SO3\text{-}3TS}$ model data.

Study	# of $w_{SO3\text{-}3TS}$ Points	Reference
EWG2.5	225	Vienna et al. 2024
APPS2	16	Russell et al. 2025
HAL24M1	30	(a)
HAL24M2	20	(a)
LAWML2	17	(b)
Total	308	--

(a) HAL24 matrix 1 and 2 $w_{SO3\text{-}3TS}$ data are found in Calculation Control Package (CCP) 300, "Comparison of predicted and measured SO_3 saturation concentrations for HAL24 glasses."

Study	# of $w_{SO3\text{-}3TS}$ Points	Reference
(b) LAWML2 $w_{SO3\text{-}3TS}$ data are found in CCP-282, "Comparison of predicted and measured SO_3 saturation concentrations for LAWML2 glasses."		

Table 2.5. Range of $w_{SO3\text{-}3TS}$ and composition data used in model development, normalized mass fraction.

Component	Min	Median	Max
Al_2O_3	0.0305	0.0790	0.2726
B_2O_3	0.0402	0.1048	0.2414
CaO	0	0.0607	0.1297
Cl	0.0004	0.0019	0.0241
Cr_2O_3	0.0001	0.0021	0.0144
F	0.0002	0.0027	0.0457
Fe_2O_3	0	0.0058	0.1210
K_2O	0	0.0037	0.0584
Li_2O	0	0.0011	0.0512
MgO	0	0.0030	0.0506
Na_2O	0.0923	0.2049	0.2704
P_2O_5	0.0007	0.0057	0.0403
SiO_2	0.2412	0.3834	0.5936
SnO_2	0	0.0075	0.0508
V_2O_5	0	0.0176	0.0573
ZnO	0	0.0198	0.0575
ZrO_2	0	0.0302	0.0932
Others	0	0.0020	0.0463
$w_{SO3\text{-}3TS}$, wt%	0.602	1.45	3.06

2.2.2 Model

A model was developed to predict the $w_{SO3\text{-}3TS}$ data described in Section 2.2.1. The distribution of each composition term was evaluated in one dimension using histogram plots and two dimensions using scatterplot matrices to determine which terms had sufficient range and variation to be used in modeling.

A first-order composition model of the following form was used:

$$w_{SO_3-3TS} = \sum_{i=1}^{n} w_i x_i$$

where w_i and x_i are the i^{th} component coefficient and normalized mass fraction, respectively, and $x_i = g_i/(1\text{-}g_{SO3})$.

It was found that Al_2O_3, B_2O_3, CaO, Cl, Cr_2O_3, F, Fe_2O_3, K_2O, Li_2O, MgO, Na_2O, P_2O_5, SiO_2, SnO_2, V_2O_5, ZnO, and ZrO_2 were statistically significant. The addition of cross-product or

quadratic terms was then investigated to determine if a few higher order terms would significantly improve the model performance using:

$$w_{SO_3-3TS} = \sum_{i=1}^{n} w_i x_i + Selected\left\{\sum_{i=1}^{n} w_{ii} x_i^2 + \sum_{i=1}^{n}\sum_{j\neq i}^{n-1} w_{ij} x_i x_j\right\}$$

where w_{ii} is the i^{th} component quadratic coefficient and w_{ij} is the i^{th}-j^{th} cross product coefficient. It was found that the addition $CaO \times SiO_2$, $Al_2O_3 \times Na_2O$, and $B_2O_3 \times CaO$ significantly improved the model fit. The partial quadratic mixture (PQM) model has an $R^2 = 0.8529$ and an RMSE = 0.1814 wt%. Three glasses (LP4-17, LP5-01, and LP5-13) were removed as outliers due to high studentized residuals.

Coefficients for the model are given in Table 2.6. The predicted vs. measured plot is shown in Figure 2.8. These coefficients do not account for the -0.33 wt% offset between melter tolerance and 3TS. Therefore, users must adjust predicted $w_{SO3\text{-}3TS}$ values to estimate melter tolerance: $w_{SO_3-MT} = w_{SO_3-3TS} - 0.33$ (Skidmore et al. 2019). The model underpredicts $w_{SO3\text{-}3TS} \geq 2.25$ wt%$w_{SO3\text{-}3TS}$. As this underprediction will result in conservative formulations, no attempt was made to correct the bias.

Table 2.6. 3TS SO_3 solubility model coefficients and summary statistics, composition in normalized mass fractions (before applying retention factors) and w_{SO3} in wt%.

Term	Coefficient		Statistic	Value
Al_2O_3	4.44357		# of points, n	305
B_2O_3	0.99677		# of terms, p	21
CaO	-16.81371		Mean	1.515
Cl	-2.66358		R^2_{fit}	0.8529
Cr_2O_3	-10.54465		R^2_{press}	0.8276
F	-1.63179		R^2_{adjust}	0.8425
Fe_2O_3	-1.85250		$RMSE_{fit}$	0.1814
K_2O	2.77687		$RMSE_{press}$	0.1898
Li_2O	15.18423		Pooled SD $w_{SO3\text{-}3TS}$	0.1548
MgO	-3.69297			
Na_2O	10.43734			
P_2O_5	4.63599			
SiO_2	-1.74459			
SnO_2	-2.51964			
V_2O_5	6.66711			
ZnO	-2.27224			
ZrO_2	-4.29299			
Others	-1.73315			
$Al_2O_3 \times Na_2O$	-45.38413			
$B_2O_3 \times CaO$	59.55168			
$CaO \times SiO_2$	44.06542			

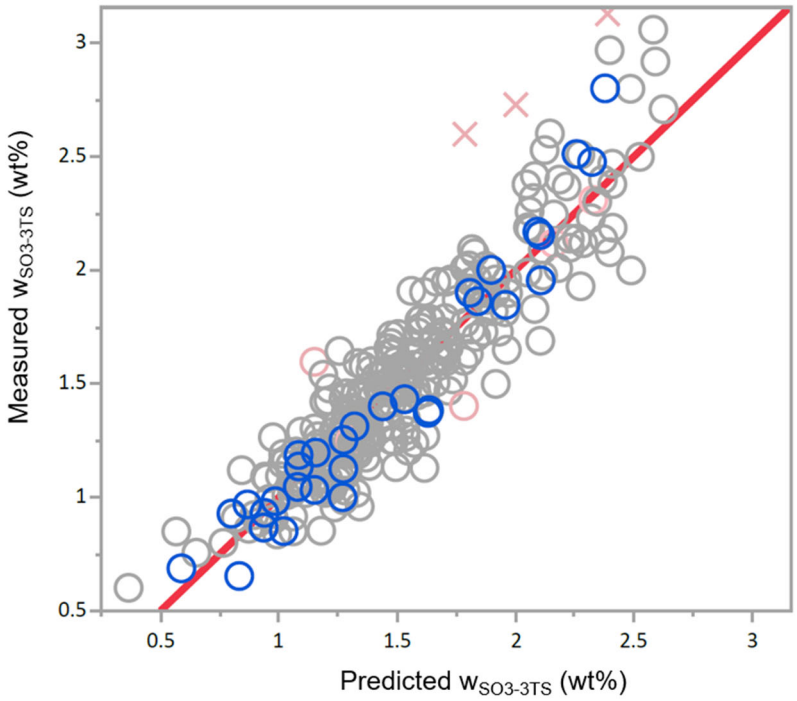

Figure 2.8. Predicted vs. measured $w_{SO3-3TS}$ in wt%. Blue circles represent the APPS and APPS2 glasses, red crosses represent outliers that have been removed from the fit, and gray/red circles represent the other data. Red line is the 1:1 line to guide the eye.

Composition effects on $w_{SO3-3TS}$ are shown in Figure 2.9. As previously reported, Li_2O, CaO, V_2O_5, and Na_2O strongly increase w_{SO3} while Al_2O_3, SiO_2, and ZrO_2 decrease w_{SO3}. One unexpected impact is that of B_2O_3, which was found to increase w_{SO3} while previous studies suggested minimal impact. Further investigation is needed to determine if this is a real effect and, if so, what chemical phenomena cause this impact.

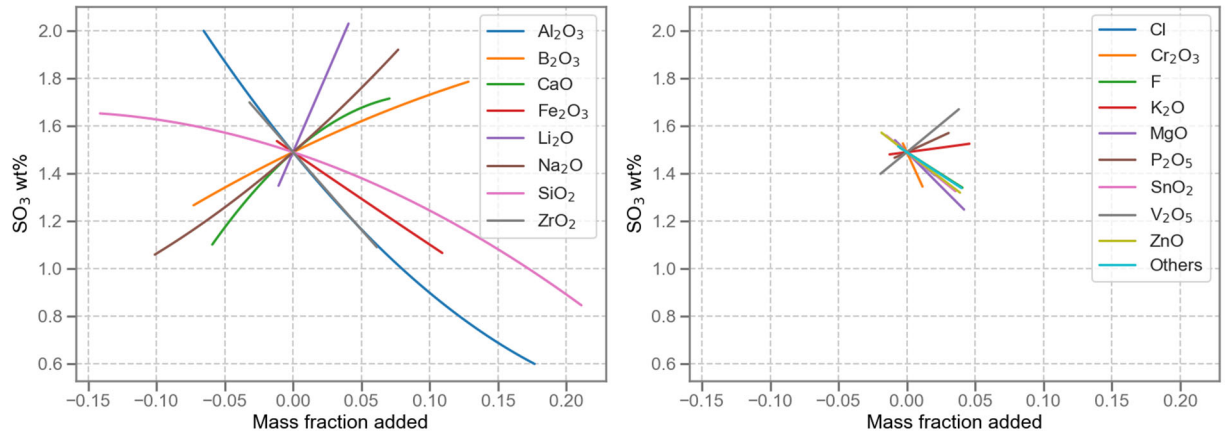

Figure 2.9. Component effects on $w_{SO3-3TS}$ (For Information Only).

2.3 K-3 Refractory Corrosion Neck Loss

The logarithm K-3 neck corrosion of APPS2 glasses was underpredicted by the EWG2.5 model as shown in Figure 2.10, particularly for values ≥ -3.5 ln[in] (≥ 0.03 in). This underprediction is not conservative and results in the failure of glasses that were predicted to pass the K-3 neck corrosion constraint. Therefore, a new model was developed.

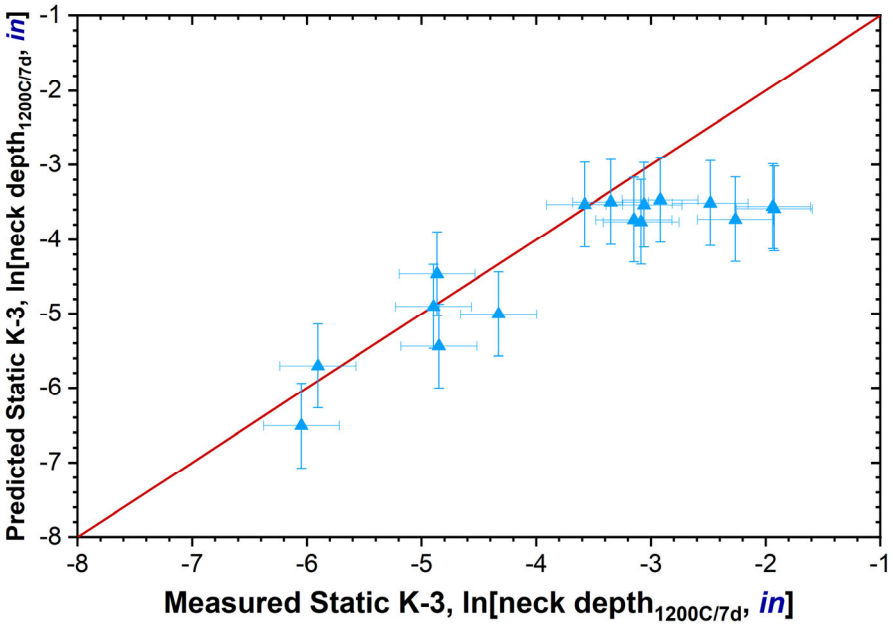

Figure 2.10. Measured vs. predicted K-3 neck corrosion by static test at 1200°C from Russell et al. 2025.

K-3 corrosion data is relatively limited in both number of glasses and composition region covered (Vienna et al. 2022b). Most of the existing data were measured for 6 days at 1208°C under bubbled conditions, with a smaller fraction of data measured using static conditions at 1150°C to 1200°C for 3, 6, and 7 days. In all cases, the refractory-air-melt triple point resulted in the highest corrosion. It is this neck region of corrosion that is used to model the impact of melt composition on K-3 corrosion. Bubbled tests result in broader but shallower corrosion at the neck compared to the static tests. The lack of data coverage by either test method necessitates the combination of data from the two methods to develop the broadest possible composition-K3 corrosion model.

2.3.1 Database

The K-3 corrosion data were drawn from two compilations: (1) Vienna et al. 2024 (EWG2.5 model report) and (2) a yet-to-be-published calculation control package.[1] The model contained data summarized in Table 2.7. The range of glass component concentrations and logarithm of K-3 neck corrosion are listed in Table 2.8.

[1] CCP-333, "EWG2.6 K3 Model."

Table 2.7. K-3 corrosion data summary.

Description	# of Data	Method
VSL LAW	327	6d, 1208°C, bubbled
VSL HLW	9	6d, 1208°C, bubbled
SRNL LAW (replicates of VSL)	4	6d, 1200°C, static
SRNL DFHLW (APPS)	15	6d, 1200°C, static
PNNL DFHLW (APPS2)	16	7d, 1200°C, static
Total	371	Various

SRNL = Savannah River National Laboratory; VSL = Vitreous State Laboratory

Table 2.8. Component concentration ranges in ln[*k*] dataset, mass fractions.

Component	Min	Median	Max
Al_2O_3	0.0300	0.0764	0.2634
B_2O_3	0.0400	0.0988	0.2229
Cl	0	0.0020	0.0120
Cr_2O_3	0	0.0008	0.0144
Fe_2O_3	0	0.0100	0.1360
K_2O	0	0.0050	0.0810
Li_2O	0	0.0000	0.0586
MnO	0	0.0000	0.0203
Na_2O	0.0247	0.2008	0.2601
P_2O_5	0	0.0012	0.0400
SiO_2	0.2477	0.4166	0.5851
V_2O_5	0	0.0000	0.0515
ZnO	0	0.0300	0.0536
ZrO_2	0	0.0351	0.0932
Other	0.0012	0.0773	0.2095
ln[k, in]	-6.0482	-3.4343	-1.6660
N_{ALK}	0.1374	0.2239	0.2725
N_{SiAl}	0.4497	0.5571	0.7206

2.3.2 Model

Due to the combination of data from two methods, the form of models considered is:

$$ln[k] = k_s S_{0/1} + \sum_{i=1}^{q} k_i g_i + Selected\left\{\sum_{i=1}^{q} k_{ii} g_i^2 + \sum_{i=1}^{q} \sum_{j \neq i}^{q-1} k_{ij} g_i g_j\right\},$$

where k_s is an offset for static corrosion (k_{stat}) data, $S_{0/1}$ is a static method counter = 0 for k_{bubb} and = 1 for k_{stat}, k_i is the i^{th} component coefficient, g_i and g_j are the i^{th} and j^{th} component mass fraction in glass, k_{ii} is the i^{th} component quadratic term, and k_{ij} is the i^{th}-j^{th} component cross-product coefficient. Initially, separate static test counters were used for 6-day and 7-day test data. No significant differences between the offsets were obtained, so for simplicity they were combined into a single counter $S_{0/1}$ and offset k_s.

A first-order model was fitted to the data to determine which components had significant effects on ln[*k*]. Al_2O_3, B_2O_3, Cl, Cr_2O_3, Fe_2O_3, K_2O, Li_2O, MnO, Na_2O, P_2O_5, SiO_2, V_2O_5, ZnO, and ZrO_2 were found to have significant effects. A PQM was developed using stepwise regression, where these second-order terms were found to improve the model statistics: Cr_2O_3×Li_2O, Cr_2O_3×V_2O_5, K_2O×Li_2O. This model was found to have the best fit statistics without overfitting with an R^2 = 0.851. The model coefficients are reported in Table 2.9. The predicted values are compared to measured values in Figure 2.11.

Table 2.9. Coefficients and summary statistics for ln[*k*, inch] model with composition in normalized mass fractions.

Term	Coefficient		Statistic	Value
$S_{0/1}$	0.5949		n	386
Al_2O_3	-20.3195		p	19
B_2O_3	-0.5937		Mean ln[*k*]	-3.52984
Cl	-24.3780		R^2_{fit}	0.8510
Cr_2O_3	-76.9256		R^2_{Adj}	0.8437
Fe_2O_3	-0.5015		R^2_{press}	0.8325
K_2O	11.2165		$RMSE_{fit}$	0.3133
Li_2O	59.6438		$RMSE_{press}$	0.3244
MnO	-41.6243		Pooled SD ln[*k*]	0.3311
Na_2O	22.1955			
P_2O_5	-20.2909			
SiO_2	-13.5721			
V_2O_5	-20.5839			
ZnO	-18.6408			
ZrO_2	-13.8232			
Other	5.3774			
Cr_2O_3 × Li_2O	-5232.2150			
Cr_2O_3 × V_2O_5	4882.3769			
K_2O × Li_2O	-611.3370			

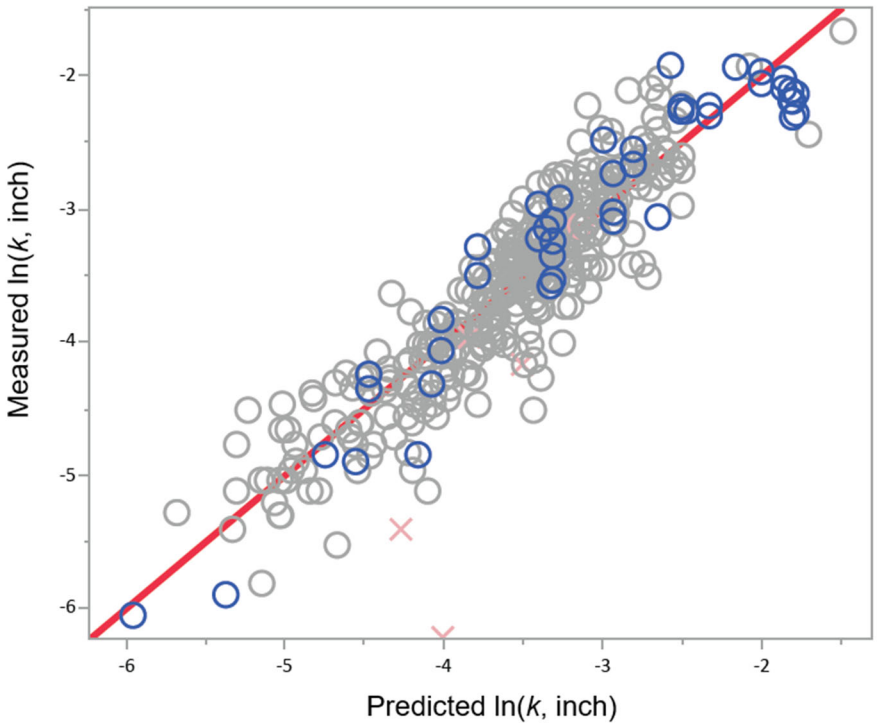

Figure 2.11. Predicted vs. measured ln[*k*, inch]. Blue circles represent the APPS and APPS2 glass data, red crosses represent outliers, and gray circles represent the remainder of the data.

Composition effects on ln[*k*] are shown in Figure 2.12. As previously reported, Li_2O and Na_2O strongly increase ln[*k*] while Cr_2O_3, Al_2O_3, SiO_2, P_2O_5, ZnO, MnO, V_2O_5, and ZrO_2 decrease ln[*k*].

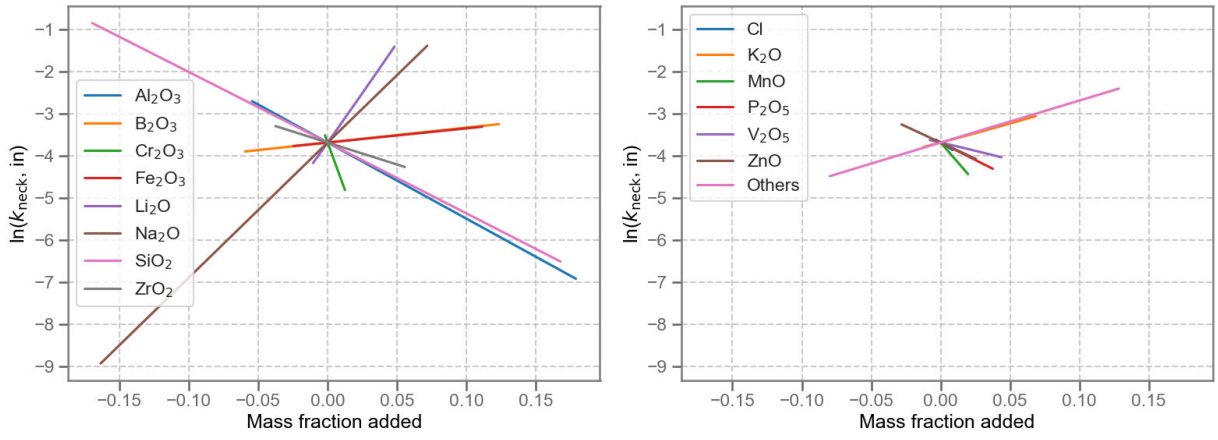

Figure 2.12. Component effects on ln[*k*, inch] (For Information Only).

2.4 P_2O_5-Bearing Phases Liquidus Temperature

Phosphate in the waste can result in formation of a range of P-containing crystalline phases and/or amorphous phase separation that may be detrimental to melter processing or waste form durability. To address melter processing concerns, a T_L model was developed that will enable formulations of glasses that avoid the formation of P-containing crystalline phases during the melting process.

2.4.1 Database

Available liquidus temperature data for P-containing crystalline phases (T_L-P) were compiled into a database, as summarized in Table 2.10. The database includes glasses that formed primarily apatite or oxyapatite [$Ca_5(PO_4)_3(F,Cl)$]. Other phosphate crystals in the database include lithium phosphate, sodium calcium phosphate, zirconium phosphate, and lanthanum phosphate. A total of 136 glasses were compiled. Table 2.11 presents the ranges of measured T_L-P values and the range of each component concentration.

Table 2.10. Phosphate T_L data summary.

Lab/Study	# of Data	Reference
PNNL/P-Sol	9	(a)
PNNL/EWG-OL	3	Russell et al. 2018
PNNL/HLW-APPS	1	Gervasio et al. 2024
PNNL/HAL24M1	2	(b)
INEEL/IG1	12	Staples et al. 1999
INEEL/IG2	10	Staples et al. 2000
INEEL/IG3	1	Scholes et al. 2000
INEEL/SBW1	15	Scholes et al. 2002
VSL/HLW-E-Al; HLW-ANa	4	Matlack et al. 2007
VSL/HLW-BP	7	Kot et al. 2007
VSL/HLW-E-Bi	7	Muller et al. 2012
VSL/HLWS	12	Matlack et al. 2012
VSL/HWBi	13	Gan et al. 2012
VSL/HLWS	5	Matlack et al. 2013
VSL/HLW13	5	Kot et al. 2014
VSL/HLW14	6	Kot et al. 2015
VSL/HLW-CP	8	Gan et al. 2015
Total	136	NA

(a) T_L-P data on P-Sol glass is found in Data Package (DP) 276, "Crystal fraction and liquidus temperature calculation for phosphorus solubility glasses."
(b) T_L-P data on HAL24M1 glass is found in CCP 291, "HAL24M1 CF XRD TL and 950C vol% crystal calculations."
INEEL = Idaho National Engineering and Environmental Laboratory

Table 2.11. Component range in glass (mass fraction) and T_L-P (°C) range for data used in model development.

Oxide	Min	Median	Max
Al_2O_3	0.0101	0.1236	0.2708
B_2O_3	0.0404	0.1204	0.2207
BaO	0.0000	0.0001	0.0470
Bi_2O_3	0.0000	0.0126	0.1040
CaO	0.0004	0.0329	0.1420
Cr_2O_3	0.0000	0.0030	0.0158
Li_2O	0.0000	0.0300	0.0676
Na_2O	0.0159	0.1101	0.2054
P_2O_5	0.0101	0.0301	0.1017
SiO2	0.2144	0.3798	0.5483
SrO	0.0000	0.0004	0.0888
ZrO_2	0.0000	0.0120	0.1052
Others[(a)]	0.0023	0.1022	0.2194
T_L-P (C°)	783	964	1278

(a) Others = Sum of remaining components: Ag_2O, CdO, Ce_2O_3, Cl, Cs_2O, CuO, F, Fe_2O_3, HfO_2, I, K_2O, La_2O_3, MgO, MnO, MoO_3, Nd_2O_3, NiO, PbO, RuO_2, SO_3, SnO_2, Tl_2O_3, ThO_2, TiO_2, UO_3, V_2O_5, WO_3, Y_2O_3, ZnO.

2.4.2 Model

The model terms were first selected based on the evaluation of range and distribution of the major glass components. Then, a linear stepwise regression model with k-fold optimization was used to further screen the significant model terms: $T_L = \sum_{i=1}^{n} c_i g_i$, where c_i is the coefficient of the i^{th} first-order component term, n is the total number of components fitted in the model, and g_i is the target mass fraction of the corresponding component. The following components were found with a high significance: BaO, CaO, Li_2O, Na_2O, and P_2O_5. The major glass components of Al_2O_3, B_2O_3, and SiO_2 were locked in as model terms for further optimization, with addition of Bi_2O_3, Cr_2O_3, SrO, and ZrO_2 to achieve the best-fitting result. This first-order model resulted in an $R^2 = 0.7184$ and an RMSE = 54.9542. A PQM model was developed with all the selected first-order terms along with second-order terms (B_2O_3xCaO, Li_2OxLi_2O, CaOxNa_2O, and BaOxP_2O_5):

$$T_L = \sum_{i=1}^{n} c_i g_i + \sum_{i=1}^{n-1} \sum_{j \geq i}^{n} c_{ij} g_i g_j$$

where c_i is the coefficient of the i^{th} first-order component term, n is the total number of components fitted in the model, g_i is the target mass fraction of the corresponding component, and c_{ij} is the quadratic coefficient for the cross-product term $g_i g_j$. This model provides the best fit statistics without overfitting. One datapoint (HLW14-23) was found to be an outlier with a studentized residual outside the 95% simultaneous Bonferroni limits and was removed from the fit. The PQM model has the fitted $R^2 = 0.8225$, a k-fold validation (k=5) $R^2 = 0.7543$, and the press $R^2 = 0.7503$. Coefficients for the PQM model are given in Table 2.12. The predicted values are compared to measured values in Figure 2.13 and component effects are shown in Figure 2.14. T_L-P is most increased by P_2O_5, BaO, CaO, and Al_2O_3 and decreased by Li_2O,

Na_2O, SrO. Further investigation is needed to determine if the impacts of SrO and BaO are a real effect and, if so, what chemical phenomena cause this behavior.

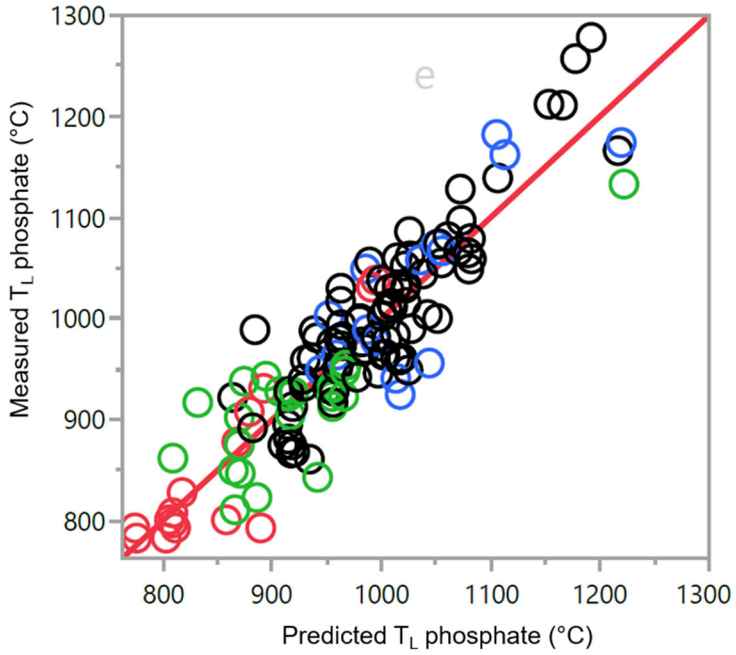

Figure 2.13. Predicted vs. measured T_L-P. Blue circles represent the PNNL glass data, black circles represent VSL glass data, and green/red circles represent INEEL glass data.

Table 2.12. Model coefficient for the T_L-P model.

Term	Coefficient		Statistic	Value
Al_2O_3	1613.5742		n	135
B_2O_3	569.88124		p	17
BaO	-7070.059		Mean T_L-P	973.0593
Bi_2O_3	652.42804		R^2_{fit}	0.8225
CaO	-2689.611		R^2_{Adj}	0.7984
Cr_2O_3	3678.4297		R^2_{press}	0.7503
Li_2O	-4995.045		$RMSE_{fit}$	44.3630
Na_2O	-572.5679		$RMSE_{press}$	49.3741
P_2O_5	2407.8577		Pooled SD	44.3633
SiO_2	1253.6389			
SrO	-755.0302			
ZrO_2	1695.3847			
Others	1327.8156			
B_2O_3 × CaO	16941.229			
BaO × P_2O_5	338443.11			
CaO × Na_2O	30932.407			
Li_2O × Li_2O	49994.82			

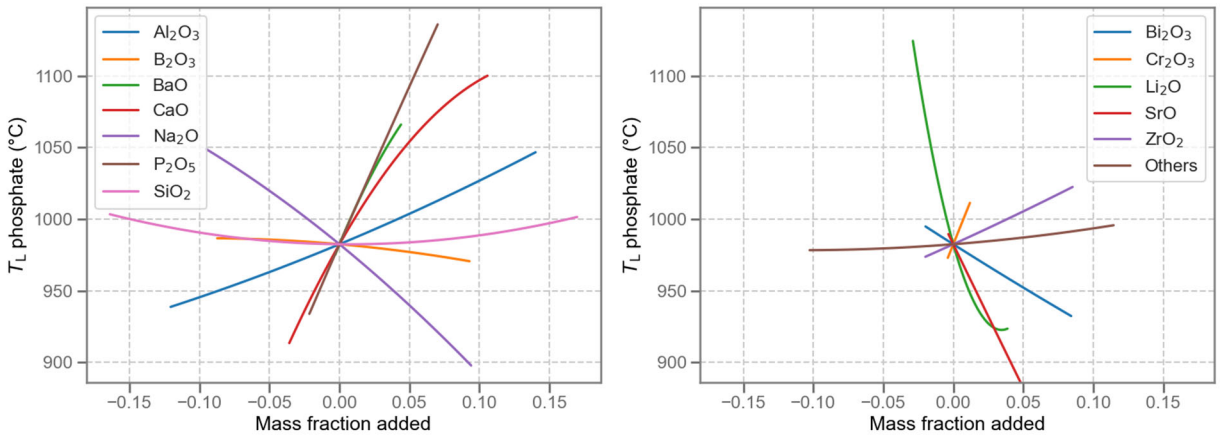

Figure 2.14. Component effects on T_L-P model (For Information Only).

2.5 ZrO_2-Bearing Phases Liquidus Temperature

Zirconium-bearing crystalline phases can settle in the melter, leading to processing upsets. To address melter processing concerns, a T_L-Zr model was developed that will enable formulations of glasses that avoid the formation of Zr-containing crystalline phases during the melting process.

2.5.1 Database

Available T_L data for Zr-containing crystalline phases were compiled into the database, as summarized in Table 2.13. The database includes glasses that formed primarily zircon ($ZrSiO_4$), baddeleyite (ZrO_2), wadeite ($K_2ZrSi_3O_9$), zektzerite ($NaLiZrSi_6O_{15}$), vlasovite ($Na_2ZrSi_4O_{11}$), or parakeldyshite ($Na_2ZrSi_2O_7$) measured by X-ray diffraction or scanning electron microscopy of glasses tested through various methods, including gradient furnace measurements and isothermal heat treatment. Table 2.14 presents the ranges of measured T_L-Zr values and the range of each component concentration.

Table 2.13. T_L-Zr data summary.

Glass ID	Lab	# of Data	Reference
Hanford CVS	PNNL	13	Hrma et al. 1994, Vienna et al. 1996
INEEL CVS phase 1	INL	5	Staples et al. 1999
INEEL CVS phase 2	INL	5	Staples et al. 2000
INEEL CVS phase 3	PNNL	3	Staples et al. 2000
SP	PNNL	2	Mika et al. 1997
TRU	PNNL	41	Crum et al. 1997
PNNL Zr	PNNL	28	Vienna et al. 2000
VSL HLW03	VSL	1	Piepel et al. 2007, 2008
VSL HLW05	VSL	3	Kot et al. 2005
VSL ALG	VSL	1	Kot et al. 2006
VSL HLW06	VSL	1	Kot et al. 2005
SBW1	INL	1	Scholes et al. 2002
VSL HLW07	VSL	4	Kruger et al. 2013
HFGI	PNNL	5	Russell et al. 2023
HAIG	PNNL	4	(a)
HAL24	PNNL	7	(b)
Total		124	

(a) HAIG matrix T_L-Zr data are found in CCP 223.
(b) HAL24 matrix 1 and 2 T_L-Zr data are found in CCPs 264 and 284, respectively.
INL = Idaho National Laboratory

Table 2.14. Range of glass data used in the T_L-Zr model development, mass fraction.

Oxide	Min	Median	Max
Al_2O_3	0.0000	0.0375	0.2857
ZrO_2	0.0269	0.1081	0.1650
Fe_2O_3	0.0000	0.0397	0.1800
SiO_2	0.2287	0.4660	0.5957

Oxide	Min	Median	Max
K_2O	0.0000	0.0028	0.0750
Na_2O	0.0362	0.1119	0.2382
ThO_2	0.0000	0.0000	0.0441
MgO	0.0000	0.0021	0.0800
F	0.0000	0.0031	0.0652
Li_2O	0.0000	0.0492	0.0901
B_2O_3	0.0000	0.0822	0.2240
Cr_2O_3	0.0000	0.0014	0.0127
MnO	0.0000	0.0014	0.0677
UO_3	0.0000	0.0000	0.0650
Others	0.0039	0.0791	0.1886

2.5.2 Model

The model terms were first selected based on the evaluation of range and distribution of the major glass components. Then, a linear stepwise regression model with k-fold optimization was used to further screen the significant model terms: $T_{L-Zr} = \sum_{i=1}^{n} c_i g_i$, where c_i is the coefficient of the i^{th} first-order component term, n is the total number of components fitted in the model, and g_i is the target mass fraction of the corresponding component. Al_2O_3, B_2O_3, Cr_2O_3, F, Fe_2O_3, K_2O, Li_2O, MgO, MnO, Na_2O, SiO_2, ThO_2, UO_3, and ZrO_2 were found to have significant effects. A PQM was developed using stepwise regression, where these second-order terms were found to improve the model statistics: B_2O_3×K_2O and Na_2O×Na_2O:

$$T_{L,-Zr} = \sum_{i=1}^{n} c_i g_i + \sum_{i=1}^{n-1} \sum_{j \geq i}^{n} c_{ij} g_i g_j$$

where c_i is the coefficient of the i^{th} first-order component term, n is the total number of components fitted in the model, g_i is the target mass fraction of the corresponding component, and c_{ij} is the coefficient for the cross-product term $g_i g_j$. This model was found to have the best fit statistics without overfitting with an $R^2 = 0.851$. The model coefficients are reported in Table 2.15. The predicted values are compared to measured values in Figure 2.15. Composition effects on T_L-Zr are shown in Figure 2.16. As previously reported, ZrO_2, Al_2O_3, MgO, ThO_2 strongly increase T_L-Zr while Li_2O and B_2O_3 decrease T_L-Zr. Unexpected impacts include:

- the non-linear impact of Na_2O which presumably increases T_L of alkali-containing phases such as zektzerite, vlasovite, parakeldyshite, and potentially wadeite;
- the positive effects of Fe_2O_3 and Cr_2O_3 on T_L;
- the negative effects of MnO and UO_3 on T_L;

Further investigation is needed to determine if this is a real effect and, if so, what chemical phenomena cause this impact.

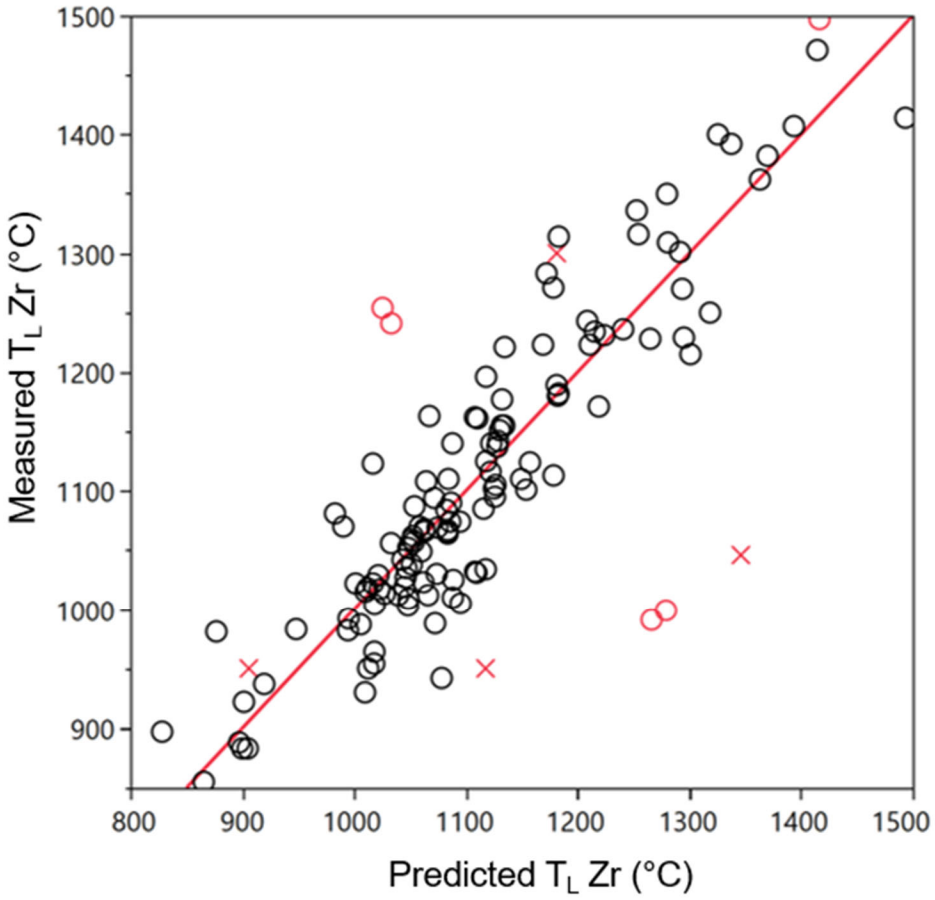

Figure 2.15. Predicted vs. measured T_L-Zr °C. Black circles represent the remainder of the data, and the red ones are outliers.

Table 2.15. Model coefficient for the T_L-Zr model.

Term	Coefficient		Statistic	Value
Al_2O_3	3397.7986		n	124
B_2O_3	529.04867		p	17
Cr_2O_3	4197.4839		Mean T_L-Zr, °C	1107.79
F	-4115.637		R^2_{fit}	0.8511
Fe_2O_3	2785.8568		R^2_{Adj}	0.8288
K_2O	11999.349		R^2_{press}	0.7848
Li_2O	-1624.633		$RMSE_{fit}$	52.3799
MgO	3300.3993		$RMSE_{press}$	58.7227

MnO	-828.6816		Pooled SD T_L-Zr, °C	11.9
Na_2O	-5334.063			
SiO_2	1050.8203			
ThO_2	8022.9858			
UO_3	-742.5985			
ZrO_2	5205.7163			
Others	1779.0088			
B_2O_3 × K_2O	-105157.6			
Na_2O × Na_2O	21008.977			

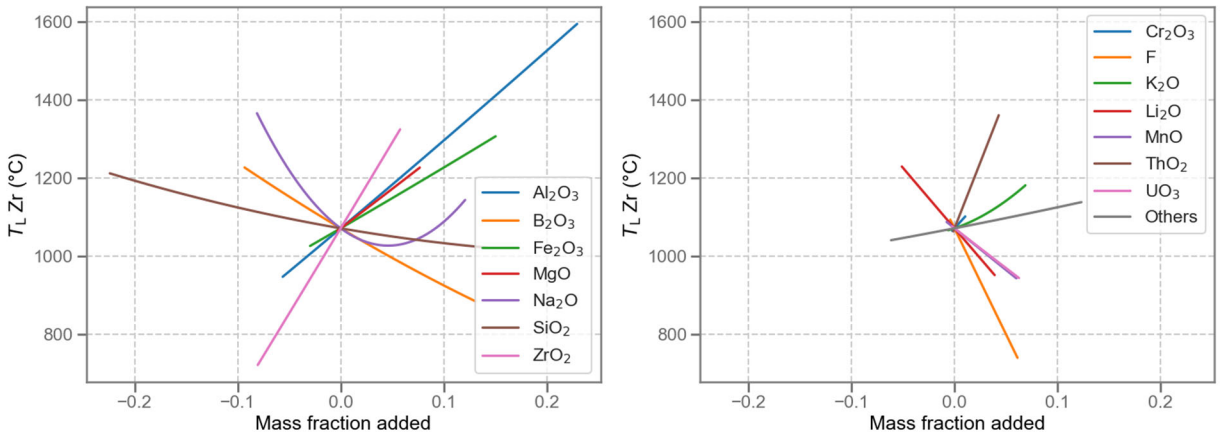

Figure 2.16. Component effects on T_L-Zr model (For Information Only).

2.6 Spinel $T_{1\%}$

Spinel crystalline phases can settle in the melter, leading to processing upsets. To address melter processing concerns, a $T_{1\%}$ model was developed that will enable formulations of glasses that avoid the accumulation of spinel during the melting process.

2.6.1 Database

Available $T_{1\%}$ data for spinel phases $T_{1\%}$-Sp were compiled into a database, as summarized in Table 2.16. The database includes glasses that formed spinels measured by X-ray diffraction or scanning electron microscopy of glasses tested through various methods, including gradient furnace measurements and isothermal heat treatment. Table 2.17 presents the ranges of measured spinel $T_{1\%}$-Sp values and the range of each component concentration.

Table 2.16. $T_{1\%}$-Sp data summary.

Glass ID	Lab	# of Data	Reference
MS	PNNL	19	Hrma 1999, Wilson et al. 2002
SP	PNNL	18	Mika et al. 2007
LSi	PNNL	30	Vienna et al. 2013
SPA	PNNL	32	Vienna et al. 2013
WTP-TL	PNNL	14	Vienna et al. 2003
EM07	PNNL	37	Schweiger et al. 2011
US	PNNL	33	Riley et al. 2018
HAL24	PNNL	9	(a)
HLW-APPS2	PNNL	4	Russell et al. 2025
ICCM	SRNL/PNNL	13	Peeler et al 2002; Vienna et al. 2013
VSL HLW02	VSL	51	Piepel et al. 2007; Piepel et al. 2008
VSL HLW03	VSL	25	Piepel et al. 2007; Piepel et al. 2008
VSL HLW05	VSL	7	Kot et al. 2005
VSL HLW06	VSL	18	Kot et al. 2005
VSL HLW07	VSL	20	Kruger et al. 2013
VSL ALG	VSL	17	Kot et al. 2006
Total		347	

(a) HAL24 matrix 1 and 2 $T_{1\%}$-Sp data are found in CCPs 264 and 284, respectively.

Table 2.17. Range of glass data used in the $T_{1\%}$-Sp model development, mass fraction.

Oxide	Min	Median	Max
Al_2O_3	0.01880	0.08969	0.25758
B_2O_3	0.03000	0.09343	0.23104
CaO	0	0.00591	0.09454
Cr_2O_3	0	0.00289	0.02000
Fe_2O_3	0.00024	0.10277	0.20001
K_2O	0	0.00520	0.06000
Li_2O	0	0.02961	0.06013
MgO	0	0.00248	0.06001

Oxide	Min	Median	Max
MnO	0	0.02124	0.08000
Na_2O	0.03910	0.13866	0.25001
NiO	0	0.00641	0.03000
SiO_2	0.24131	0.40743	0.53011
SO_3	0	0.00140	0.00925
SrO	0	0.01845	0.10089
ZnO	0	0.00950	0.04053
ZrO_2	0	0.02644	0.09605
Others	0	0.03848	0.15958

2.6.2 Model

The model terms were first selected based on the evaluation of range and distribution of the major glass components. Then, a linear stepwise regression model with k-fold optimization was used to further screen the significant model terms: $T_{1\%} = \sum_{i=1}^{n} c_i g_i$, where c_i is the coefficient of the i^{th} first-order component term, n is the total number of components fitted in the model, and g_i is the target mass fraction of the corresponding component, i. Al_2O_3, B_2O_3, CaO, Cr_2O_3, Fe_2O_3, K_2O, Li_2O, MgO, MnO, Na_2O, NiO, SiO_2, SO_3, SrO, ZnO, and ZrO_2 were found to have significant effects. A PQM was developed using stepwise regression, where the second-order term that was found to improve the model statistics was MnO×SiO_2:

$$T_{1\%} = \sum_{i=1}^{n} c_i g_i + \sum_{i=1}^{n-1} \sum_{j \geq i}^{n} c_{ij} g_i g_j$$

where c_{ij} is the quadratic coefficient for the cross-product term $g_i g_j$. This model was found to have the best fit statistics without overfitting with an $R^2 = 0.754$. The model coefficients are reported in Table 2.18. The predicted values are compared to measured values in Figure 2.17. Figure 2.18 displays the component effects on $T_{1\%}$-Sp. $T_{1\%}$-Sp is strongly increased by spinel forming components (Cr_2O_3, NiO, ZnO, MnO, MgO, Fe_2O_3, and Al_2O_3) and also by ZrO_2. $T_{1\%}$-Sp is strongly increased by Li_2O, Na_2O, K_2O, CaO, and B_2O_3. These impacts have been widely reported and were expected. More surprising is the strong negative effect of SO_3. Removal of the SO_3 terms significantly reduced model predictability. Previous studies of composition effects on spinel formation didn't include significant concentrations of SO_3. Perhaps there is a solubility competition between CrO_4^{2-} and SO_4^{2-} which indirectly effects T_L-Sp. This warrants further evaluation.

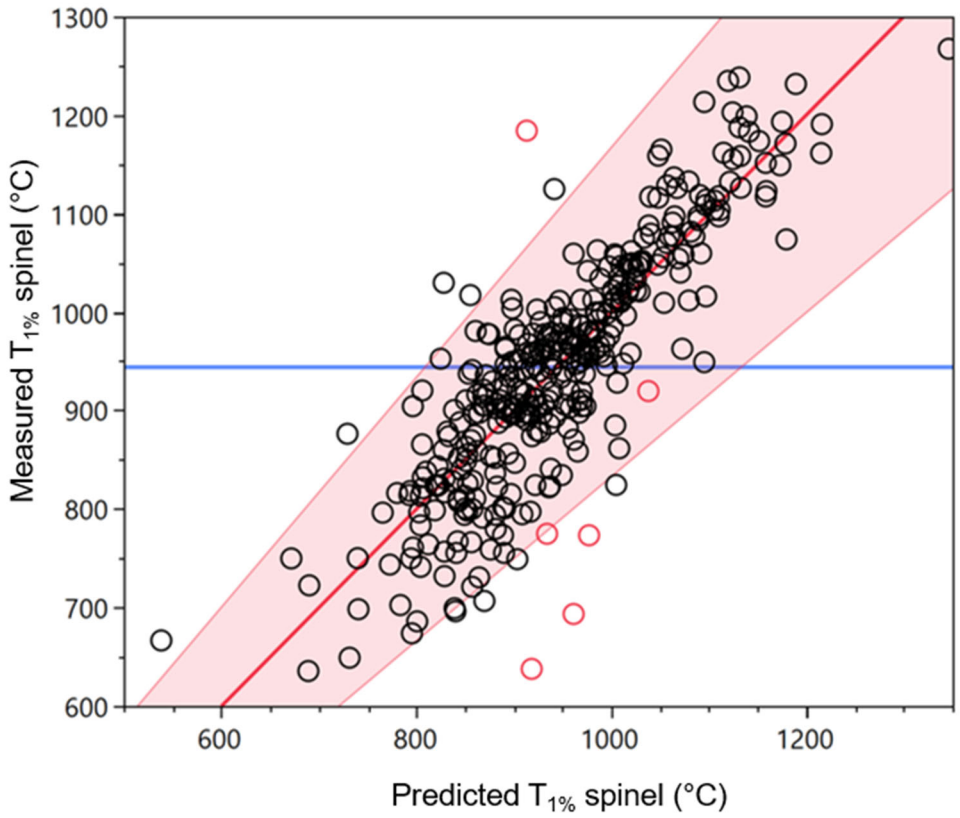

Figure 2.17. Predicted vs. measured $T_{1\%}$-Sp, °C. Red circles represent outliers and black circles represent the remainder of the data.

Table 2.18. Model coefficient for the $T_{1\%}$-Sp model.

Term	Coefficient		Statistic	Value
Al_2O_3	2815.5448		n	347
B_2O_3	-120.6229		p	18
CaO	-207.9127		Mean $T_{1\%}$-Sp, °C	944.9581
Cr_2O_3	11538.132		R^2_{fit}	0.7540
Fe_2O_3	2911.5517		R^2_{Adj}	0.7413
K_2O	-934.5138		R^2_{press}	0.7211
Li_2O	-1524.845		$RMSE_{fit}$	61.1044
MgO	3383.5339		$RMSE_{press}$	63.4350
MnO	9343.5046		Pooled $T_{1\%}$-Sp SD, °C	32.1151
Na_2O	-882.5007			
NiO	11986.565			
SiO_2	746.07398			
SO_3	-15074.44			
SrO	308.62547			
ZnO	3196.7892			
ZrO_2	1779.187			
Others	999.00555			
MnO × SiO_2	-16698.33			

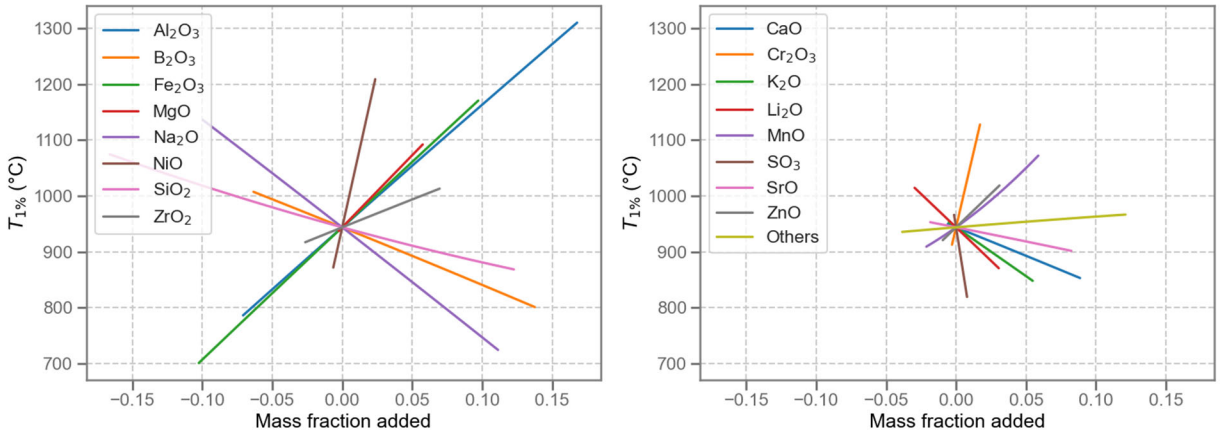

Figure 2.18. Component effects on $T_{1\%}$-Sp model (For Information Only).

3.0 Formulation Methods and Constraints

This section summarizes the property constraints (Section 3.1), MV ranges (Section 3.2), and optimization criteria (Section 3.3) for the EWG2.6 formulation algorithm. Example calculations can be found in Section 3.4.

3.1 Property Constraints

A combination of models from the literature and those developed in this report are recommended to predict the properties of example DFHLW glasses while glass property data gaps are being filled. These models are summarized in Table 3.1.

Table 3.1. List of property constraints for DFHLW glass composition estimation

Property	Reference	Constraint	U_{pred}[(a)]	Comp.[(b)]	Note
PCT	Vienna and Crum (2018)	$NL_{Ave} \le 6.44$ g/m^2	Applied	AR, MO	(c)
TCLP	Kim and Vienna (2004)	$C_{Cd} \le 0.48$ mg/L	None	AR, MO	(d)
Nepheline	Lu et al. (2021)	$p \ge 0.031$ (distance to the line)	None	AR, MO	(e)
Viscosity	This report, Section 2.1	$2 \le \eta_{1150} \le 8$ Pa·s $\eta_{1100} < 15$ Pa·s	Applied	AR, MA	(f)
EC	This report, Section 2.1	$\varepsilon_{1100} \ge 10$ S/m $\varepsilon_{1200} \le 70$ S/m	Applied	AR, MA	(f)
Sulfate	This report, Section 2.2	$g_{SO3} \le w_{SO3\text{-}3TS}$ - offset, wt%	Applied	BR, MA	(g)
Immiscibility	Peeler and Hrma (1994)	$N_{NaLi} \ge 20$ wt%	None	AR, MA	(h)
K-3 corrosion	This report, Section 2.3	$k_{1208} \le 0.025$ in	Applied	BR, MA	(i)
Phosphate	This report, Section 2.4	T_L-P ≤ 1050 °C (for $g_{P2O5} \ge 0.01$)	Applied	AR, MA	(j)
Zirconia	This report, Section 2.5	T_L-Zr ≤ 1050°C (for $g_{ZrO2} \ge 0.027$)	None	AR, MA	(k)
Spinel	This report, Section 2.6	$T_{1\%}$-Sp ≤ 950 °C	None	AR, MA	(l)

(a) Prediction uncertainties (U_{pred}) are applied to the limits associated with all models generated in this report. They are calculated based on confidence intervals (CIs) for processing related properties: $U_{pred} = t_{1-\alpha,n-p}\sqrt{\mathbf{g}^{\mathrm{T}}[s^2(\mathbf{G}^{\mathrm{T}}\mathbf{G})^{-1}]\,\mathbf{g}}$, where n is the total number of points used to fit a model (i.e., total observations), p is the total number of model terms/coefficients. n and p values of each model can be found in the coefficient table. α is the statistical significance level (e.g., α = 0.10 for 90% confidence), and $t_{1-\alpha,n-p}$ represents 100(1−α)-percentile of the Student's t-distribution with $n - p$ degrees of freedom. For PCT response, a simultaneous upper confidence interval (SUCI): $U_{pred} = \sqrt{pF_{1-2\alpha,(p,n-p)}}\sqrt{\mathbf{g}^{\mathrm{T}}s^2(\mathbf{G}^{\mathrm{T}}\mathbf{G})^{-1}\mathbf{g}}$, where $F_{1-2\alpha,(p,n-p)}$ represents 100(1−2α)-percentile of the F-distribution with p and $n - p$ degrees of freedom. The variance covariance matrices ($s^2[\mathbf{G}^{\mathrm{T}}\mathbf{G}]^{-1}$) are reported in Appendix A. More details on the statistical methods to develop, evaluate and validate property-composition models can be found in Appendix B by Vienna et al. 2022b.

(b) Compositions to be used for model predictions: AR (after applying retention factors), BR (before applying retention factors), MA (mass fractions) and MO (molar fractions).

(c) The Ave ln[NL] of the Defense Waste Processing Facility (DWPF) EA glass = (ln[8.350] + ln[6.675] + ln[4.785])/3 = 1.862. Applying an exponential function to Ave ln[NL] yields a NL_{Ave} = 6.44 g/m^2, which will be used to limit PCT response for the model in this report.

(d) The TCLP model was found to be conservative for APPS1 and APPS2 glasses; therefore, no U_{pred} is applied.

(e) Lu et al. (2021) model provides the probability of nepheline formation based on the compositional distance above a dividing line (p), where the standard model with a limit of $p > 0$ results in a roughly 10% failure rate. Increasing the threshold to $p \ge 0.031$ reduces the failure rate to 0 for the model dataset and would exclude the APPS2 glass that precipitated nepheline.

(f) Viscosity limits changed from $4 \le \eta_{1150} \le 6$ Pa·s in EWG2.5 to $2 \le \eta_{1150} \le 8$ Pa·s in EWG2.6, while there was no change for EC limits (Peters 2025).

(g) The w_{SO3} model in this report was based on 3TS solubility data, which have been shown to be 0.33 wt% SO_3 higher than the melter tolerance data as reported by Skidmore et al. (2019). Therefore, the predicted $g_{SO3} \le w_{SO3\text{-}3TS} - 0.33$ is the bounding limit. Here, g_{SO3} is before accounting for any volatile loss of SO_3.

(h) Immiscibility limit is given by $N_{NaLi} = (g_{Na_2O} + 2.07g_{Li_2O})/(g_{Na_2O} + 2.07g_{Li_2O} + g_{B_2O_3} + g_{SiO_2}) \ge 0.2$ mass fraction.

(i) k_{1208} limit was ≤ 0.04 inch in EWG2.5 (Vienna et al. 2024), but after review of all glass processing related limits, WTP revised the limit to $k_{1208} \le 0.025$ inch in future glass designs (Peters 2025).

	Property	Reference	Constraint	U_{pred}[a]	Comp.[b]	Note
(j)	Model for phosphate-containing phases was changed from a probability model in EWG2.5 to a T_L-P model in EWG2.6. A sigmoid function was added to the T_L-P model predictions to avoid a singularity in the first derivative of composition vs. predicted response with 0 for g_{P2O5} < 0.01 and much greater than zero predicted T_L-P for g_{P2O5} ≥ 0.01. The equation used is: $T_L\ P = \frac{\sum T_i g_i}{1+e^{-2000(g_{P_2O_5}-0.009)}}$.					
(k)	A sigmoid function was also added to the T_L-Zr model predictions with 0 for g_{ZrO2} < 0.027 and much greater than zero predicted T_L-Zr for g_{ZrO2} ≥ 0.027. The equation used is: $T_L\ Zr = \frac{\sum T_i g_i}{1+e^{-2000(g_{ZrO_2}-0.026)}}$.					
(l)	In EWG2.5, spinel fraction in glass was limited to 2 vol% at 950°C ($T_{2\%}$ ≤ 950°C). WTP revised the limit to $T_{1\%}$-Sp ≤ 950°C in future glass designs (Peters 2025).					

3.2 Model Validity Constraints

The empirical models used to predict DFHLW glass properties are only valid within the range of data used to develop and validate the models. These MV ranges are summarized in Table 3.2. The “overall” limits in the last two columns are recommended to be used in EWG2.6. The minimum limits were generally developed by taking the maximum of the minimum values for each property and likewise the maximum limits are the minimum of the maximums for individual properties. Some exceptions were made when multiple models were used for a given property and/or if the model was validated across a broader range. Some recommended models use compositions in mole fractions, which are not given in the table. The range of validity does not directly translate into mole fractions; however, the key components were spot-checked and found to be well bound by the overall limits. In addition to the single-component limits, some of the models have additional multi-component limits. These include:

- K-3 corrosion model: $N_{Alk} = g_{Na_2O} + 2.07 g_{Li_2O} + 0.66 g_{K_2O}$ is between 0.1374 and 0.2725
- K-3 corrosion model: $N_{SiAl} = g_{SiO_2} + 1.6970 g_{Al_2O_3}$ is between 0.4497 and 0.7206

In these cases, the normalized concentration ratios are based on ratios of molecular weights. Based on these data limits, it is recommended that the following multi-component limits be added:

- 0.1374 ≤ N_{Alk} ≤ 0.2725
- 0.4497 ≤ N_{SiAl} ≤ 0.7206

F limits were based on model validity. However, F is known to affect corrosion of metallic components in the melter for which no current model is available. There are studies underway to help assess the ultimate F concentration limits but at the time of this report they are not sufficiently developed to rationally reduce the F concentration limit.

Table 3.2. Model validity constraints in mass fractions.

	EWG2.5 overall		w_{SO3}		K_{1208}		η		ε		$T_{1\%}$		T_L-Zr		T_L-P		**EWG2.6 overall**	
Bound	Min	Max	Min	Max	Min	Max	Min	Max	Min	Max	Min	Max	Min	Max	Min	Max	**Min**	**Max**
Al_2O_3	0.0300	0.3000	**0.0305**[a]	**0.2726**	**0.0300**	**0.2634**	**0.0301**	**0.2711**	**0.0301**	**0.2621**	**0.0188**[b]	**0.2576**	**0**	**0.2857**	**0.0101**	**0.2708**	**0.0300**	**0.3000**
B_2O_3	0.0400	0.2200	**0.0402**	**0.2414**	**0.0400**	**0.2229**	**0**	**0.2392**	**0**	**0.2229**	**0.0300**	**0.2310**	**0**	**0.2240**	**0.0404**	**0.2207**	**0.0404**	**0.2207**
Bi_2O_3	0	0.0700	0[c]	0.0155	0	0.0155	0	0.0537	0	0.0537	0	0.0700	0	0.1000	**0**	**0.1040**	**0**	**0.0537**
CaO	0	0.1270	**0**	**0.1297**	0	0.1225	**0**	**0.1276**	**0**	**0.1276**	**0**	**0.0945**	0	0.0934	**0.0004**	**0.1420**	**0**	**0.1276**
CdO			-	-	0	0.0001	0	0.0150	0	0.0150	0	0.0200	0	0.0165	0	0.0096	**0**	**0.0150**
Cl			**0.0004**	**0.0241**	**0**	**0.0120**	**0**	**0.0117**	**0**	**0.0117**	0	0.0034	0	0.0034	-	-	**0**	**0.0117**
Cr_2O_3	0	0.0145	**0.0001**	**0.0144**	**0**	**0.0144**	**0**	**0.0143**	**0**	**0.0143**	**0**	**0.0200**	**0**	**0.0127**	**0**	**0.0158**	**0**	**0.0144**
F	0	0.0450	**0.0002**	**0.0457**	0	0.0452	**0**	**0.0453**	**0**	**0.0453**	0	0.0200	**0**	**0.0652**	0	0.0250	**0**	**0.0450**
Fe_2O_3	0	0.1198	**0**	**0.1210**	**0**	**0.1360**	**0**	**0.1206**	**0**	**0.1206**	**0.0002**	**0.2000**	**0**	**0.1800**	0	0.1003	**0**	**0.1206**
K_2O	0	0.0584	**0**	**0.0584**	**0**	**0.0810**	**0**	**0.0809**	**0**	**0.0809**	**0**	**0.0600**	**0**	**0.0750**	0	0.0895	**0**	**0.0584**
LN_2O_3	0	0.0111	-	-	0	0.0288	0	0.0494	0	0.0440	-	-	-	-	0	0.0152	**0**	**0.0152**
Li_2O	0	0.0512	**0**	**0.0512**	**0**	**0.0586**	**0**	**0.0633**	**0**	**0.0633**	**0**	**0.0601**	**0**	**0.0901**	**0**	**0.0676**	**0**	**0.0512**
MgO	0	0.0502	**0**	**0.0506**	0	0.0451	**0**	**0.0818**	**0**	**0.0502**	**0**	**0.0600**	**0**	**0.0800**	0	0.0432	**0**	**0.0432**
MnO	0	0.0204	0	0.0077	**0**	**0.0203**	0	0.0500	0	0.0500	**0**	**0.0800**	**0**	**0.0677**	0	0.0807	**0**	**0.0203**
Na_2O	0.0410	0.2700	**0.0923**	**0.2704**	**0.0247**	**0.2601**	**0.0247**	**0.2695**	**0.0247**	**0.2695**	**0.0391**	**0.2500**	**0.0362**	**0.2382**	**0.0159**	**0.2054**	**0.0391**	**0.2601**
NiO	0	0.0297	0	0.0096	0	0.0096	0	0.0360	0	0.0154	**0**	**0.0300**	0	0.0129	0	0.0266	**0**	**0.0266**
P_2O_5	0	0.0400	**0.0007**	**0.0403**	**0**	**0.0400**	**0**	**0.0402**	**0**	**0.0402**	0	0.0327	0	0.0500	**0.0101**	**0.1017**	**0**	**0.0400**
SiO_2	0.2493	0.5300	**0.2412**	**0.5936**	**0.2477**	**0.5851**	**0.2405**	**0.5872**	**0.2459**	**0.5872**	**0.2413**	**0.5301**	**0.2287**	**0.5957**	**0.2144**	**0.5483**	**0.2459**	**0.5300**
SO_3	0	0.0280	-	-	0.0001	0.0197	**0**	**0.0133**	**0**	**0.0133**	**0**	**0.0093**	0	0.0098	0	0.0156	**0**	**0.028**
SrO	0	0.0788	0	0.0002	0	0.0788	0	0.0788	0	0.0788	**0**	**0.1009**	0	0.1029	**0**	**0.0888**	**0**	**0.0788**
SnO_2	0	0.0503	**0**	**0.0508**	0	0.0500	**0**	**0.0504**	**0**	**0.0504**	0	0.0023	0	0.0023	0	0.0073	**0**	**0.0500**
ThO_2			-	-	-	-	0	0.0534	0	0.0440	0	0.0601	**0**	**0.0441**	0	0.0183	**0**	**0.0440**
TiO_2	0	0.0294	0	0.0294	0	0.0501	**0**	**0.0501**	**0**	**0.0501**	0	0.0305	0	0.0100	0	0.0059	**0**	**0.0294**
UO_3	0	0.0630	-	-	-	-	0	0.0367	0	0.0367	0	0.0650	**0**	**0.0650**	0	0.0359	**0**	**0.0650**
V_2O_5	0	0.0508	**0**	**0.0573**	**0**	**0.0515**	**0**	**0.0570**	**0**	**0.0570**	0	0.0495	0	0.0332	0	0.0406	**0**	**0.0495**
ZnO	0	0.0400	**0**	**0.0575**	**0**	**0.0536**	**0**	**0.0982**	**0**	**0.0581**	**0**	**0.0405**	0	0.0390	0	0.0400	**0**	**0.0400**
ZrO_2	0	0.0924	**0**	**0.0932**	**0**	**0.0932**	**0**	**0.0932**	**0**	**0.0932**	**0**	**0.0960**	**0.0269**	**0.1650**	**0**	**0.1052**	**0**	**0.0932**
Others[d]	0	0.0377	-	-	-	-	-	-	-	-	-	-	-	-	**0.0002**	**0.0199**	**0**	**0.0199**

(a) Red entries represent values that are within the overall MV limits (i.e., the overall limits exceed these component concentrations, where the models are extrapolating).
(b) Green entries represent values that significantly exceed the overall MV limits (i.e., the overall limits do not exceed these component concentrations).
(c) Gray entries represent components that are not in the recommended models.
(d) "Others" here represent the other components not listed in the table. To reduce the upper limit of "Others," LN_2O_3 (all the lanthanide oxides) is excluded from "Others" even though it is not a model term in EWG2.6 models. Upper limit of "Others" was calculated using the T_L-P model data, where the model has the smallest upper MV limit for "Others".

3.3 Optimization Criteria

The glass compositions are optimized by varying the concentrations of glass-forming chemicals (GFCs) and waste to maximize the waste loading while simultaneously satisfying the property and composition constraints. Unguided optimization often results in selection of GFCs that are not ideal – for example, Cr_2O_3 addition in cases of low K-3 corrosion glasses or V_2O_5 addition in cases of low SO_3 glasses. To address these concerns, the following logic statements are used in the optimization: 1) V_2O_5 is not added when the waste loading increase by V_2O_5 addition is smaller than 0.6 wt% and 2) a Cr_2O_3 upper limit of 0.6 wt% in the final glass is imposed if Cr_2O_3 is selected as a GFC.

These optimization criteria will result in a reasonable set of glasses for design, testing, and planning purposes in the near-term. As data collection and modeling efforts continue, glass formulation approaches and compositions will evolve without jeopardizing the validity of the work performed.

3.4 Example Calculations

To demonstrate the glass formulation approach suggested, example calculations are described here. Five example waste compositions (high in Al_2O_3, F, Na_2O, P_2O_5, and SO_3, respectively) were selected from the feed vector supplied by Britton (2023), as summarized in Table 3.3 and Appendix B. Glass was optimized for each of the five example wastes using the constraints presented in Table 3.1 and Table 3.2. Appendix C presents the nominal compositions of the current list of GFCs. For PCT, 99% SUCI was used, and for the other properties, 99% CI was used – although the confidence level should be adjusted to match the desired application of the models. The formulations, resulting glass compositions, and predicted properties are summarized in Table 3.4, Table 3.5, and Table 3.6, respectively.

Table 3.3. Composition (mass fraction of oxides and halogen) of the five wastes used in example calculations. Compositions in mg/L element can be found in Appendix B.

Example #	1	2	3	4	5
	High Al	High F	High Na	High P	High S
Ac_2O_3	2.005E-12	4.392E-13	9.360E-13	2.542E-13	8.536E-13
Ag_2O	1.035E-04	6.046E-04	1.716E-05	0.000E+00	0.000E+00
Al_2O_3	6.241E-01	4.492E-02	1.267E-01	1.962E-01	1.593E-01
Am_2O_3	7.214E-09	6.811E-08	8.465E-07	3.325E-06	9.012E-06
As_2O_5	5.421E-04	3.424E-05	7.257E-04	0.000E+00	0.000E+00
B_2O_3	2.936E-03	4.120E-03	6.985E-04	0.000E+00	0.000E+00
BaO	1.970E-04	7.422E-05	1.164E-04	1.745E-13	3.530E-13
BeO	4.899E-05	1.739E-04	1.991E-05	0.000E+00	0.000E+00
Bi_2O_3	9.619E-05	5.008E-04	5.008E-05	1.839E-02	4.659E-05
CaO	1.113E-03	1.054E-03	1.618E-03	3.652E-03	6.674E-03
CdO	7.087E-05	4.724E-05	1.709E-04	1.385E-11	5.614E-11
Ce_2O_3	4.139E-04	7.537E-06	4.142E-04	0.000E+00	0.000E+00
Cl	4.198E-03	3.368E-03	8.362E-03	2.759E-03	2.546E-03
Cm_2O_3	1.655E-14	1.230E-13	2.817E-10	2.365E-11	1.376E-09

Example #	1	2	3	4	5
CoO	3.871E-04	3.208E-06	4.106E-05	2.787E-12	1.531E-11
Cr_2O_3	3.886E-03	1.049E-02	3.113E-03	2.503E-03	4.271E-03
Cs_2O	3.922E-06	2.592E-06	1.142E-05	6.098E-06	1.237E-05
CuO	4.427E-05	9.002E-06	9.940E-05	0.000E+00	0.000E+00
Eu_2O_3	6.944E-11	1.998E-11	7.093E-10	5.414E-10	4.451E-09
F	3.559E-03	1.449E-01	3.490E-03	1.495E-02	6.399E-02
Fe_2O_3	4.191E-04	2.282E-03	3.028E-02	2.392E-01	1.658E-01
Gd_2O_3	0.000E+00	0.000E+00	0.000E+00	0.000E+00	0.000E+00
HgO	2.719E-06	5.375E-07	1.197E-06	1.104E-04	9.815E-05
I	4.293E-07	4.563E-07	6.609E-07	6.229E-06	1.183E-06
K_2O	8.083E-03	1.624E-02	3.747E-03	1.389E-03	4.056E-03
La_2O_3	2.405E-09	4.856E-04	1.178E-04	5.143E-04	7.750E-03
Li_2O	2.640E-04	1.540E-05	1.392E-04	0.000E+00	0.000E+00
MgO	5.867E-04	1.779E-03	9.938E-04	0.000E+00	0.000E+00
MnO	4.554E-05	1.331E-04	3.017E-03	1.055E-02	1.172E-02
MoO_3	3.482E-04	1.946E-05	1.890E-04	0.000E+00	0.000E+00
Na_2O	3.350E-01	5.151E-01	7.807E-01	3.558E-01	4.910E-01
Nb_2O_5	4.807E-10	1.126E-10	2.415E-10	1.016E-10	3.750E-09
Nd_2O_3	4.127E-04	1.592E-04	8.332E-04	0.000E+00	0.000E+00
NiO	8.925E-05	1.576E-04	6.714E-04	6.427E-03	7.177E-03
NpO_2	1.547E-06	6.851E-07	6.365E-06	3.370E-07	1.248E-05
P_2O_5	2.869E-03	1.222E-02	1.352E-02	9.039E-02	1.310E-02
Pa_2O_5	3.574E-09	8.895E-10	2.377E-09	5.197E-10	1.812E-09
PbO	3.804E-04	9.625E-05	1.247E-03	1.775E-02	3.255E-03
PdO	0.000E+00	0.000E+00	0.000E+00	0.000E+00	0.000E+00
Pr_2O_3	0.000E+00	0.000E+00	0.000E+00	0.000E+00	0.000E+00
PuO_2	1.716E-07	7.311E-06	7.450E-06	6.758E-05	4.386E-05
RaO	1.459E-13	3.948E-14	9.104E-14	4.923E-13	7.696E-13
Rb_2O	0.000E+00	0.000E+00	0.000E+00	0.000E+00	0.000E+00
Rh_2O_3	0.000E+00	0.000E+00	0.000E+00	0.000E+00	0.000E+00
RuO_2	1.315E-24	2.901E-24	1.343E-04	6.733E-25	5.489E-24
SO_3	3.366E-03	3.850E-02	1.405E-02	1.145E-02	4.727E-02
Sb_2O_3	2.539E-04	3.552E-06	5.894E-05	2.959E-14	1.297E-13
SeO_2	4.972E-04	1.207E-05	3.583E-04	2.630E-08	8.428E-08
SiO_2	4.595E-03	5.274E-03	9.071E-04	8.060E-03	1.687E-03
Sm_2O_3	1.576E-06	2.827E-07	1.417E-05	1.130E-05	2.989E-05
SnO_2	7.630E-07	1.777E-07	3.273E-07	1.240E-07	7.362E-06
SrO	2.834E-07	2.119E-06	3.536E-05	4.881E-04	4.587E-04
Ta_2O_5	0.000E+00	0.000E+00	0.000E+00	0.000E+00	0.000E+00
Tc_2O_7	5.837E-05	7.725E-06	2.690E-06	8.374E-06	1.095E-05
TeO_2	0.000E+00	0.000E+00	0.000E+00	0.000E+00	0.000E+00
ThO_2	2.667E-06	9.522E-06	1.549E-04	1.210E-03	1.916E-03
TiO_2	5.903E-05	1.453E-05	1.368E-05	0.000E+00	0.000E+00

Example #	1	2	3	4	5
Tl_2O	0.000E+00	4.252E-06	1.698E-04	0.000E+00	0.000E+00
UO_3	3.226E-04	1.627E-02	7.860E-04	1.790E-02	3.288E-03
V_2O_5	3.154E-04	6.327E-05	7.317E-05	0.000E+00	0.000E+00
WO_3	0.000E+00	0.000E+00	9.424E-04	0.000E+00	0.000E+00
Y_2O_3	1.231E-12	3.861E-05	2.881E-04	3.343E-09	7.562E-09
ZnO	2.640E-04	1.897E-05	1.961E-04	0.000E+00	0.000E+00
ZrO_2	4.375E-05	1.808E-01	7.641E-04	1.877E-04	4.539E-03
SUM	1	1	1	1	1

Table 3.4. Formulation of example glasses (mass fraction of component oxide in glass).

Component	1	2	3	4	5
Kyanite	0	0.02683	0.05416	0	0
Boric acid	0.22026	0.08733	0.05394	0.04056	0.10514
Wollastonite	0	0.22185	0.09993	0.10685	0.20161
Na_2CO_3	0	0	0	0	0
Li_2CO_3	0.01529	0.01086	0	0.01987	0
Cr_2O_3	0	0.00312	0.00527	0	0
Silica	0.27675	0.35767	0.38841	0.36839	0.33536
Zincite	0.02471	0	0.03979	0.01293	0
Zircon	0	0	0.03952	0.00806	0
V_2O_5	0.04988	0	0	0	0.05000
Waste	0.41311	0.29234	0.31896	0.44334	0.30789

Table 3.5. Target glass composition (after applying retention factors) in mass fraction of oxides and halogen.

Example #	1	2	3	4	5
Ac_2O_3	8.320E-13	1.303E-13	2.995E-13	1.131E-13	2.653E-13
Ag_2O	4.212E-05	1.758E-04	5.384E-06	0.000E+00	0.000E+00
Al_2O_3	**2.598E-01**	3.000E-02	7.270E-02	8.831E-02	5.058E-02
Am_2O_3	2.935E-09	1.981E-08	2.657E-07	1.451E-06	2.748E-06
As_2O_5	1.739E-04	7.852E-06	1.796E-04	0.000E+00	0.000E+00
B_2O_3	2.207E-01	8.913E-02	5.393E-02	4.040E-02	1.053E-01
BaO	8.174E-05	2.201E-05	3.724E-05	7.763E-14	1.097E-13
BeO	2.032E-05	5.157E-05	6.370E-06	0.000E+00	0.000E+00
Bi_2O_3	3.914E-05	1.457E-04	1.572E-05	8.025E-03	1.420E-05
CaO	6.288E-04	1.085E-01	4.870E-02	5.333E-02	9.983E-02
CdO	3.189E-05	1.401E-05	5.871E-05	1.301E-06	1.746E-11
Ce_2O_3	1.717E-04	2.235E-06	1.326E-04	0.000E+00	0.000E+00
Cl	9.520E-04	5.462E-04	1.460E-03	6.721E-04	4.319E-04
Cm_2O_3	6.868E-15	3.648E-14	9.015E-11	1.052E-11	4.278E-10
CoO	1.606E-04	9.514E-07	1.314E-05	1.245E-12	4.776E-12

Example #	1	2	3	4	5
Cr_2O_3	1.544E-03	6.000E-03	6.000E-03	1.069E-03	1.268E-03
Cs_2O	1.435E-06	6.777E-07	3.221E-06	2.393E-06	3.390E-06
CuO	1.837E-05	2.670E-06	3.181E-05	0.000E+00	0.000E+00
Eu_2O_3	2.881E-11	5.925E-12	2.270E-10	2.409E-10	1.384E-09
F	1.081E-03	**3.145E-02**	8.175E-04	4.869E-03	1.456E-02
Fe_2O_3	2.393E-04	1.874E-03	1.064E-02	1.071E-01	5.249E-02
Gd_2O_3	0.000E+00	0.000E+00	0.000E+00	0.000E+00	0.000E+00
HgO	0.000E+00	0.000E+00	0.000E+00	0.000E+00	0.000E+00
I	9.102E-08	6.916E-08	1.081E-07	1.416E-06	1.879E-07
K_2O	3.253E-03	4.673E-03	1.178E-03	6.106E-04	1.231E-03
La_2O_3	9.977E-10	1.440E-04	3.771E-05	2.288E-04	2.409E-03
Li_2O	1.526E-02	1.088E-02	4.450E-05	1.968E-02	0.000E+00
MgO	2.711E-04	7.557E-04	4.434E-04	1.264E-04	2.001E-04
MnO	1.930E-05	2.665E-04	1.067E-03	4.801E-03	3.848E-03
MoO_3	1.417E-04	5.659E-06	5.932E-05	0.000E+00	0.000E+00
Na_2O	1.382E-01	1.520E-01	**2.486E-01**	1.575E-01	1.518E-01
Nb_2O_5	1.994E-10	3.339E-11	7.728E-11	4.522E-11	1.166E-09
Nd_2O_3	1.712E-04	4.721E-05	2.666E-04	0.000E+00	0.000E+00
NiO	3.683E-05	4.648E-05	2.137E-04	2.845E-03	2.219E-03
NpO_2	6.419E-07	2.032E-07	2.037E-06	1.500E-07	3.878E-06
P_2O_5	1.184E-03	3.604E-03	4.301E-03	**4.000E-02**	4.051E-03
Pa_2O_5	1.483E-09	2.638E-10	7.607E-10	2.313E-10	5.633E-10
PbO	1.568E-04	2.828E-05	3.959E-04	7.827E-03	1.002E-03
PdO	0.000E+00	0.000E+00	0.000E+00	0.000E+00	0.000E+00
Pr_2O_3	0.000E+00	0.000E+00	0.000E+00	0.000E+00	0.000E+00
PuO_2	7.120E-08	2.168E-06	2.384E-06	3.007E-05	1.363E-05
RaO	4.681E-14	9.055E-15	2.253E-14	1.694E-13	1.850E-13
Rb_2O	0.000E+00	0.000E+00	0.000E+00	0.000E+00	0.000E+00
Rh_2O_3	0.000E+00	0.000E+00	0.000E+00	0.000E+00	0.000E+00
RuO_2	5.412E-25	8.533E-25	4.214E-05	2.972E-25	1.692E-24
SO_3	1.202E-03	9.635E-03	3.792E-03	4.307E-03	**1.239E-02**
Sb_2O_3	8.145E-05	8.147E-07	1.459E-05	1.023E-14	3.131E-14
SeO_2	1.595E-04	2.768E-06	8.866E-05	9.048E-09	2.026E-08
SiO_2	2.797E-01	4.910E-01	4.765E-01	4.310E-01	4.436E-01
Sm_2O_3	6.539E-07	8.383E-08	4.534E-06	5.031E-06	9.292E-06
SnO_2	3.165E-07	5.271E-08	1.047E-07	5.518E-08	2.289E-06
SrO	1.176E-07	6.285E-07	1.132E-05	2.172E-04	1.426E-04
Ta_2O_5	0.000E+00	0.000E+00	0.000E+00	0.000E+00	0.000E+00
Tc_2O_7	1.045E-05	9.890E-07	3.716E-07	1.609E-06	1.470E-06
TeO_2	0.000E+00	0.000E+00	0.000E+00	0.000E+00	0.000E+00
ThO_2	1.107E-06	2.824E-06	4.958E-05	5.386E-04	5.955E-04
TiO_2	6.624E-05	3.437E-04	6.023E-04	8.550E-05	9.191E-05
Tl_2O	0.000E+00	9.752E-07	4.203E-05	0.000E+00	0.000E+00

Example #	1	2	3	4	5
UO_3	1.338E-04	4.824E-03	2.696E-04	7.970E-03	1.022E-03
V_2O_5	4.924E-02	1.840E-05	2.296E-05	0.000E+00	4.950E-02
WO_3	0.000E+00	0.000E+00	3.016E-04	0.000E+00	0.000E+00
Y_2O_3	5.117E-13	1.145E-05	9.220E-05	1.491E-09	2.356E-09
ZnO	2.494E-02	5.627E-06	4.000E-02	1.298E-02	0.000E+00
ZrO_2	1.828E-05	5.375E-02	2.682E-02	5.503E-03	1.415E-03
SUM	1.000E+00	1.000E+00	1.000E+00	1.000E+00	1.000E+00

Table 3.6. Predicted glass properties, limiting values are bold

Property	Model	1	2	3	4	5
Melt temperature, °C	--	1150	1150	1150	1150	1150
PCT NL_{Ave} (no U), g/m^2	Vienna and Crum (2018)	1.20	2.43	0.64	0.23	1.06
PCT NL_{Ave}+U_{pred}, g/m^2	Vienna and Crum (2018)	1.99	6.21	0.84	0.33	1.81
TCLP c_{Cd}, mg/L	Kim and Vienna (2003)	0.00267	0.00366	0.01185	0.00007	0.00000
NP p	Lu et al. (2021)	**0.031**	0.098	**0.031**	**0.031**	0.085
Immisc N_{NaLi}, wt%	Peeler and Hrma (1994)	0.253	0.231	0.319	0.296	0.217
w_{SO3}-offset (no U), wt%	This report	0.874	1.319	1.079	0.769	1.577
w_{SO3}-offset (-U_{pred}), wt%	This report	0.721	**1.127**	0.984	0.572	**1.456**
SO_3 in glass (BR), wt%	This report	0.142	1.127	0.449	0.509	1.456
η_{1150} (no U), Pa·s	This report	7.6	4.0	7.7	7.7	3.6
η_{1150}+U_{pred}, Pa·s	This report	**8.0**	4.2	**8.0**	**8.0**	3.7
η_{1150}-U_{pred}, Pa·s	This report	7.2	3.8	7.5	7.3	3.4
η_{1100}+U_{pred}, Pa·s	This report	13.2	6.7	13.2	13.2	5.9
ε_{1150} (no U), S/m	This report	33.7	25.6	59.5	32.1	27.5
ε_{1100}-U_{pred}, S/m	This report	26.1	19.4	49.5	25.1	21.4
ε_{1200}+U_{pred}, S/m	This report	42.3	32.8	**70.0**	40.0	34.2
K-3 (no U), in	This report	0.001	0.019	0.021	0.017	0.018
K-3 +U_{pred}, in	This report	0.002	**0.025**	**0.025**	**0.025**	**0.025**
$T_{1\%}$, °C	This report	901	332	557	810	396
$T_{1\%}$ + U_{pred}, °C	This report	**950**	450	637	864	508
T_L-Zs, °C	This report	1042	733	1127	967	776
T_L-Zs + Sigmoid, °C	This report	0	733	945	0	0
T_L-Zs + Sigmoid + U_{pred}, °C	This report	69	814	**1050**	69	72
T_L-P, °C	This report	873	1156	1051	1010	1194
T_L-P + Sigmoid, °C	This report	0	0	0	1010	0
T_L-P + Sigmoid + U_{pred}, °C	This report	53	65	59	**1050**	57

3.5 Model Recommendations

Table 3.7 summarizes the models and constraints recommendations for immobilizing DFHLW. With the range of flowsheet options currently being considered, it may also be useful to consider how these and previously existing models can be applied to estimate loading of pretreated HLW (PTHLW). The current system plan (Schubick et al. 2023) utilizes a combination of models and constraints based on those from Vienna et al. 2016 (EWG1) and augmented with revised nepheline model (Lu et al. 2021), increased F limit (Jin et al. 2020), and various additional tweaks in Glass Model Calculator (GMC v1.4) for convenience, we'll call these models EWG1.4. Starting with these models, we've selected alternative models for those cases when the same property can be predicted significantly more precisely in the PTHLW glass composition region (primarily using EWG2.6 models). This revised PTHLW model and constraint set is also listed in Table 3.7 as EWG1.5.

Similarly, a number of different LAW glass models and constraints are available. Table 3.7 summarizes two such model and constraint sets. The WTP baseline models based on Piepel et al. 2007 and Kim and Vienna 2012. Version 1 of the enhanced LAW glass models (ELG) are reported by Vienna et al. 2022. It's our recommendation that for operations under the TSCR flowsheet, the WTP baseline be used for design of LAW glasses while for operations after the Advanced Modular Pretreatment System (AMPS) begins processing, the rate of LAW generation should match LAW Facility throughput giving advantage to the use of ELG1 formulations.

Table 3.8 lists the modal validity ranges for HLW and LAW glass formulation algorithms. Table 3.9 lists the GFCs used in DFHLW, pretreated HLW, LAW (TSCR) and LAW (AMPS) glass formulation algorithms.

Table 3.7. Models and constraints recommendations for treating DFHLW, pretreated HLW, LAW (TSCR), and LAW (AMPS).

	DFHLW (EWG2.6)		PTHLW (EWG1.5)		LAW (TSCR) (WTP Baseline)		LAW (AMPS) (ELG1)	
Property	Model	Constraint	Model	Constraint	Model	Constraint	Model	Constraint
PCT	Vienna and Crum (2018)	$NL_{Ave}+U_{pred} \leq 6.44$ g/m^2	Vienna and Crum (2018)	$NL_{Ave} \leq 6.44$ g/m^2	Kim and Vienna (2012)	NL+U_{pred} < 2 g/m^2, (for B, Na and Si)	Vienna et al. (2022b)	$NL \leq 2$ g/m^2, (for B and Na)
VHT	NA	NA	NA	NA	Kim and Vienna (2012)	$r_a + U_{pred} < 50$ g/m^2/d	Vienna et al. (2022b)	p < 0.190
TCLP	Kim and Vienna (2003)	$C_{Cd} \leq 0.48$ mg/L	Kim and Vienna (2003)	$C_{Cd} \leq 0.48$ mg/L	NA	NA	NA	NA
Nepheline	Lu et al. (2021)	$p \geq 0.031$	Lu et al. (2021)	$p \geq 0.000$	NA	NA	Lu et al. (2021)	$p \geq 0.028$
Viscosity	EWG2.6	$2 \leq \eta_{1150} \pm U_{pred} \leq 8$ Pa·s $\eta_{1100} + U_{pred} < 15$ Pa·s	EWG2.6	$2 \leq \eta_{1150} \leq 8$ Pa·s $\eta_{1100} < 15$ Pa·s	Kim and Vienna (2012)	$2 \leq \eta_{1150} \pm U_{pred} \leq 8$ Pa·s $\eta_{1100} + U_{pred} < 15$ Pa·s	Vienna et al. (2022b)	$2 \leq \eta_{1150} \leq 8$ Pa·s $\eta_{1100} < 15$ Pa·s
EC	EWG2.6	$\varepsilon_{1100} - U_{pred} \geq 0.1$ S/cm $\varepsilon_{1200} + U_{pred} \leq 0.7$ S/cm	EWG2.6	$\varepsilon_{1100} \geq 0.1$ S/cm $\varepsilon_{1200} \leq 0.7$ S/cm	Kim and Vienna (2012)	$\varepsilon_{1100} - U_{pred} \geq 0.2$ S/cm $\varepsilon_{1200} + U_{pred} \leq 0.7$ S/cm	Vienna et al. (2022b)	$\varepsilon_{1100} \geq 0.2$ S/cm $\varepsilon_{1200} \leq 0.7$ S/cm
Sulfate	EWG2.6	$g_{SO3} \leq w_{SO3}$ – offset - U_{pred}, wt%	EWG2.6	$g_{SO3} \leq w_{SO3}$ - offset, wt%	NA	NA	Vienna et al. (2022b)	$g_{SO3} \leq w_{SO3}$, wt%
Immiscibility	Peeler and Hrma (1994)	$N_{NaLi} \geq 20$ wt%	Peeler and Hrma (1994)	$N_{NaLi} \geq 20$ wt%	NA	NA	NA	NA
K-3 corrosion	EWG2.6	$k_{1208} + U_{pred} \leq 0.025$ in	NA	NA	NA	NA	Vienna et al. (2022b)	$k_{1208} \leq 0.04$ in
Phosphate	EWG2.6	T_L-P + $U_{pred} \leq$ 1050°C (for $g_{P2O5} > 0.01$)	EWG2.6	T_L-P ≤ 1050°C (for $g_{P2O5} \geq 0.01$)	NA	NA	NA	NA
Zirconia	EWG2.6	T_L-Zr + $U_{pred} \leq$ 1050°C (for $g_{ZrO2} \geq 0.027$)	EWG2.6	T_L-Zr ≤ 1050°C (for $g_{ZrO2} \geq 0.027$)	NA	NA	NA	NA
Spinel	EWG2.6	$T_{1\%} + U_{pred} \leq 950$ °C	Vienna et al. (2016)	$T_{2\%} \leq 950$°C	NA	NA	NA	NA
Melter and CCC crystallization constraint	NA	NA	NA	NA	NA	NA	Vienna et al. (2022b)	Section 9.9
Multi MV limits	EWG2.6	This report, Section 3.2	Vienna et al. (2016)	$SiO_2+B_2O_3 > 32$ wt%	Kim and Vienna (2012)	Table 13	Vienna et al. (2022b)	13.5 wt% ≤NAlk≤27.018 wt% $SiO_2 + 1.697Al_2O_3$ ≤61.6 wt%
Additional considerations	Sigmoid for T_L models				Formulation correlation in Kim and Vienna (2012)			

AMPS = Advanced Modular Pretreatment System.

Table 3.8. Modal validity ranges for HLW and LAW glass formulation algorithms.

Waste type	HLW						LAW			
Algorithm	WTP-2014		EWG-1.5 (PTHLW)		EWG2.6 (DFHLW)		WTP baseline (TSCR)		ELG1 (AMPS)	
Reference	Vienna and Kim (2014)		Vienna et al. (2016)		This report		Kim and Vienna (2012)		Vienna et al. (2022b)	
	Min	Max	Min	Max	Min	Max	Min	Max	Min	Max
Al_2O_3	0.018 [0.019]	0.13 [0.085]	0.019	0.3	0.03	0.3	0.035	0.09	0.035	0.1475
B_2O_3	0.045	0.15	0.04	0.22	0.0404	0.2229	0.06	0.131	0.06	0.1383
Bi_2O_3	0	In others	0	0.07	0	0.0537	-	-	-	-
CaO	0	0.01	0	0.1	0	0.1276	0	0.105	0	0.1278
CdO	0	0.001 [0.016]	0	0.015	0	0.015	-	-	-	-
Cr_2O_3	0	0.006 [0.005]	0	0.03	0	0.0144	0	0.0059	0	0.0063
F	0	0.0044	0	0.025	0	0.045	0	0.0035	0	0.013
Fe_2O_3	0.014 [0.019]	0.15 [0.14]	0	0.2	0	0.1206	0	0.08	0	0.1198
K_2O	0	0.016	0	0.06	0	0.0584	0	0.054	0	0.059
Li_2O	0 [0.019]	0.06	0	0.06	0	0.0512	0	0.058	0	0.0584
MgO	0	0.012	0	0.06	0	0.0432	0	0.05	0	0.0502
MnO	0	0.08 [0.07]	0	0.08	0	0.0203	-	-	-	-
Na_2O	0.039	0.2 [0.15]	0.041	0.24	0.0391	0.2601	0.025	0.23	0.0247	0.2657
NiO	0	0.01	0	0.03	0	0.0266	-	-	-	-
P_2O_5	0	0.045	0	0.045	0	0.04	0	0.03	0	0.0403
SiO_2	0.35	0.53	0.22	0.53	0.2459	0.53	0.384	0.521	0.3352	0.5226
SrO	0	0.1	0	0.101	0	0.0788	-	-	-	-
ThO_2	0	0.06	0	0.06	0	0.044	-	-	-	-
TiO_2	0	0.01	0	0.05	0	0.0294	0	0.03	0	0.0501
UO_3	0	0.065 [0.063]	0	0.063	0	0.065	-	-	-	-
ZnO	0	0.04	0	0.04	0	0.04	0.01	0.054	0	0.0582
ZrO_2	0	0.096 [0.091]	0	0.135	0	0.0932	0	0.05	0	0.0675

Table 3.9. GFCs used (labeled as Y) in DFHLW, pretreated HLW, LAW (TSCR) and LAW (AMPS) glass formulation algorithms.

GFCs	EWG2.6 (DFHLW)	EWG1.5 (PTHLW)	WTP Baseline (LAW TSCR)	ELG1 (LAW AMPS)
Kyanite	Y	Y	Y	Y
Boric acid	Y	Y	Y	Y
Borax	**N**	**N**	**N**	**N**
Wollastonite	Y	Y	Y	Y
Na_2CO_3	Y	Y	Y	**N**
Li_2CO_3	Y	Y	Y	Y
Cr_2O_3	Y	Y	**N**	Y
Silica	Y	Y	Y	Y
Zincite	Y	Y	Y	Y
Zircon	Y	Y	Y	Y
V_2O_4	Y	Y	**N**	Y
SnO_2	**N**	**N**	**N**	Y
Olivine	**N**	Y	Y	Y
Rutile	**N**	**N**	Y	Y
Fe_2O_3	**N**	**N**	Y	**N**
Sucrose	Y	Y	Y	Y

4.0 Conclusions

The EWG1 formulation method was developed in 2016 for application to pretreated waste at the Hanford Site (Vienna et al. 2016). It was applied to designing preliminary DFHLW glasses for the WTP, and a subset of these glasses was tested to evaluate how well the models and constraints for pretreated wastes applied to DFHLW glasses (Gervasio et al. 2024). Measured property data for the 15 APPS glasses were only partially predicted by the original EWG1 models. The shortcomings were largely explained by the combination of LAW and HLW in the DFHLW feeds and therefore DFHLW glasses. A new set of models and constraints were developed for datasets that combined LAW glasses with DFHLW glasses – EWG2.5.

A second set of glasses (APPS2) were formulated using then current estimates of DFHLW feed from Britton and Andersen (2024) and the EWG2.5 properties and constraints. Many (7/16) of the APPS2 glasses failed at least one design constraint (Russell et al. 2025). In addition, it was suggested that the crystallinity (from 2% to 1% spinel ≤ 950°C) and K_{1208} (from 0.04 to 0.025 in.) constraints be tightened to reduce risk of complications to melter testing (Peters 2025). Based on the tightening of constraints and the failure to conservatively estimate key properties, it was decided that an additional set of intermediate models (EWG2.6) would be needed for use before EWG3 models become available in 2026.

This report documents the development and proposed method of applying the EWG2.6 models to form a method to formulate DFHLW glasses. Seven new models were developed to predict η_T, ε_T, w_{SO3}, k_{1208}, T_L-P, T_L-Zr, and $T_{1\%}$-Sp of DFHLW glasses. These models include data not available during the fitting of EWG2.5 models and represent an incremental improvement in the ability to design glasses.

The property and composition constraints are tabulated along with the proposed use of prediction uncertainty and which GFCs should be used. Based on the EWG2.6 models and constraints, five example glass compositions were designed to demonstrate the proper application of the method.

5.0 References

10 CFR 830, *Nuclear Safety Management*. Code of Federal Regulations, as amended.

Bernards JK, GA Hersi, KT Pak, AJ Schubick, LM Bergmann, AN Praga, and SN Tilanus. 2021. *High-Level Waste Analysis of Alternatives Model Results Report*. RPP-RPT-61957, Rev. 2, Washington River Protection Solutions, Richland, WA.

Bernards JK, GA Hersi, TM Hohl, RT Jasper, PD Mahoney, NK Pak, SD Reaksecker, AJ Schubick, EB West, LM Bergmann, et al. 2020. *River Protection Project System Plan*. ORP-11242, Rev. 9, U.S. Department of Energy, Office of River Protection, Richland, WA.

Britton MD and CK Anderson. 2024. *Direct-Feed High-Level Waste Feed Vectors Assessment*. RPP-RPT-64878, Rev. 0, Washington River Protection Solutions, Richland, WA.

Britton MD. 2023. *Revised DFHLW Washing and Blending Study Campaign Inventory*. WRPS-2300881, Washington River Protection Solutions, Richland, WA.

Chapman 2007, *High Level Waste Vitrification Plant Capacity Enhancement Study*, 24590-HLW-RPT-PE-07-001, Waste Treatment and Immobilization Plant, Richland, WA.

Crum JV et al. 1996. “Liquidus temperature model for Hanford high-level waste glasses with high concentrations of zirconia.” *MRS Online Proceedings Library* 465:79.

DOE Order 414.1D, *Quality Assurance*. U.S. Department of Energy, Washington, D.C.

DOE. 2013. *Hanford Tank Waste Retrieval, Treatment, and Disposition Framework*. U.S. Department of Energy, Washington, D.C.

Gan H, K Gilbo, AE Papathanassiu, WK Kot, and IL Pegg. 2015. *Calcium Phosphate Constraints in HLW Glasses: Phosphate Liquidus Model.* VSL-15R3420-1, Vitreous State Laboratory, the Catholic University of America, Washington, D.C.

Gan H, WK Kot, and IL Pegg. 2012. *Development of High Waste-Loading HLW Glasses for High Bismuth Phosphate Wastes.* VSL-12R2550-1, Vitreous State Laboratory, the Catholic University of America, Washington, D.C.

Gervasio V, JJ Neeway, JD Vienna, JB Lang, BE Westman, JT Reiser, CE Lonergan, X Lu, SM Baird, DA Cutforth, and M Peterson. 2023. *Enhanced Hanford Low-Activity Waste Glass Property Data Development: Phase 5 and Phase 6.* PNNL-34331, Pacific Northwest National Laboratory, Richland, WA.

Gervasio V, X Lu, JT Reiser, M Peterson, NL Canfield, JB Lang, JC Rigby, JL George, DA Cutforth, JM Westman, RA Brown, JM Oshiro, BK Boehnke, EA Cordova, JV Crum, NA Lumetta, and JD Vienna. 2024. *Direct Feed High-Level Waste APPS Model Glass Testing (DFHLW APPS) Matrix*. PNNL-35503, Pacific Northwest National Laboratory, Richland, WA.

Heredia-Langner A, V Gervasio, SK Cooley, CE Lonergan, DS Kim, AA Kruger, and JD Vienna. 2022. “Hanford low-activity waste glass composition-temperature-melt viscosity relationships.” *International Journal of Applied Glass Science* 13(4):514-525. https://doi.org/10.1111/ijag.1658

Hrma P, JD Vienna, M Mika et al. 1999. *Liquidus Temperature Data for DWPF Glass*. PNNL-11790, Pacific Northwest National Laboratory, Richland, WA.

Hrma PR, GF Piepel, MJ Schweiger et al. 1994. *Property/composition relationships for Hanford high-level waste glasses melting at 1150°C*. PNL-10359; Vol. 1, Pacific Northwest National Laboratory, Richland, WA.

Jin T, D Kim, JD Vienna, and MS Fountain. 2020. *Fluorine Limits and Impacts in High-Level Waste Glass Compositions,* PNNL-30072, Pacific Northwest National Laboratory, Richland, WA.

Kim DS and JD Vienna. 2003. *Model for TCLP Releases from Waste Glasses*. PNNL-14061, Rev. 1, Pacific Northwest National Laboratory, Richland, WA.

Kim DS and JD Vienna. 2012. Preliminary ILAW Formulation Algorithm Description, 24590-LAW-RPT-RT-04-0003, Rev. 1, River Protection Project, Hanford Tank Waste Treatment and Immobilization Plant, Richland, WA

Kim DS and JD Vienna. 2004. *Glass Composition-TCLP Response Model for Waste Glasses*. PNNL-SA-40102, Pacific Northwest National Laboratory, Richland, WA.

Kot WK, H Gan and IL Pegg. 2006. *Preparation and Testing of HLW Glasses to Support Development of WTP IHLW Formulation Algorithm*. VSL-06R1240-1, Vitreous State Laboratory, the Catholic University of America, Washington, D.C.

Kot WK, H Gan, and IL Pegg. 2005. *Preparation and testing (T1% and PCT) of HLW matrix glasses to support WTP property-composition model development*. VSL-05R5780-2, Vitreous State Laboratory, The Catholic University of America, Washington, D.C.

Kot WK, H Gan, and IL Pegg. 2006. *Preparation and testing of HLW matrix glasses to support development of WTP phase 2 property-composition models*. VSL-06R6780-2, Vitreous State Laboratory, the Catholic University of America, Washington, D.C.

Kot WK, H Gan, and IL Pegg. 2016. *Preparation and Testing of HLW Glasses to Support Development of WTP IHLW Formulation Algorithm*. VSL-06R1240-1, Vitreous State Laboratory, the Catholic University of America, Washington, D.C.

Kot WK, K Gilbo, H Gan, I Joseph, and IL Pegg. 2014. *Enhanced HLW Glass Property-Composition Models – Phase 1*. VSL-14R3080-1, Vitreous State Laboratory, the Catholic University of America, Washington, D.C.

Kot WK, K Gilbo, H Gan, I Joseph, and IL Pegg. 2015. *Enhanced HLW Glass Property-Composition Models – Phase 2*. VSL-15R3400-1, Vitreous State Laboratory, the Catholic University of America, Washington, D.C.

Kot WK, L Myers and IL Pegg. 2007. *Baseline HLW Glass Formulations for Bismuth Phosphate Wastes*. VSL-07R1240-2, Vitreous State Laboratory, the Catholic University of America, Washington, D.C.

Kruger AA, et al. 2013. *IHLW PCT, Spinel T1%, Electrical Conductivity, and Viscosity Model Development*. VSL-07R1240-4; ORP-56320, Rev. 0. Vitreous State Laboratory, the Catholic University of America, Washington, D.C.

Lu et al. 2024a, DFHLW Process Control Chemical Limits Memo (PNNL-SA-199714)

Lu X and JD Vienna. 2023. “Selection of Example DFHLW Glasses for Validation Tests.” Memo to RL Hanson, dtd 7/26/2023. CCN-335241, River Protection Project, Waste Treatment and Immobilization Plant, Richland, WA.

Lu X, I Sargin, and JD Vienna. 2021. “Predicting nepheline precipitation in waste glasses using ternary submixture model and machine learning.” *Journal of American Ceramic Society* 104:5636-5647. https://doi.org/10.1111/jace.17983

Lu X, JD Vienna, and P Ferkl. 2024b. *Evaluation of DFHLW EWG Formulations and Processing Rates*. PNNL-36196, Pacific Northwest National Laboratory, Richland, WA.

Matlack KS, H Gan, W Gong, IL Pegg, CC Chapman, and I Joseph. 2007. *High Level Waste Vitrification System Improvements*. VSL-07R1010-1; ORP-56297, Vitreous State Laboratory, the Catholic University of America, Washington, D.C.

Matlack KS, W Kot, H Gan, and IL Pegg. 2012. *Enhanced Sulfate Management in HLW Glass Formulations*. VSL-12R2540-1, Vitreous State Laboratory, the Catholic University of America, Washington, D.C.

Matlack KS, W Kot, H Gan, Z Feng, and IL Pegg. 2013. *Management of High Sulfur HLW*. VSL-13R2920-1, Vitreous State Laboratory, the Catholic University of America, Washington, D.C.

Matlack KS, W Kot, W Gong, and IL Pegg. 2008a. *Small Scale Melter Testing of HLW Algorithm Glasses: Matrix 2 Tests*. VSL-08R1220-1, Vitreous State Laboratory, the Catholic University of America, Washington, D.C.

Mika M, MJ Schweiger, JD Vienna, et al. 1997. “Liquidus temperature of spinel precipitating high-level waste glasses.” *MRS Online Proceedings Library* 465:71

Muller I, WK Kot, HK Pasieka, K Gilbo, F Perez-Cardenas, I Joseph, and IL Pegg. 2012. *Compilation and Management of ORP Glass Formulation Database*. VSL-12R2470-1, Vitreous State Laboratory, the Catholic University of America, Washington, D.C.

NQA-1-2012, *Quality Assurance Requirements for Nuclear Facility Application*. American Society of Mechanical Engineers, New York, NY.

Parsons. 2023. *Waste Treatment and Immobilization Plant High Level Waste Treatment Analysis of Alternatives*. DE-NA0002895, Parsons Corporation, Boston, MA.

Peeler DK and P Hrma. 1994. “Predicting liquid immiscibility in multicomponent nuclear waste glasses.” *Ceramics Transactions* 45:219-229.

Peeler DK, TB Edwards, CC Herman et al. 2002. *Development of High Waste Loading Glasses for Advanced Melter Technologies*. WSRC-TR-2002-00426, Rev. 0, Savannah River National Laboratory, Aiken, SC.

Peters R. 2025. “DFHLW Glass Constraints – Supersedes CCN 342375.” Memo to D Bauer dtd 2/21/25. CCN 342390, Bechtel National Inc, Richland, WA.

Piepel GF, SK Cooley, IS Muller, H Gan, I Joseph, and IL Pegg. 2007. *ILAW PCT, VHT, Viscosity, and Electrical Conductivity Model Development: VSL-07R1230-1,* ORP-56502, Vitreous State Laboratory, The Catholic University of America, Washington, D.C.

Piepel GF, A Heredia-Langner, and SK Cooley. 2008. "Property–composition–temperature modeling of waste glass melt data subject to a randomization restriction." *Journal of the American Ceramic Society* 91(10):3222-3228. https://doi.org/10.1111/j.1551-2916.2008.02590.x

Piepel GF, SK Cooley, A Heredia-Langner et al, 2008. *Final Report IHLW PCT, Spinel T1% , Electrical Conductivity , and Viscosity Model Development*. VSL-07R1240-4, Rev. 0; Vitreous State Laboratory, The Catholic University of America, Washington, D.C.

Riley 2009: Riley BJ, P Hrma, JV Crum, JD Vienna, MJ Schweiger, CP Rodriguez, and JA Peterson. 2018. "Liquidus temperature in the spinel primary phase field: A comparison between optical and crystal fraction methods." Journal of Non-Crystalline Solids 483:1-9. https://doi.org/10.1016/j.jnoncrysol.2017.11.033

Russell RL JB Lang, YS Chou, SK Cooley, BP McCarthy, JD Vienna, LP Darnell, GF Piepel, V Gervasio, MJ Schweiger and JL Mayer. 2018. *Glass Compositions and Properties of Enhanced Waste Glass with High Alumina Content for High-Level Waste*, PNNL-27138, Pacific Northwest National Laboratory, Richland, WA.

Russell RL, DS Kim, JD Vienna, JB Lang, SM Baird, DL Bellofatto et al. 2023. *Enhanced Hanford High-Fluoride Waste Glass Property Data Development: Phase 1*. PNNL-35037; EWG-RPT-043, Pacific Northwest National Laboratory Richland, WA.

Russell RL, V Gervasio, X Lu, S Chong, JT Reiser, NL Canfield, JL George, et al. 2025. *Direct Feed High-Level Waste APPS Model Glass Testing (DFHLW APPS) Matrix, Phase 2*. PNNL-37506. Richland, WA: Pacific Northwest National Laboratory.

Scholes BA, DK Peeler, and JD Vienna. 2000. *The Preparation and Characterization of INTEC Phase 3 Composition Variation Study Glasses*. INEEL/EXT-2000-01566, Idaho National Engineering and Environmental Laboratory, Idaho Falls, ID.

Schubick AJ, LM Bergmann, TM Hohl, RT Jasper, J Mcmullin, KT Pak, GV Smith, UE Zaher, SD Reaksecker, and SL Weld. 2023. *River Protection Project System Plan*, ORP-11242, Rev. 10, U.S. Department of Energy, Office of River Protection, Richland, WA.

Scholes BA, JD Vienna, DK Peeler, and TB Edwards. 2002. *The preparation and Characterization of INTEC Sodium Bearing Waste Phase 1 Composition Variation Study Glasses*. INEEL/EXT-02-00386, Idaho National Engineering and Environmental Laboratory, Idaho Falls, ID.

Skidmore CH, JD Vienna, T Jin, DS Kim, BA Stanfill, KM Fox, and AA Kruger. 2019. "Sulfur solubility in low activity waste glass and its correlation to melter tolerance." *International Journal of Applied Glass Science* 10(4): 558-568. https://doi.org/10.1111/ijag.13272

Staples BA, BA Scholes, DK Peeler, LL Torres, JD Vienna, CA Musick, and BR Boyle. 2000. *The Preparation and Characterization of INTEC Phase 2b Composition Variation Study Glasses*. INEEL/EXT-99-01322, Idaho National Engineering and Environmental Laboratory, Idaho Falls, ID.

Staples BA, DK Peeler, JD Vienna, BA Scholes, and CA Musick. 1999. *The Preparation and Characterization of INTEC HAW Phase 1 Composition Variation Study Glasses*. INEEL/EXT-98-00970, Idaho National Engineering and Environmental Laboratory, Idaho Falls, ID.

Vienna JD and DS Kim. 2014. *Preliminary IHLW Formulation Algorithm Description*. 24590-HLW-RPT-RT-05-001, Rev. 1, River Protection Project, Waste Treatment Plant, Richland, WA.

Vienna JD and JV Crum. 2018. "Non-linear effects of alumina concentration on Product Consistency Test response of waste glasses." *Journal of Nuclear Materials* 511:396-405. https://doi.org/10.1016/j.jnucmat.2018.09.040

Vienna JD, A Fluegel, DS Kim, and P Hrma. 2009. *Glass Property Data and Models for Estimating High-Level Waste Glass Volume*. PNNL-18501, Pacific Northwest National Laboratory, Richland, WA.

Vienna JD, DK Peeler, RL Plaisted et al. 2000. *Glass Formulation for Idaho National Engineering and Environmental Laboratory Zirconia Calcine High-Activity Waste*. PNNL-12202, Pacific Northwest National Laboratory, Richland, WA.

Vienna JD, DS Kim, DC Skorski, and J Matyas. 2013. *Glass Property Models and Constraints for Estimating the Glass to be Produced at Hanford by Implementing Current Advanced Glass Formulation Efforts*. PNNL-22631, Rev. 1; ORP-58289, Pacific Northwest National Laboratory, Richland, WA.

Vienna JD, DS Kim, and P Hrma. 2002. *Database and Interim Glass Property Models for Hanford HLW and LAW Glasses*. PNNL-14060, Pacific Northwest National Laboratory, Richland, WA.

Vienna JD, GF Piepel, DS Kim, JV Crum, CE Lonergan, BA Stanfill, BJ Riley, SK Cooley, and T Jin. 2016. *Update of Hanford Glass Property Models and Constraints for Use in Estimating the Glass Mass to be Produced at Hanford by Implementing Current Enhanced Glass Formulation Efforts*. PNNL-25835, Pacific Northwest National Laboratory, Richland, WA.

Vienna JD, PR Hrma, MJ Schweiger et al. 1996. *Effect of Composition and Temperature on the Properties of High-Level Waste (HLW) Glass Melting Above 1200 degrees Celsius*. PNNL-10987, Pacific Northwest National Laboratory, Richland, WA.

Vienna JD, X Lu, P Ferkl, J Marcial, MS Fountain, and CL Bottenus. 2022a. *Initial Evaluation of Direct-Feed High-Level Waste Glass Formulations and Processing Rates*. PNNL-32866, Rev. 1, Pacific Northwest National Laboratory, Richland, WA.

Vienna JD, A Heredia-Langner, SK Cooley, AE Holmes, DS Kim, and NA Lumetta. 2022b. *Glass Property-Composition Models for Support of Hanford WTP LAW Facility Operation*. PNNL-30932, Rev. 2, Pacific Northwest National Laboratory, Richland, WA.

Vienna JD, X Lu, P Ferkl, J Marcial, MS Fountain, M Trenidad, R Hanson, MD Britton, L Cree, and W Abdul. 2023. "High-Level Waste Glass Processing over Broad Range of Alternative Feed Compositions." In *Proceedings of the 2023 Waste Management Symposia*, Phoenix, AZ.

Vienna JD, X Lu, P Ferkl, LL Gunnell, A Heredia-Langner, NA Lumetta, T Jin, et al. 2024. *Glass Property-Composition Models Update for use in Direct Feed High-Level Waste Flowsheet Development*. PNNL-35884, Pacific Northwest National Laboratory, Richland, WA.

Westesen AM, EL Campbell, SK Fiskum, AM Carney, TT Trang-Le, and RA Peterson. 2022. "Impact of feed variability on cesium removal with multiple actual waste samples from the Hanford site." *Separation Science and Technology* 57(15). https://doi.org/10.1080/01496395.2022.2059378

Wilson BK., P Hrma, J Alton, TJ Plaisted, and JD Vienna. 2002. "The effect of composition on spinel equilibrium and crystal size in high-level waste glass." *Journal of Materials Science* 37:5327-5331. https://doi.org/10.1023/A:1021081126162

Appendix A – Variance-Covariance Matrices

Table A.1. Variance-covariance table for product consistency test model (Vienna and Crum 2018).

Terms	Al_2O_3	B_2O_3	CaO	F	Fe_2O_3	K_2O	Li_2O	MgO	Na_2O	Nd_2O_3	P_2O_5
Al_2O_3	10.842200	-0.110010	-0.135940	0.474933	-0.219750	-0.296440	-0.186090	-0.002060	-0.218320	-0.689960	-0.715070
B_2O_3	-0.110010	0.958308	-0.009670	-0.038380	-0.049380	-0.112860	-0.019050	-0.046190	-0.013400	-0.596150	-0.285410
CaO	-0.135940	-0.009670	0.156770	-0.077860	0.011473	0.033719	0.008622	-0.029940	0.010959	-0.064120	0.040199
F	0.474933	-0.038380	-0.077860	2.804084	0.125234	-0.153440	0.050057	0.059267	-0.034340	-0.301120	-1.021250
Fe_2O_3	-0.219750	-0.049380	0.011473	0.125234	0.294468	-0.035100	-0.014570	-0.006640	-0.009740	0.930843	-0.154200
K_2O	-0.296440	-0.112860	0.033719	-0.153440	-0.035100	0.672862	0.038532	-0.012880	0.033665	0.471352	-0.214970
Li_2O	-0.186090	-0.019050	0.008622	0.050057	-0.014570	0.038532	0.075209	-0.000490	0.030691	-0.223860	0.115593
MgO	-0.002060	-0.046190	-0.029940	0.059267	-0.006640	-0.012880	-0.000490	0.287977	-0.002900	0.312449	-0.039220
Na_2O	-0.218320	-0.013400	0.010959	-0.034340	-0.009740	0.033665	0.030691	-0.002900	0.054068	0.043926	0.056038
Nd_2O_3	-0.689960	-0.596150	-0.064120	-0.301120	0.930843	0.471352	-0.223860	0.312449	0.043926	23.379630	-1.378670
P_2O_5	-0.715070	-0.285410	0.040199	-1.021250	-0.154200	-0.214970	0.115593	-0.039220	0.056038	-1.378670	6.381845
SiO_2	-0.180980	-0.063820	-0.002560	-0.021010	-0.004490	0.000430	-0.011340	-0.004140	-0.009570	0.003079	0.030982
SO_3	-1.640700	0.237811	-0.445740	-1.771410	0.259406	-0.403010	-0.150640	-0.053950	0.082167	4.528378	-0.615960
TiO_2	-0.301580	0.009407	-0.004590	0.181973	-0.012440	-0.042460	-0.000570	0.033836	-0.011000	-0.790580	0.006796
UO_3	-0.475850	0.243186	0.012155	0.101860	-0.042810	0.201202	-0.097770	0.013465	-0.043380	0.994202	-0.252600
ZnO	-1.097850	-0.270020	-0.086940	0.121723	0.045571	0.079777	0.088583	-0.085500	0.017193	-0.291710	0.406175
ZrO_2	0.176132	-0.082800	0.008898	-0.066870	0.086833	0.019180	-0.034230	0.053932	-0.026690	0.398691	-0.176220
Others	-0.111140	0.009814	0.009466	0.000942	-0.073840	0.002791	-0.005850	0.013830	0.003183	-0.171380	0.026749
$(B_2O_3)^2$	-0.000260	-4.339500	0.027293	0.061767	0.182455	0.377241	0.105084	0.180834	0.107145	2.048592	0.769805
$(Al_2O_3)^2$	-191.870000	0.309899	2.378166	-7.140640	3.823359	5.243662	3.295892	0.834569	3.124850	11.669480	9.178304
$(Al_2O_3)^3$	1204.687000	4.933771	-15.146800	27.616150	-21.047200	-31.500000	-23.698200	-7.276770	-19.242600	-42.605300	-52.429500
$(Al_2O_3)^4$	-2453.660000	-21.802500	29.636880	-26.249100	38.966520	62.171420	52.895160	16.603320	39.481710	38.483050	105.417300

Table A.2. Variance-covariance table for product consistency model (Vienna and Crum 2018).

Terms	SiO_2	SO_3	TiO_2	UO_3	ZnO	ZrO_2	Others	$(B_2O_3)^2$	$(Al_2O_3)^2$	$(Al_2O_3)^3$	$(Al_2O_3)^4$
Al_2O_3	-0.180980	-1.640700	-0.301580	-0.475850	-1.097850	0.176132	-0.111140	-0.000260	-191.8700	1204.6870	-2453.6600
B_2O_3	-0.063820	0.237811	0.009407	0.243186	-0.270020	-0.082800	0.009814	-4.339500	0.309899	4.933771	-21.802500
CaO	-0.002560	-0.445740	-0.004590	0.012155	-0.086940	0.008898	0.009466	0.027293	2.378166	-15.146800	29.636880
F	-0.021010	-1.771410	0.181973	0.101860	0.121723	-0.066870	0.000942	0.061767	-7.140640	27.616150	-26.249100
Fe_2O_3	-0.004490	0.259406	-0.012440	-0.042810	0.045571	0.086833	-0.073840	0.182455	3.823359	-21.047200	38.966520
K_2O	0.000430	-0.403010	-0.042460	0.201202	0.079777	0.019180	0.002791	0.377241	5.243662	-31.500000	62.171420
Li_2O	-0.011340	-0.150640	-0.000570	-0.097770	0.088583	-0.034230	-0.005850	0.105084	3.295892	-23.698200	52.895160
MgO	-0.004140	-0.053950	0.033836	0.013465	-0.085500	0.053932	0.013830	0.180834	0.834569	-7.276770	16.603320
Na_2O	-0.009570	0.082167	-0.011000	-0.043380	0.017193	-0.026690	0.003183	0.107145	3.124850	-19.242600	39.481710
Nd_2O_3	0.003079	4.528378	-0.790580	0.994202	-0.291710	0.398691	-0.171380	2.048592	11.669480	-42.605300	38.483050
P_2O_5	0.030982	-0.615960	0.006796	-0.252600	0.406175	-0.176220	0.026749	0.769805	9.178304	-52.429500	105.417300
SiO_2	0.016267	-0.009240	-0.000310	-0.019160	0.031198	-0.000570	0.001357	0.274283	3.198964	-19.046300	37.371870
SO_3	-0.009240	24.585190	-0.045030	0.207054	-0.895630	0.161689	0.094661	-0.497610	9.953430	21.789890	-163.94500
TiO_2	-0.000310	-0.045030	0.596379	0.324276	-0.058140	0.034605	0.001438	0.016438	6.012219	-39.61560	82.30849
UO_3	-0.019160	0.207054	0.324276	6.155863	0.089334	0.176920	-0.272380	-0.786030	9.947577	-60.68220	116.1953
ZnO	0.031198	-0.895630	-0.058140	0.089334	1.350052	-0.233850	0.016484	1.195863	19.998790	-126.1090	258.3208
ZrO_2	-0.000570	0.161689	0.034605	0.176920	-0.233850	0.542998	-0.040880	0.199568	-1.949250	13.48843	-31.5528
Others	0.001357	0.094661	0.001438	-0.272380	0.016484	-0.040880	0.201357	0.000565	1.104123	-4.57934	6.038681
$(B_2O_3)^2$	0.274283	-0.497610	0.016438	-0.786030	1.195863	0.199568	0.000565	21.266940	7.505606	-99.55050	290.1129
$(Al_2O_3)^2$	3.198964	9.95343	6.012219	9.947577	19.99879	-1.949250	1.104123	7.505606	3594.974	-23530.90	49387.980
$(Al_2O_3)^3$	-19.046300	21.78989	-39.615600	-60.68220	-126.10900	13.488430	-4.579340	-99.550500	-23530.900	160159.10	-346496.0
$(Al_2O_3)^4$	37.371870	-163.9450	82.308490	116.19530	258.32080	-31.552800	6.038681	290.112900	49387.980	-346496.00	768358.5

Table A.3. Variance-covariance table for viscosity model.

Terms	A	B_Al_2O_3	B_B_2O_3	B_CaO	B_Cl	B_Cr_2O_3	B_F	B_Fe_2O_3	B_K_2O	B_Li_2O	B_MgO
A	0.0049402	-14.2085226	-3.6915724	-4.2509636	-11.4262561	-8.2118732	-0.0834687	-7.1371039	-5.0212532	10.1621620	-6.9209328
B_Al_2O_3	-14.208523	42705.7050	9996.4428	12075.8753	33299.3899	21012.5029	-1293.3016	20817.8450	14402.7122	-30799.4754	20139.0231
B_B_2O_3	-3.691572	9996.4428	4006.6456	3243.1992	10430.5430	3293.1347	976.3333	5163.4375	4134.0829	-7562.2672	5205.3079
B_CaO	-4.250964	12075.8753	3243.1992	5582.6772	9441.1782	6760.8479	-1519.0141	6412.0313	4706.1506	-8552.3877	5947.2634
B_Cl	-11.426256	33299.3899	10430.5430	9441.1782	362497.5280	8882.1372	-14731.4969	13464.1338	8484.9001	-16175.4944	7214.8092
B_Cr_2O_3	-8.211873	21012.5029	3293.1347	6760.8479	8882.1372	452396.5529	-924.1720	9966.1330	2696.7434	-13957.0243	9478.8256
B_F	-0.083469	-1293.3016	976.3333	-1519.0141	-14731.4969	-924.1720	71447.0986	1803.8719	-1461.3298	-1208.3245	1339.3966
B_Fe_2O_3	-7.137104	20817.8450	5163.4375	6412.0313	13464.1338	9966.1330	1803.8719	12460.6760	6938.5735	-15093.1787	9657.8045
B_K_2O	-5.021253	14402.7122	4134.0829	4706.1506	8484.9001	2696.7434	-1461.3298	6938.5735	10107.4886	-10371.5577	7857.8645
B_Li_2O	10.162162	-30799.4754	-7562.2672	-8552.3877	-16175.4944	-13957.0243	-1208.3245	-15093.1787	-10371.5577	31594.1201	-14587.1787
B_MgO	-6.920933	20139.0231	5205.3079	5947.2634	7214.8092	9478.8256	1339.3966	9657.8045	7857.8645	-14587.1787	21075.7801
B_Na_2O	-2.552920	6706.7165	2039.1555	2466.3716	1069.1328	2170.1482	555.5075	3769.5163	2771.6374	-2970.1079	4113.7061
B_P_2O_5	-10.092443	28323.1437	7414.7073	8778.7412	18878.1297	-1116.6864	-8517.4713	13508.0640	7931.3741	-20231.9229	13832.9201
B_SO_3	-8.758486	27343.7849	4949.3654	287.5458	-7489.6830	-10429.9529	5921.1810	14664.4368	9346.1393	-20731.9434	10683.8311
B_SiO_2	-12.137360	35340.6746	8946.2523	10237.6989	29679.5277	21912.5141	-103.8471	17470.5726	12179.5539	-26293.3890	16745.5376
B_SnO_2	-10.794398	32178.2542	7797.4521	9275.0725	26844.2900	-1562.2350	3030.8075	16916.8082	9693.5710	-23837.2752	13529.0099
B_TiO_2	-7.700730	23191.6619	4805.9796	7084.3024	3369.7232	36311.1008	-326.2500	10395.8417	6657.7104	-16026.9160	7701.3502
B_V_2O_5	-6.492845	19164.4106	4143.7011	5236.8473	18654.6448	9664.9500	-2946.6393	9927.0419	6843.3126	-14852.0017	8244.5837
B_ZnO	-6.461156	18868.4478	4635.3906	5411.3129	9053.4450	-485.2307	3902.3923	9025.2341	7151.9602	-13476.8919	7375.8956
B_ZrO_2	-11.019567	32613.4347	7997.2731	9153.3308	23642.2434	18100.1281	-4010.2673	16759.0322	10613.1562	-24887.1567	15392.1281
B_Others	-6.393690	18470.9149	4529.7722	5911.7640	17708.3628	7736.6773	-4141.6060	8262.5812	6953.9286	-14395.2782	9550.6557
T_0	1.0262004	-3001.6924	-769.1478	-884.5089	-2470.7497	-1726.6429	3.7763	-1502.3436	-1053.4740	2169.7929	-1447.2213

Table A.4. Variance-covariance table for viscosity model.

Terms	B_Na_2O	B_P_2O_5	B_SO_3	B_SiO_2	B_SnO_2	B_TiO_2	B_V_2O_5	B_ZnO	B_ZrO_2	B_Others	T_0
A	-2.5529200	-10.0924430	-8.7584856	-12.1373604	-10.7943976	-7.7007305	-6.4928449	-6.4611557	-11.0195674	-6.3936902	1.0262004
B_Al_2O_3	6706.7165	28323.1437	27343.7849	35340.6746	32178.2542	23191.6619	19164.4106	18868.4478	32613.4347	18470.9149	-3001.6924
B_B_2O_3	2039.1555	7414.7073	4949.3654	8946.2523	7797.4521	4805.9796	4143.7011	4635.3906	7997.2731	4529.7722	-769.1478
B_CaO	2466.3716	8778.7412	287.5458	10237.6989	9275.0725	7084.3024	5236.8473	5411.3129	9153.3308	5911.7640	-884.5089
B_Cl	1069.1328	18878.1297	-7489.6830	29679.5277	26844.2900	3369.7232	18654.6448	9053.4450	23642.2434	17708.3628	-2470.7497
B_Cr_2O_3	2170.1482	-1116.6864	-10429.9529	21912.5141	-1562.2350	36311.1008	9664.9500	-485.2307	18100.1281	7736.6773	-1726.6429
B_F	555.5075	-8517.4713	5921.1810	-103.8471	3030.8075	-326.2500	-2946.6393	3902.3923	-4010.2673	-4141.6060	3.7763394
B_Fe_2O_3	3769.5163	13508.0640	14664.4368	17470.5726	16916.8082	10395.8417	9927.0419	9025.2341	16759.0322	8262.5812	-1502.3436
B_K_2O	2771.6374	7931.3741	9346.1393	12179.5539	9693.5710	6657.7104	6843.3126	7151.9602	10613.1562	6953.9286	-1053.4740
B_Li_2O	-2970.1079	-20231.9229	-20731.9434	-26293.3890	-23837.2752	-16026.9160	-14852.0017	-13476.8919	-24887.1567	-14395.2782	2169.7929
B_MgO	4113.7061	13832.9201	10683.8311	16745.5376	13529.0099	7701.3502	8244.5837	7375.8956	15392.1281	9550.6557	-1447.2213
B_Na_2O	2504.7573	5479.1546	4263.2734	5830.0171	4571.5639	3783.0020	2464.7248	3229.0504	4951.1109	3148.8356	-524.0527
B_P_2O_5	5479.1546	45100.3533	13214.7307	24767.8900	22587.3421	18264.0938	13439.2703	14887.7593	22477.2386	13517.2923	-2098.2804
B_SO_3	4263.2734	13214.7307	238717.5826	21068.6243	25723.5574	17493.5962	-5553.4135	3797.4805	23129.3937	13459.6503	-1892.7594
B_SiO_2	5830.0171	24767.8900	21068.6243	30342.6824	26918.1255	18983.8791	16251.8105	16037.5767	27405.2417	15694.4949	-2559.9656
B_SnO_2	4571.5639	22587.3421	25723.5574	26918.1255	41541.0734	17153.1781	12329.3097	14451.1411	23490.7079	14231.2124	-2273.8022
B_TiO_2	3783.0020	18264.0938	17493.5962	18983.8791	17153.1781	44866.6069	11727.9664	6622.4866	18177.2975	11275.3711	-1625.9975
B_V_2O_5	2464.7248	13439.2703	-5553.4135	16251.8105	12329.3097	11727.9664	22910.4358	9027.8685	15658.7479	9411.0571	-1347.7286
B_ZnO	3229.0504	14887.7593	3797.4805	16037.5767	14451.1411	6622.4866	9027.8685	17544.3491	13109.9103	10161.4057	-1373.0813
B_ZrO_2	4951.1109	22477.2386	23129.3937	27405.2417	23490.7079	18177.2975	15658.7479	13109.9103	29746.3154	14409.7135	-2335.1117
B_Others	3148.8356	13517.2923	13459.6503	15694.4949	14231.2124	11275.3711	9411.0571	10161.4057	14409.7135	14266.6241	-1340.1500
T_0	-524.0527	-2098.2804	-1892.7594	-2559.9656	-2273.8022	-1625.9975	-1347.7286	-1373.0813	-2335.1117	-1340.1500	218.9304

Table A.5. Variance-covariance matrix for electrical conductivity model.

Terms	A	B_Al_2O_3	B_B_2O_3	B_CaO	B_Cl	B_Cr_2O_3	B_F	B_Fe_2O_3	B_K_2O	B_Li_2O	B_MgO
A	0.0031443	-7.2379331	-5.0240803	-6.6615015	-9.0243538	-0.4736346	-8.6395682	-5.5539933	-4.1532810	8.0320970	-4.3690965
B_Al_2O_3	-7.2379331	18367.8203	11008.1957	15547.1439	20715.2243	-3309.2105	20616.8985	12896.9536	9754.5905	-20386.8358	10341.1258
B_B_2O_3	-5.0240803	11008.1957	9916.6794	10890.8411	15555.7217	952.4747	15252.4052	8917.6390	6417.9462	-13499.4321	6989.3720
B_CaO	-6.6615015	15547.1439	10890.8411	15674.0891	19733.3304	1273.0510	17935.2541	12184.8259	9096.2805	-17852.9932	9419.2861
B_Cl	-9.0243538	20715.2243	15555.7217	19733.3304	248350.1357	1779.3150	17454.0522	15057.2287	15266.2122	-23887.8464	8045.4105
B_Cr_2O_3	-0.4736346	-3309.2105	952.4747	1273.0510	1779.3150	289210.7365	-13001.5838	4134.2282	-9745.7827	-7200.2863	2882.7853
B_F	-8.6395682	20616.8985	15252.4052	17935.2541	17454.0522	-13001.5838	127965.1984	16526.0070	9604.8269	-25447.9979	13984.9631
B_Fe_2O_3	-5.5539933	12896.9536	8917.6390	12184.8259	15057.2287	4134.2282	16526.0070	12712.9951	7344.8101	-15207.5242	7827.2219
B_K_2O	-4.1532810	9754.5905	6417.9462	9096.2805	15266.2122	-9745.7827	9604.8269	7344.8101	10201.1535	-9575.8896	5470.2233
B_Li_2O	8.0320970	-20386.8358	-13499.4321	-17852.9932	-23887.8464	-7200.2863	-25447.9979	-15207.5242	-9575.8896	34146.1770	-13027.6875
B_MgO	-4.3690965	10341.1258	6989.3720	9419.2861	8045.4105	2882.7853	13984.9631	7827.2219	5470.2233	-13027.6875	18023.2526
B_Na_2O	2.3136732	-6072.6499	-3882.7787	-5046.5072	-11748.1073	-2683.1347	-6789.5238	-4057.8175	-2870.1522	9201.6025	-3303.3230
B_P_2O_5	-7.2937306	16876.2992	11089.0119	15357.6030	24046.8585	-11236.6178	7458.7938	12957.9706	10541.7840	-18509.3045	9429.3238
B_SO_3	-8.2785314	20080.8490	9883.1260	13622.4437	22222.8765	654.5795	27865.6508	22351.1397	13312.2703	-24926.7729	15305.8644
B_SiO_2	-6.6150898	15591.5847	10435.0880	14010.7356	20214.8838	1529.3009	17654.1297	11457.4070	8696.6752	-18184.0544	9068.5246
B_SnO_2	-8.0620569	19216.4519	13446.2831	17512.3878	23375.6444	-3089.0481	24753.7642	15213.7269	9173.8189	-23809.3498	10529.3193
B_TiO_2	-4.4717836	10298.4013	7556.4600	10320.3304	-3156.6016	16496.2360	12364.6155	6513.7245	3609.1692	-10865.5158	1884.7364
B_V_2O_5	-3.2877200	7803.1318	5158.3613	6712.9678	11215.9175	4345.3012	5802.3623	6062.9238	3956.1878	-9622.0330	2891.8783
B_ZnO	-5.5875426	13033.8808	9109.7575	12087.0491	13924.3722	974.4448	21804.9523	9844.5600	6798.8629	-15991.4248	5841.3471
B_ZrO_2	-6.6657904	15535.0474	10833.9678	14344.0261	20279.7582	411.2077	18004.1885	12275.4830	8666.0757	-17979.3089	10037.2692
B_Others	-5.9395814	13982.6150	9111.0817	13318.9872	17661.6481	-1390.1921	17451.8691	8730.6810	8196.1216	-16671.0961	10110.3272
T_0	-1.7737345	4168.8613	2878.3127	3836.8888	5276.2539	288.0501	4992.3191	3186.0111	2375.8635	-4706.5478	2499.3914

Table A.6. Variance-covariance matrix for electrical conductivity model.

Terms	B_Na_2O	B_P_2O_5	B_SO_3	B_SiO_2	B_SnO_2	B_TiO_2	B_V_2O_5	B_ZnO	B_ZrO_2	B_Others	T_0
A	2.3136732	-7.2937306	-8.2785314	-6.6150898	-8.0620569	-4.4717836	-3.2877200	-5.5875426	-6.6657904	-5.9395814	-1.7737345
B_Al_2O_3	-6072.6499	16876.2992	20080.8490	15591.5847	19216.4519	10298.4013	7803.1318	13033.8808	15535.0474	13982.6150	4168.8613
B_B_2O_3	-3882.7787	11089.0119	9883.1260	10435.0880	13446.2831	7556.4600	5158.3613	9109.7575	10833.9678	9111.0817	2878.3127
B_CaO	-5046.5072	15357.6030	13622.4437	14010.7356	17512.3878	10320.3304	6712.9678	12087.0491	14344.0261	13318.9872	3836.8888
B_Cl	-11748.1073	24046.8585	22222.8765	20214.8838	23375.6444	-3156.6016	11215.9175	13924.3722	20279.7582	17661.6481	5276.2539
B_Cr_2O_3	-2683.1347	-11236.6178	654.5795	1529.3009	-3089.0481	16496.2360	4345.3012	974.4448	411.2077	-1390.1921	288.0501
B_F	-6789.5238	7458.7938	27865.6508	17654.1297	24753.7642	12364.6155	5802.3623	21804.9523	18004.1885	17451.8691	4992.3191
B_Fe_2O_3	-4057.8175	12957.9706	22351.1397	11457.4070	15213.7269	6513.7245	6062.9238	9844.5600	12275.4830	8730.6810	3186.0111
B_K_2O	-2870.1522	10541.7840	13312.2703	8696.6752	9173.8189	3609.1692	3956.1878	6798.8629	8666.0757	8196.1216	2375.8635
B_Li_2O	9201.6025	-18509.3045	-24926.7729	-18184.0544	-23809.3498	-10865.5158	-9622.0330	-15991.4248	-17979.3089	-16671.0961	-4706.5478
B_MgO	-3303.3230	9429.3238	15305.8644	9068.5246	10529.3193	1884.7364	2891.8783	5841.3471	10037.2692	10110.3272	2499.3914
B_Na_2O	3035.4580	-5545.2373	-5336.0790	-5420.1619	-6951.0704	-3160.3743	-3163.9279	-4543.5679	-5555.4354	-4700.4738	-1383.6746
B_P_2O_5	-5545.2373	44032.4504	19013.6509	15484.4984	16323.9729	8363.8081	7564.5911	14546.3246	16624.7896	11893.9000	4180.4207
B_SO_3	-5336.0790	19013.6509	198990.1850	16007.3919	26100.1170	4689.6619	-4482.8464	12484.6346	18359.7847	19571.6345	4778.1781
B_SiO_2	-5420.1619	15484.4984	16007.3919	14418.2258	17287.8792	9077.4978	7185.1884	11604.3607	14039.8922	12530.6777	3806.3615
B_SnO_2	-6951.0704	16323.9729	26100.1170	17287.8792	29109.8752	12330.1521	7736.5067	15404.9218	16632.4762	15896.6541	4653.1012
B_TiO_2	-3160.3743	8363.8081	4689.6619	9077.4978	12330.1521	28296.0808	6809.6531	8301.9703	10234.1971	11054.1251	2530.3497
B_V_2O_5	-3163.9279	7564.5911	-4482.8464	7185.1884	7736.5067	6809.6531	12097.3989	7000.8489	7676.2733	5929.2491	1871.6439
B_ZnO	-4543.5679	14546.3246	12484.6346	11604.3607	15404.9218	8301.9703	7000.8489	18056.5486	11316.5176	12291.1605	3209.5421
B_ZrO_2	-5555.4354	16624.7896	18359.7847	14039.8922	16632.4762	10234.1971	7676.2733	11316.5176	18351.7794	13006.2153	3837.2485
B_Others	-4700.4738	11893.9000	19571.6345	12530.6777	15896.6541	11054.1251	5929.2491	12291.1605	13006.2153	20452.0620	3409.6368
T_0	-1383.6746	4180.4207	4778.1781	3806.3615	4653.1012	2530.3497	1871.6439	3209.5421	3837.2485	3409.6368	1031.3188

Table A.7. Variance-covariance matrix for w_{SO3} model.

Terms	Al_2O_3	B_2O_3	CaO	Cl	Cr_2O_3	F	Fe_2O_3	K_2O	Li_2O	MgO	Na_2O
Al_2O_3	0.8190800	-0.2068292	-1.1264864	-0.2067684	0.1727451	-0.1032908	-0.0452754	0.0559650	0.1226666	-0.0308165	0.4036345
B_2O_3	-0.2068292	0.2293198	0.5167499	-0.0089845	-0.1809842	0.0650137	-0.0344561	0.0081930	-0.1010432	0.0146707	-0.0924670
CaO	-1.1264864	0.5167499	5.7457434	-0.7496438	-1.7619077	-0.4206645	-0.3378202	-0.3399867	-0.6731786	-0.4052539	-0.8298825
Cl	-0.2067684	-0.0089845	-0.7496438	10.1573134	0.9542452	0.6745881	0.3653246	-0.4608179	-1.0129539	0.6308182	-0.4109518
Cr_2O_3	0.1727451	-0.1809842	-1.7619077	0.9542452	23.7343830	-0.6722488	-0.3092008	-0.3312545	0.2383473	-0.2038333	-0.0249861
F	-0.1032908	0.0650137	-0.4206645	0.6745881	-0.6722488	3.8484247	-0.1431452	0.1221428	-0.2307172	0.1063835	0.0306060
Fe_2O_3	-0.0452754	-0.0344561	-0.3378202	0.3653246	-0.3092008	-0.1431452	0.5839115	0.0890693	-0.0318412	0.0881880	-0.0113693
K_2O	0.0559650	0.0081930	-0.3399867	-0.4608179	-0.3312545	0.1221428	0.0890693	0.5391219	0.0106614	-0.0710806	0.0520632
Li_2O	0.1226666	-0.1010432	-0.6731786	-1.0129539	0.2383473	-0.2307172	-0.0318412	0.0106614	1.2331049	-0.2140589	0.3586613
MgO	-0.0308165	0.0146707	-0.4052539	0.6308182	-0.2038333	0.1063835	0.0881880	-0.0710806	-0.2140589	0.9829596	-0.0542736
Na_2O	0.4036345	-0.0924670	-0.8298825	-0.4109518	-0.0249861	0.0306060	-0.0113693	0.0520632	0.3586613	-0.0542736	0.3661319
P_2O_5	-0.0998699	-0.0270731	-0.3352954	0.0823860	-0.3750547	-0.2491870	-0.1207801	0.0575907	-0.0123273	0.0750927	-0.0089392
SiO_2	-0.1341866	0.0080684	0.4840916	0.0479354	-0.1201408	-0.0699388	-0.0176188	-0.0475385	-0.1328330	-0.0226687	-0.1347286
SnO_2	0.0469474	-0.0317013	-0.6679246	0.2778368	0.7685944	0.3474998	0.0891661	0.0279359	-0.1986280	-0.0151216	-0.0265506
V_2O_5	0.0002530	-0.0284952	-0.0202772	0.1030037	0.2252488	-0.1078740	0.0100485	-0.0279815	-0.0814193	-0.0735757	-0.0216304
ZnO	-0.1319557	0.0269196	-0.2055015	0.4312315	-0.1074935	0.1449545	0.0160414	-0.0257356	-0.0998165	-0.0264545	-0.1086979
ZrO_2	0.0446303	-0.0208093	-0.2980841	-0.1807586	0.0112021	-0.1314728	0.0759407	-0.0135650	-0.0018846	0.0973502	-0.0183493
Others	-0.2438964	-0.0455627	0.3416017	-1.1978374	0.9467350	0.0229225	-0.3344538	-0.2361570	-0.0036575	-0.1458599	-0.1400563
$Al_2O_3 \times Na_2O$	-4.3548595	0.6454717	4.8235766	2.6181083	-1.4472761	0.2987185	0.3652194	-0.2229070	-1.1158377	0.4868765	-2.5464177
$B_2O_3 \times CaO$	2.1507497	-2.6671469	-12.0505791	0.7880322	0.6427521	1.0091932	0.6921593	0.3035754	2.3223543	0.4587122	1.8108159
$CaO \times SiO_2$	2.2133042	-0.5913088	-11.7646664	1.7409799	4.3554693	0.8479633	0.7555743	0.8883534	1.1259769	1.0287862	1.6226031

Table A.8. Variance-covariance matrix for w_{SO3} model.

Terms	P_2O_5	SiO_2	SnO_2	V_2O_5	ZnO	ZrO_2	Others	$Al_2O_3 \times Na_2O$	$B_2O_3 \times CaO$	$CaO \times SiO_2$
Al_2O_3	-0.0998699	-0.1341866	0.0469474	0.0002530	-0.1319557	0.0446303	-0.2438964	-4.3548595	2.1507497	2.2133042
B_2O_3	-0.0270731	0.0080684	-0.0317013	-0.0284952	0.0269196	-0.0208093	-0.0455627	0.6454717	-2.6671469	-0.5913088
CaO	-0.3352954	0.4840916	-0.6679246	-0.0202772	-0.2055015	-0.2980841	0.3416017	4.8235766	-12.0505791	-11.7646664
Cl	0.0823860	0.0479354	0.2778368	0.1030037	0.4312315	-0.1807586	-1.1978374	2.6181083	0.7880322	1.7409799
Cr_2O_3	-0.3750547	-0.1201408	0.7685944	0.2252488	-0.1074935	0.0112021	0.9467350	-1.4472761	0.6427521	4.3554693
F	-0.2491870	-0.0699388	0.3474998	-0.1078740	0.1449545	-0.1314728	0.0229225	0.2987185	1.0091932	0.8479633
Fe_2O_3	-0.1207801	-0.0176188	0.0891661	0.0100485	0.0160414	0.0759407	-0.3344538	0.3652194	0.6921593	0.7555743
K_2O	0.0575907	-0.0475385	0.0279359	-0.0279815	-0.0257356	-0.0135650	-0.2361570	-0.2229070	0.3035754	0.8883534
Li_2O	-0.0123273	-0.1328330	-0.1986280	-0.0814193	-0.0998165	-0.0018846	-0.0036575	-1.1158377	2.3223543	1.1259769
MgO	0.0750927	-0.0226687	-0.0151216	-0.0735757	-0.0264545	0.0973502	-0.1458599	0.4868765	0.4587122	1.0287862
Na_2O	-0.0089392	-0.1347286	-0.0265506	-0.0216304	-0.1086979	-0.0183493	-0.1400563	-2.5464177	1.8108159	1.6226031
P_2O_5	1.4984568	-0.0180918	-0.0006796	0.0134550	0.0200840	0.0123376	-0.0451134	0.4090621	0.8438039	0.6798109
SiO_2	-0.0180918	0.0799837	-0.0486083	-0.0054717	-0.0070180	-0.0259758	0.0407940	0.7927337	-0.5804868	-1.1607564
SnO_2	-0.0006796	-0.0486083	0.6905931	0.0601319	0.0322586	-0.0143926	0.0506196	0.2043382	1.2416525	1.5069827
V_2O_5	0.0134550	-0.0054717	0.0601319	0.4585850	-0.0427217	0.0485392	-0.0739722	0.1616560	-0.0356591	-0.0332816
ZnO	0.0200840	-0.0070180	0.0322586	-0.0427217	0.6153012	0.0133312	0.3570345	0.8440714	0.0575446	0.6806569
ZrO_2	0.0123376	-0.0259758	-0.0143926	0.0485392	0.0133312	0.3153276	0.0220804	-0.0126308	0.1567901	0.7295669
Others	-0.0451134	0.0407940	0.0506196	-0.0739722	0.3570345	0.0220804	2.5648779	1.2920295	-0.1536897	-0.6608805
$Al_2O_3 \times Na_2O$	0.4090621	0.7927337	0.2043382	0.1616560	0.8440714	-0.0126308	1.2920295	27.1123656	-7.0991653	-9.6135379
$B_2O_3 \times CaO$	0.8438039	-0.5804868	1.2416525	-0.0356591	0.0575446	0.1567901	-0.1536897	-7.0991653	56.0766051	16.4747576
$CaO \times SiO_2$	0.6798109	-1.1607564	1.5069827	-0.0332816	0.6806569	0.7295669	-0.6608805	-9.6135379	16.4747576	26.9617022

Table A.9. Variance-covariance matrix for K-3 corrosion model.

Terms	Stat, 1200	Al_2O_3	B_2O_3	Cl	Cr_2O_3	Fe_2O_3	K_2O	Li_2O	MnO	Na_2O
Stat, 1200	0.00706809	-0.02117640	0.00077995	0.13783591	-0.02592841	0.00511060	0.01051786	0.01681053	0.04373656	0.00782901
Al_2O_3	-0.02117640	0.73140645	-0.40691382	-0.20863390	0.01253817	-0.02306911	-0.04455745	-1.16232547	-0.99409795	-0.41896301
B_2O_3	0.00077995	-0.40691382	0.50919706	-0.63718448	-0.72066906	-0.03333872	0.00456205	0.29564974	0.40195325	0.15442817
Cl	0.13783591	-0.20863390	-0.63718448	60.15097688	11.54652238	-0.81347425	2.57173583	2.07416693	11.76934063	-1.54686087
Cr_2O_3	-0.02592841	0.01253817	-0.72066906	11.54652238	100.42031913	2.66737532	-3.34369334	-6.87787369	-2.08203543	-2.15208007
Fe_2O_3	0.00511060	-0.02306911	-0.03333872	-0.81347425	2.66737532	0.90300083	-0.24605852	0.07083527	-4.20439095	0.09574747
K_2O	0.01051786	-0.04455745	0.00456205	2.57173583	-3.34369334	-0.24605852	1.81900712	1.86903844	-0.59429660	0.20779551
Li_2O	0.01681053	-1.16232547	0.29564974	2.07416693	-6.87787369	0.07083527	1.86903844	11.61550732	-3.34321197	2.37570378
MnO	0.04373656	-0.99409795	0.40195325	11.76934063	-2.08203543	-4.20439095	-0.59429660	-3.34321197	90.59545695	-0.93611317
Na_2O	0.00782901	-0.41896301	0.15442817	-1.54686087	-2.15208007	0.09574747	0.20779551	2.37570378	-0.93611317	0.73718046
P_2O_5	-0.07894752	0.03421580	-0.35394434	2.13142263	-6.85992249	-0.63802975	0.37692961	1.05408790	1.09800361	-0.02310980
SiO_2	-0.01226017	0.19396098	-0.08871005	0.27162293	0.59009383	-0.11645654	-0.15832251	-1.04267619	0.23066212	-0.31381002
V_2O_5	0.01332965	-0.05844185	-0.12836678	3.09750091	10.60782872	0.77495404	-0.22734449	-2.02062541	0.08228007	-0.51820477
ZnO	0.11606586	-0.41913362	-0.18541003	3.20665462	1.64572265	-0.26901575	-0.19370964	-0.50369979	6.41356651	0.13103338
ZrO_2	0.01520902	0.13492303	-0.07511666	-0.63108424	-0.70857315	0.28183519	-0.12367841	-0.69703135	-0.76367459	-0.30684890
Other	-0.00259008	0.00044765	0.02899076	-1.32298759	0.42521037	0.13821482	0.05387142	-0.26320789	0.33544394	0.04959579
$Cr_2O_3 \times Li_2O$	9.99487928	14.22843547	-26.25812172	217.57817823	-209.11474797	55.16052975	-121.04522829	-813.36994221	-20.81280257	-71.49508223
$Cr_2O_3 \times V_2O_5$	-5.64727825	11.29642662	53.58048772	-406.03332769	-3886.56291229	-181.32797823	217.61488784	658.94861553	-262.41433283	103.70479322
$K_2O \times Li_2O$	-0.05269964	9.94463287	-3.18355952	-95.88451230	52.55772060	-11.43370218	-58.79594630	-130.79033322	62.05887597	-20.51895228

Table A.10. Variance-covariance matrix for K-3 corrosion model.

Terms	P_2O_5	SiO_2	V_2O_5	ZnO	ZrO_2	Other	$Cr_2O_3 \times Li_2O$	$Cr_2O_3 \times V_2O_5$	$K_2O \times Li_2O$
Stat, 1200	-0.07894752	-0.01226017	0.01332965	0.11606586	0.01520902	-0.00259008	9.99487928	-5.64727825	-0.05269964
Al_2O_3	0.03421580	0.19396098	-0.05844185	-0.41913362	0.13492303	0.00044765	14.22843547	11.29642662	9.94463287
B_2O_3	-0.35394434	-0.08871005	-0.12836678	-0.18541003	-0.07511666	0.02899076	-26.25812172	53.58048772	-3.18355952
Cl	2.13142263	0.27162293	3.09750091	3.20665462	-0.63108424	-1.32298759	217.57817823	-406.03332769	-95.88451230
Cr_2O_3	-6.85992249	0.59009383	10.60782872	1.64572265	-0.70857315	0.42521037	-209.11474797	-3886.56291229	52.55772060
Fe_2O_3	-0.63802975	-0.11645654	0.77495404	-0.26901575	0.28183519	0.13821482	55.16052975	-181.32797823	-11.43370218
K_2O	0.37692961	-0.15832251	-0.22734449	-0.19370964	-0.12367841	0.05387142	-121.04522829	217.61488784	-58.79594630
Li_2O	1.05408790	-1.04267619	-2.02062541	-0.50369979	-0.69703135	-0.26320789	-813.36994221	658.94861553	-130.79033322
MnO	1.09800361	0.23066212	0.08228007	6.41356651	-0.76367459	0.33544394	-20.81280257	-262.41433283	62.05887597
Na_2O	-0.02310980	-0.31381002	-0.51820477	0.13103338	-0.30684890	0.04959579	-71.49508223	103.70479322	-20.51895228
P_2O_5	13.90965532	0.01177797	-0.70695653	0.46257664	0.53249559	-0.19698577	-174.12690391	264.23724237	-2.33417006
SiO_2	0.01177797	0.19406514	0.06631369	-0.28819429	0.03437941	-0.11063994	33.56424216	-17.05821642	13.84245029
V_2O_5	-0.70695653	0.06631369	6.09886644	0.79903256	0.38981777	-0.01299632	301.22079672	-1326.17217238	-23.61469897
ZnO	0.46257664	-0.28819429	0.79903256	4.92226622	-0.32087474	-0.02984889	250.76738750	-259.05468541	20.92532648
ZrO_2	0.53249559	0.03437941	0.38981777	-0.32087474	1.31388327	-0.01220079	8.19461059	-36.42798429	5.64333205
Other	-0.19698577	-0.11063994	-0.01299632	-0.02984889	-0.01220079	0.50369082	-47.50456406	-34.66190902	-13.10949916
$Cr_2O_3 \times Li_2O$	-174.12690391	33.56424216	301.22079672	250.76738750	8.19461059	-47.50456406	429723.56283836	-190441.02073129	1838.85845481
$Cr_2O_3 \times V_2O_5$	264.23724237	-17.05821642	-1326.17217238	-259.05468541	-36.42798429	-34.66190902	-190441.02073129	534881.11789488	-137.61649628
$K_2O \times Li_2O$	-2.33417006	13.84245029	-23.61469897	20.92532648	5.64333205	-13.10949916	1838.85845481	-137.61649628	7257.46021033

Table A.11. Variance-covariance matrix for P_2O_5 T_L model.

Terms	Al_2O_3	B_2O_3	BaO	Bi_2O_3	CaO	Cr_2O_3	Li_2O	Na_2O	P_2O_5
Al_2O_3	14806.8586	-11814.2269	15262.9799	1885.8322	-34503.7533	-7537.7372	-42958.6034	-10986.5037	3575.8993
B_2O_3	-11814.2269	27697.4392	5848.6468	-6113.4967	85948.0796	-12466.5697	5093.3346	5279.2587	-5655.9586
BaO	15262.9799	5848.6468	2974661.6403	-27504.8946	79071.8975	529492.2399	-216871.1045	-72353.3155	210276.2872
Bi_2O_3	1885.8322	-6113.4967	-27504.8946	58135.5530	-31813.1113	-65641.6228	8869.1984	-886.4621	-12956.1835
CaO	-34503.7533	85948.0796	79071.8975	-31813.1113	726723.0877	-89726.2578	2129.4428	71632.0889	1931.8938
Cr_2O_3	-7537.7372	-12466.5697	529492.2399	-65641.6228	-89726.2578	1895423.6553	-150796.6406	-49637.1756	-27845.0085
Li_2O	-42958.6034	5093.3346	-216871.1045	8869.1984	2129.4428	-150796.6406	614660.2769	39453.9083	-15154.8585
Na_2O	-10986.5037	5279.2587	-72353.3155	-886.4621	71632.0889	-49637.1756	39453.9083	39590.2799	-14140.5514
P_2O_5	3575.8993	-5655.9586	210276.2872	-12956.1835	1931.8938	-27845.0085	-15154.8585	-14140.5514	82025.4485
SiO_2	4121.3783	-5638.8496	-13604.5458	2820.2483	-31399.6006	18132.9518	-13916.6848	-10632.2195	-1416.8028
SrO	6476.9185	7880.1196	333654.3655	-26312.2127	22326.7588	16772.1596	-75353.8693	5980.0328	4714.5955
ZrO_2	6475.0117	-2205.4422	91052.8751	232.6448	-9280.1855	78975.3964	-26918.9861	-9529.1184	-613.9038
Others	-2078.2486	-3840.4188	8655.0310	-15091.8876	-22540.6327	-12062.6123	6465.5276	3833.5757	-1498.7180
B_2O_3 × CaO	103597.6897	-475799.2532	-477443.7273	113060.2233	-3186078.9679	582557.7926	360545.7066	-149364.9498	-63018.4549
BaO × P_2O_5	-185820.3418	101541.9018	-149477130.5174	2724282.6263	-3766683.2713	-25315019.9250	6295167.1991	2392000.0428	-9155111.0368
CaO × Na_2O	192296.8640	-236765.1221	45621.5276	299585.1777	-3045458.5183	-418860.1189	-522652.4082	-527964.0547	236654.5768
Li_2O × Li_2O	414916.7018	120910.2297	3278551.8590	-15835.7857	318852.3379	1678569.8659	-9161632.2312	-209529.0726	33204.3569

Table A.12. Variance-covariance matrix for P_2O_5 T_L model.

Terms	SiO_2	SrO	ZrO_2	Others	B_2O_3 × CaO	BaO × P_2O_5	CaO × Na_2O	Li_2O × Li_2O
Al_2O_3	4121.3783	6476.9185	6475.0117	-2078.2486	103597.6897	-185820.3418	192296.8640	414916.7018
B_2O_3	-5638.8496	7880.1196	-2205.4422	-3840.4188	-475799.2532	101541.9018	-236765.1221	120910.2297
BaO	-13604.5458	333654.3655	91052.8751	8655.0310	-477443.7273	-149477130.5174	45621.5276	3278551.8590
Bi_2O_3	2820.2483	-26312.2127	232.6448	-15091.8876	113060.2233	2724282.6263	299585.1777	-15835.7857
CaO	-31399.6006	22326.7588	-9280.1855	-22540.6327	-3186078.9679	-3766683.2713	-3045458.5183	318852.3379
Cr_2O_3	18132.9518	16772.1596	78975.3964	-12062.6123	582557.7926	-25315019.9250	-418860.1189	1678569.8659
Li_2O	-13916.6848	-75353.8693	-26918.9861	6465.5276	360545.7066	6295167.1991	-522652.4082	-9161632.2312
Na_2O	-10632.2195	5980.0328	-9529.1184	3833.5757	-149364.9498	2392000.0428	-527964.0547	-209529.0726
P_2O_5	-1416.8028	4714.5955	-613.9038	-1498.7180	-63018.4549	-9155111.0368	236654.5768	33204.3569
SiO_2	5460.7166	-3535.9820	-374.8817	-2660.7022	120222.3392	550580.2945	136285.1475	17260.5665
SrO	-3535.9820	276765.8258	-291.7936	-5502.2701	-99518.2678	-20484282.0742	-175936.1145	1229760.2097
ZrO_2	-374.8817	-291.7936	42717.1539	1395.1757	14227.5043	-3571324.7366	49296.1046	147978.3793
Others	-2660.7022	-5502.2701	1395.1757	18012.3019	153274.3322	-1781120.1733	-49132.6382	16884.6170
B_2O_3 × CaO	120222.3392	-99518.2678	14227.5043	153274.3322	16579457.8823	8065970.8617	9932969.8237	-6907414.7270
BaO × P_2O_5	550580.2945	-20484282.0742	-3571324.7366	-1781120.1733	8065970.8617	8916490214.6793	35392629.3633	-73727295.7395
CaO × Na_2O	136285.1475	-175936.1145	49296.1046	-49132.6382	9932969.8237	35392629.3633	20483942.9800	7306965.9725
Li_2O × Li_2O	17260.5665	1229760.2097	147978.3793	16884.6170	-6907414.7270	-73727295.7395	7306965.9725	161253726.4253

Table A.13. Variance-covariance matrix for Zr T_L model.

Terms	Al_2O_3	B_2O_3	Cr_2O_3	F	Fe_2O_3	K_2O	Li_2O	MgO	MnO
Al_2O_3	25721.9756	-11839.8180	-77414.9954	14568.4920	4848.7986	-39885.1200	-22526.7370	16347.5167	23076.6262
B_2O_3	-11839.8180	23270.1772	-56216.7906	-20430.3756	3980.2727	93561.1345	7438.0358	-13523.1645	27112.4193
Cr_2O_3	-77414.9954	-56216.7906	7731830.3560	-151369.4667	-122551.5685	347981.2294	-105906.9158	370744.7048	-704553.8741
F	14568.4920	-20430.3756	-151369.4667	768880.4614	5643.8312	-268582.8861	38103.9561	-97453.9817	96313.5328
Fe_2O_3	4848.7986	3980.2727	-122551.5685	5643.8312	44699.7106	44390.9375	8974.5461	-21605.7987	4802.8395
K_2O	-39885.1200	93561.1345	347981.2294	-268582.8861	44390.9375	1502318.6585	-26908.1516	-16590.8282	60905.6311
Li_2O	-22526.7370	7438.0358	-105906.9158	38103.9561	8974.5461	-26908.1516	138928.6217	-55817.1321	52434.0450
MgO	16347.5167	-13523.1645	370744.7048	-97453.9817	-21605.7987	-16590.8282	-55817.1321	422461.8762	-23304.0535
MnO	23076.6262	27112.4193	-704553.8741	96313.5328	4802.8395	60905.6311	52434.0450	-23304.0535	511973.6664
Na_2O	-27918.5930	-9775.7770	-328108.1899	161418.6244	-15985.5900	-118175.9551	28659.4047	-95725.3426	-34594.7582
SiO_2	4511.8972	-2397.7698	17032.6555	9355.1456	-3887.4238	-3180.4591	-15079.1840	-7752.7488	2327.8876
ThO_2	-3871.6545	-19611.2235	521554.2012	-59120.5540	878.4700	18282.1875	-53388.5423	56531.9115	-364230.6762
UO_3	-3655.9437	6396.6159	-8115.8862	187954.9223	-41751.3833	-91207.0735	1874.0801	-53808.7832	127958.1641
ZrO_2	13709.9626	-6878.4354	173977.2458	-81256.7548	10099.4241	7325.8697	-36122.4953	94788.6899	-47069.0591
Others	-4243.0660	-4448.1704	127.7649	-62958.3930	-6889.4371	-34472.7485	13818.0849	17253.7291	-50587.0587
$B_2O_3 \times K_2O$	257856.8269	-940531.9235	-451451.8336	1813649.4174	-531602.0407	-13982822.5309	362740.9395	792415.0649	-661318.5822
$Na_2O \times Na_2O$	46604.6938	83994.9481	1025973.8299	-925637.8658	65573.0143	601715.0748	-29737.4171	348038.4733	142167.8189

Table A.14. Variance-covariance matrix for Zr T_L model.

Terms	Na_2O	SiO_2	ThO_2	UO_3	ZrO_2	Others	B_2O_3· × K_2O	Na_2O × Na_2O
Al_2O_3	-27918.5930	4511.8972	-3871.6545	-3655.9437	13709.9626	-4243.0660	257856.8269	46604.6938
B_2O_3	-9775.7770	-2397.7698	-19611.2235	6396.6159	-6878.4354	-4448.1704	-940531.9235	83994.9481
Cr_2O_3	-328108.1899	17032.6555	521554.2012	-8115.8862	173977.2458	127.7649	-451451.8336	1025973.8299
F	161418.6244	9355.1456	-59120.5540	187954.9223	-81256.7548	-62958.3930	1813649.4174	-925637.8658
Fe_2O_3	-15985.5900	-3887.4238	878.4700	-41751.3833	10099.4241	-6889.4371	-531602.0407	65573.0143
K_2O	-118175.9551	-3180.4591	18282.1875	-91207.0735	7325.8697	-34472.7485	-13982822.5309	601715.0748
Li_2O	28659.4047	-15079.1840	-53388.5423	1874.0801	-36122.4953	13818.0849	362740.9395	-29737.4171
MgO	-95725.3426	-7752.7488	56531.9115	-53808.7832	94788.6899	17253.7291	792415.0649	348038.4733
MnO	-34594.7582	2327.8876	-364230.6762	127958.1641	-47069.0591	-50587.0587	-661318.5822	142167.8189
Na_2O	297031.6714	-13198.7014	-71688.3409	87470.4942	-64464.8652	-23315.1972	789321.3766	-1170514.5714
SiO_2	-13198.7014	7346.2117	5671.9300	14354.6638	-10579.9040	-4724.8523	-33785.9506	30605.5966
ThO_2	-71688.3409	5671.9300	965659.2163	-261347.9312	49388.7970	46053.2926	81546.3446	215422.0268
UO_3	87470.4942	14354.6638	-261347.9312	443491.8935	-78185.2426	-54165.3712	566555.4308	-397299.0840
ZrO_2	-64464.8652	-10579.9040	49388.7970	-78185.2426	84535.9866	16922.4976	152757.3074	233111.5585
Others	-23315.1972	-4724.8523	46053.2926	-54165.3712	16922.4976	30758.4716	481494.7446	117398.6271
B_2O_3 × K_2O	789321.3766	-33785.9506	81546.3446	566555.4308	152757.3074	481494.7446	149723875.8432	-3920182.2067
Na_2O × Na_2O	-1170514.5714	30605.5966	215422.0268	-397299.0840	233111.5585	117398.6271	-3920182.2067	5064721.7850

Table A.15. Variance-covariance matrix for T1% spinel model.

Terms	Al_2O_3	B_2O_3	CaO	Cr_2O_3	Fe_2O_3	K_2O	Li_2O	MgO	MnO
Al_2O_3	12372.6337	-5304.0026	-6212.7521	12489.2428	2208.1178	-4132.4559	-6795.1510	-7304.9251	-9437.1427
B_2O_3	-5304.0026	11265.0688	-4295.8123	-6740.7776	1590.5922	2737.6999	5856.4584	11130.9616	-32024.9837
CaO	-6212.7521	-4295.8123	153783.0979	-60254.1339	-3240.2312	-990.0183	-1271.8327	-45501.0810	-21874.6756
Cr_2O_3	12489.2428	-6740.7776	-60254.1339	1871553.9869	-3430.4153	-84224.4838	-36300.4671	8412.6324	139839.3392
Fe_2O_3	2208.1178	1590.5922	-3240.2312	-3430.4153	16229.2568	1566.8951	-1252.0804	5209.5863	-63596.2447
K_2O	-4132.4559	2737.6999	-990.0183	-84224.4838	1566.8951	109892.9612	4757.4924	5583.1719	-102741.4560
Li_2O	-6795.1510	5856.4584	-1271.8327	-36300.4671	-1252.0804	4757.4924	75931.9009	18693.7075	-84448.0363
MgO	-7304.9251	11130.9616	-45501.0810	8412.6324	5209.5863	5583.1719	18693.7075	691003.7983	-94874.4038
MnO	-9437.1427	-32024.9837	-21874.6756	139839.3392	-63596.2447	-102741.4560	-84448.0363	-94874.4038	1617098.6338
Na_2O	-5727.5258	2509.6915	2759.8227	-26280.7872	-4352.4136	4011.0158	13689.4473	4600.1409	-37003.7659
NiO	8792.4650	-960.0795	8674.2362	-97698.3660	2853.1930	-24345.7493	-22620.6968	-7770.6718	81865.8105
SiO_2	64.5103	-2634.4027	2116.7236	5632.8108	-4243.7894	-2265.4881	-9075.9771	-11031.6374	47735.8299
SO_3	-69142.0791	-64711.0878	-86326.5645	-707486.5094	36329.1249	55778.8632	50144.0828	61512.9491	130045.9932
SrO	-3518.3617	4241.7804	1577.3201	5728.3183	-738.0195	872.0110	13303.2281	11015.9030	-72528.6651
ZnO	5335.6094	-11876.8901	-15220.7905	58791.7900	1392.1009	4048.8889	-8192.2441	4511.4918	35767.7180
ZrO_2	6307.0439	-3700.0669	1095.1002	-4014.4074	5586.3325	8751.0465	-12264.4091	-7624.6288	-10228.8975
Others	1174.7589	1365.9111	-9561.5063	-16399.4631	2876.2560	-7137.5154	417.3046	14716.2148	-28643.9371
MnO × SiO_2	25947.0195	79587.4971	53923.4021	-420627.5644	162919.9553	245117.2641	210205.2779	263941.6640	-3919879.4245

Table A.16. Variance-covariance matrix for T1% spinel model.

Terms	Na_2O	NiO	SiO_2	SO_3	SrO	ZnO	ZrO_2	Others	MnO × SiO_2
Al_2O_3	-5727.5258	8792.4650	64.5103	-69142.0791	-3518.3617	5335.6094	6307.0439	1174.7589	25947.0195
B_2O_3	2509.6915	-960.0795	-2634.4027	-64711.0878	4241.7804	-11876.8901	-3700.0669	1365.9111	79587.4971
CaO	2759.8227	8674.2362	2116.7236	-86326.5645	1577.3201	-15220.7905	1095.1002	-9561.5063	53923.4021
Cr_2O_3	-26280.7872	-97698.3660	5632.8108	-707486.5094	5728.3183	58791.7900	-4014.4074	-16399.4631	-420627.5644
Fe_2O_3	-4352.4136	2853.1930	-4243.7894	36329.1249	-738.0195	1392.1009	5586.3325	2876.2560	162919.9553
K_2O	4011.0158	-24345.7493	-2265.4881	55778.8632	872.0110	4048.8889	8751.0465	-7137.5154	245117.2641
Li_2O	13689.4473	-22620.6968	-9075.9771	50144.0828	13303.2281	-8192.2441	-12264.4091	417.3046	210205.2779
MgO	4600.1409	-7770.6718	-11031.6374	61512.9491	11015.9030	4511.4918	-7624.6288	14716.2148	263941.6640
MnO	-37003.7659	81865.8105	47735.8299	130045.9932	-72528.6651	35767.7180	-10228.8975	-28643.9371	-3919879.4245
Na_2O	10645.9130	-23645.5363	-2287.2744	30654.7003	4483.7080	-1061.4131	-4033.6616	-848.2956	90470.9637
NiO	-23645.5363	570101.4591	-1567.1762	-76547.6776	5557.7360	42386.8630	-4901.8633	-2706.8183	-183474.6768
SiO_2	-2287.2744	-1567.1762	3733.4916	-16118.6423	-2607.0957	-899.6930	-1566.5928	-1425.6454	-124278.5037
SO_3	30654.7003	-76547.6776	-16118.6423	6716967.0561	20364.1927	126795.0482	46454.4799	-16048.2084	-283589.9165
SrO	4483.7080	5557.7360	-2607.0957	20364.1927	25938.6530	-3030.4872	-6710.8799	-1201.4052	145156.2211
ZnO	-1061.4131	42386.8630	-899.6930	126795.0482	-3030.4872	135781.6605	9055.8547	-17422.0832	-101388.4000
ZrO_2	-4033.6616	-4901.8633	-1566.5928	46454.4799	-6710.8799	9055.8547	30354.6478	-4103.1211	38764.1192
Others	-848.2956	-2706.8183	-1425.6454	-16048.2084	-1201.4052	-17422.0832	-4103.1211	16386.2856	68410.1526
MnO × SiO_2	90470.9637	-183474.6768	-124278.5037	-283589.9165	145156.2211	-101388.4000	38764.1192	68410.1526	9768641.1456

Appendix B – Waste Compositions

Table B.1. Waste compositions.

Example #	Unit	1	2	3	4	5
Ac	mg/L	0.000E+00	0.000E+00	0.000E+00	0.000E+00	0.000E+00
Ag	mg/L	1.073E+01	1.095E+02	3.313E+00	0.000E+00	0.000E+00
Al	mg/L	3.678E+04	4.625E+03	1.391E+04	1.595E+04	1.336E+04
Am	mg/L	0.000E+00	0.000E+00	0.000E+00	0.000E+00	0.000E+00
As	mg/L	3.935E+01	4.342E+00	9.814E+01	0.000E+00	0.000E+00
B	mg/L	1.015E+02	2.489E+02	4.500E+01	0.000E+00	0.000E+00
Ba	mg/L	1.965E+01	1.293E+01	2.162E+01	2.400E-08	5.009E-08
Be	mg/L	1.966E+00	1.219E+01	1.488E+00	0.000E+00	0.000E+00
Bi	mg/L	9.607E+00	8.738E+01	9.317E+00	2.533E+03	6.623E+00
Ca	mg/L	8.858E+01	1.465E+02	2.399E+02	4.009E+02	7.559E+02
Cd	mg/L	6.908E+00	8.045E+00	3.104E+01	1.863E-06	7.792E-06
Ce	mg/L	3.935E+01	1.252E+00	7.336E+01	0.000E+00	0.000E+00
Cl	mg/L	4.675E+02	6.551E+02	1.734E+03	4.237E+02	4.035E+02
Cm	mg/L	0.000E+00	0.000E+00	0.000E+00	0.000E+00	0.000E+00
Co	mg/L	3.390E+01	4.908E-01	6.698E+00	3.379E-07	1.915E-06
Cr	mg/L	2.960E+02	1.397E+03	4.417E+02	2.630E+02	4.632E+02
Cs	mg/L	4.120E-01	4.757E-01	2.234E+00	8.836E-01	1.849E+00
Cu	mg/L	3.938E+00	1.399E+00	1.647E+01	0.000E+00	0.000E+00
Eu	mg/L	0.000E+00	0.000E+00	0.000E+00	0.000E+00	0.000E+00
F	mg/L	3.963E+02	2.819E+04	7.240E+02	2.296E+03	1.014E+04
Fe	mg/L	3.264E+01	3.104E+02	4.392E+03	2.570E+04	1.837E+04
Gd	mg/L	0.000E+00	0.000E+00	0.000E+00	0.000E+00	0.000E+00
Hg	mg/L	2.804E-01	9.683E-02	2.299E-01	1.570E+01	1.441E+01
I	mg/L	0.000E+00	0.000E+00	0.000E+00	0.000E+00	0.000E+00
K	mg/L	7.472E+02	2.623E+03	6.452E+02	1.771E+02	5.336E+02
La	mg/L	2.283E-04	8.055E+01	2.084E+01	6.735E+01	1.047E+03
Li	mg/L	1.366E+01	1.392E+00	1.342E+01	0.000E+00	0.000E+00
Mg	mg/L	3.940E+01	2.087E+02	1.243E+02	0.000E+00	0.000E+00
Mn	mg/L	3.927E+00	2.006E+01	4.846E+02	1.254E+03	1.438E+03
Mo	mg/L	2.584E+01	2.523E+00	2.613E+01	0.000E+00	0.000E+00
Na	mg/L	2.767E+04	7.433E+04	1.201E+05	4.053E+04	5.772E+04
Nb	mg/L	0.000E+00	0.000E+00	0.000E+00	0.000E+00	0.000E+00
Nd	mg/L	3.940E+01	2.655E+01	1.482E+02	0.000E+00	0.000E+00
Ni	mg/L	7.809E+00	2.409E+01	1.094E+02	7.757E+02	8.937E+02
Np	mg/L	0.000E+00	0.000E+00	0.000E+00	0.000E+00	0.000E+00
P	mg/L	1.394E+02	1.037E+03	1.224E+03	6.058E+03	9.063E+02
Pa	mg/L	0.000E+00	0.000E+00	0.000E+00	0.000E+00	0.000E+00
Pb	mg/L	3.932E+01	1.738E+01	2.401E+02	2.531E+03	4.789E+02
Pd	mg/L	0.000E+00	0.000E+00	0.000E+00	0.000E+00	0.000E+00

Example #	Unit	1	2	3	4	5
Pr	mg/L	0.000E+00	0.000E+00	0.000E+00	0.000E+00	0.000E+00
Pu	mg/L	0.000E+00	0.000E+00	0.000E+00	0.000E+00	0.000E+00
Ra	mg/L	0.000E+00	0.000E+00	0.000E+00	0.000E+00	0.000E+00
Rb	mg/L	0.000E+00	0.000E+00	0.000E+00	0.000E+00	0.000E+00
Rh	mg/L	0.000E+00	0.000E+00	0.000E+00	0.000E+00	0.000E+00
Ru	mg/L	1.125E-19	4.335E-19	2.115E+01	7.943E-20	6.682E-19
S	mg/L	1.501E+02	3.000E+03	1.167E+03	7.042E+02	3.000E+03
Sb	mg/L	2.361E+01	5.772E-01	1.021E+01	3.812E-09	1.724E-08
Se	mg/L	3.940E+01	1.670E+00	5.288E+01	2.874E-03	9.503E-03
Si	mg/L	2.391E+02	4.796E+02	8.795E+01	5.786E+02	1.250E+02
Sm	mg/L	0.000E+00	0.000E+00	0.000E+00	0.000E+00	0.000E+00
Sn	mg/L	0.000E+00	0.000E+00	0.000E+00	0.000E+00	0.000E+00
Sr	mg/L	2.669E-02	3.486E-01	6.202E+00	6.340E+01	6.148E+01
Ta	mg/L	0.000E+00	0.000E+00	0.000E+00	0.000E+00	0.000E+00
Tc	mg/L	0.000E+00	0.000E+00	0.000E+00	0.000E+00	0.000E+00
Te	mg/L	0.000E+00	0.000E+00	0.000E+00	0.000E+00	0.000E+00
Th	mg/L	2.610E-01	1.628E+00	2.824E+01	1.634E+02	2.668E+02
Ti	mg/L	3.940E+00	1.694E+00	1.700E+00	0.000E+00	0.000E+00
Tl	mg/L	0.000E+00	7.960E-01	3.390E+01	0.000E+00	0.000E+00
U	mg/L	2.989E+01	2.633E+03	1.357E+02	2.288E+03	4.337E+02
V	mg/L	1.967E+01	6.894E+00	8.502E+00	0.000E+00	0.000E+00
W	mg/L	0.000E+00	0.000E+00	1.550E+02	0.000E+00	0.000E+00
Y	mg/L	1.082E-07	5.914E+00	4.706E+01	4.053E-04	9.459E-04
Zn	mg/L	2.362E+01	2.964E+00	3.268E+01	0.000E+00	0.000E+00
Zr	mg/L	3.623E+00	2.603E+04	1.174E+02	2.135E+01	5.327E+02
^{59}Ni	mCi/L	3.311E-03	1.096E-03	1.893E-03	1.212E-03	1.350E-02
^{60}Co	mCi/L	3.166E-05	7.043E-05	3.456E-05	3.821E-04	2.166E-03
^{63}Ni	mCi/L	2.459E-01	8.098E-02	2.181E-01	8.960E-02	7.845E-01
^{79}Se	mCi/L	4.229E-04	2.398E-04	2.945E-04	2.003E-04	6.623E-04
^{90}Sr	mCi/L	5.916E-02	1.818E+00	2.063E+01	2.217E+02	5.174E+02
^{90}Y	mCi/L	5.880E-02	1.807E+00	2.050E+01	2.204E+02	5.143E+02
^{93m}Nb	mCi/L	8.927E-03	3.653E-03	8.355E-03	2.603E-03	9.913E-02
^{93}Zr	mCi/L	9.113E-03	3.848E-03	1.013E-02	2.764E-03	1.036E-01
^{99}Tc	mCi/L	7.100E-02	1.642E-02	6.096E-03	1.405E-02	1.897E-02
^{106}Ru	mCi/L	3.767E-16	1.452E-15	3.601E-16	2.660E-16	2.238E-15
^{113m}Cd	mCi/L	1.656E-03	9.350E-04	7.097E-04	4.307E-04	1.801E-03
^{125}Sb	mCi/L	3.634E-07	4.364E-06	3.827E-07	3.953E-06	1.788E-05
^{126}Sn	mCi/L	1.923E-03	7.827E-04	1.537E-03	4.311E-04	2.642E-02
^{129}I	mCi/L	8.452E-06	1.569E-05	2.424E-05	1.691E-04	3.315E-05
^{134}Cs	mCi/L	6.825E-10	5.947E-09	2.914E-09	1.281E-09	8.032E-09
^{137m}Ba	mCi/L	6.025E+00	6.931E+00	3.252E+01	1.291E+01	2.696E+01
^{137}Cs	mCi/L	6.347E+00	7.328E+00	3.442E+01	1.361E+01	2.849E+01
^{151}Sm	mCi/L	3.986E+00	1.249E+00	6.675E+01	3.943E+01	1.076E+02

Example #	Unit	1	2	3	4	5
^{152}Eu	mCi/L	9.641E-05	3.203E-05	1.322E-03	7.324E-04	6.601E-03
^{154}Eu	mCi/L	1.611E-03	8.382E-04	3.171E-02	1.782E-02	1.521E-01
^{155}Eu	mCi/L	8.299E-05	3.682E-05	1.138E-03	8.550E-04	4.581E-03
^{226}Ra	mCi/L	1.490E-08	6.467E-09	1.020E-08	4.461E-09	1.326E-08
^{227}Ac	mCi/L	1.461E-05	5.588E-06	1.270E-05	2.554E-06	8.848E-06
^{228}Ra	mCi/L	2.703E-08	1.719E-07	1.996E-06	1.803E-05	2.742E-05
^{229}Th	mCi/L	6.376E-09	3.986E-09	7.891E-09	3.712E-06	1.784E-07
^{231}Pa	mCi/L	1.602E-05	6.967E-06	1.985E-05	3.214E-06	1.156E-05
^{232}Th	mCi/L	2.281E-08	1.753E-07	3.084E-06	1.792E-05	2.782E-05
^{232}U	mCi/L	2.046E-07	1.621E-05	9.297E-07	1.364E-05	1.249E-06
^{233}U	mCi/L	1.795E-05	1.423E-03	8.154E-05	1.204E-03	1.100E-03
^{234}U	mCi/L	1.274E-05	1.194E-03	5.777E-05	7.775E-04	1.766E-04
^{235}U	mCi/L	5.018E-07	4.641E-05	2.514E-06	3.333E-05	7.020E-06
^{236}U	mCi/L	8.619E-07	9.679E-05	3.912E-06	1.344E-05	1.418E-05
^{237}Np	mCi/L	1.070E-04	8.274E-05	8.197E-04	3.213E-05	1.228E-03
^{238}Pu	mCi/L	5.340E-05	5.087E-03	1.707E-02	8.911E-03	6.016E-02
^{238}U	mCi/L	9.964E-06	8.772E-04	4.519E-05	7.636E-04	1.445E-04
^{239}Pu	mCi/L	9.750E-04	7.225E-02	7.565E-02	5.432E-01	3.496E-01
^{240}Pu	mCi/L	2.535E-04	1.991E-02	1.952E-02	8.901E-02	1.074E-01
^{241}Am	mCi/L	2.475E-03	4.118E-02	5.036E-01	1.583E+00	4.297E+00
^{241}Pu	mCi/L	7.842E-04	8.453E-02	3.311E-02	8.078E-02	6.049E-01
^{242}Cm	mCi/L	2.935E-07	4.208E-06	2.916E-03	5.496E-04	1.823E-02
^{242}Pu	mCi/L	2.693E-08	2.469E-06	2.208E-04	4.208E-06	4.079E-05
^{243}Am	mCi/L	1.648E-06	6.822E-06	2.545E-03	4.727E-04	8.979E-03
^{243}Cm	mCi/L	7.976E-09	1.021E-07	2.621E-04	1.599E-05	9.777E-04
^{244}Cm	mCi/L	1.155E-07	1.491E-06	3.802E-03	2.278E-04	1.401E-02

Appendix C – Glass-Forming Chemical Compositions

Table C.1. Nominal glass-forming chemical composition in mass fractions.

Oxide	Kyanite	Boric acid	Wollastonite	Na_2CO_3	Li_2CO_3	Cr_2O_3	Silica	Zincite	Zircon	V_2O_5
Al_2O_3	0.570223	0	0.002003	0	0	0	0.001657	0	0.002502	0
B_2O_3	0	0.565221	0	0	0	0	0	0	0	0
CaO	0.000267	0	0.475099	1.29×10^{-5}	0.003657	0	0.0001	0	0	0
CdO	0	0	0	0	0	0	0	0.0001	0	0
Cl	0	0	0	0.000174	8.32×10^{-5}	0	0	0	0	0
Cr_2O_3	0	0	0	7.77×10^{-5}	0.0001	0.990223	0	0	0	0
Fe_2O_3	0.007568	0	0.004003	1.3×10^{-5}	1.67×10^{-5}	3.88×10^{-5}	0.000217	1.66×10^{-5}	0.000783	0.000074
K_2O	0.000116	0	0	0	1.66×10^{-5}	0	3.35×10^{-5}	0	0	2.34×10^{-5}
Li_2O	0	0	0	0	0.402062	0	0	0	0	0
MgO	0.000133	0	0.000835	1.3×10^{-5}	9.99×10^{-5}	0	8.33×10^{-5}	0	0	0
MnO	0	0	0.001	0	0	0	0	1.66×10^{-5}	0	0
Na_2O	0.003495	0	0	0.58376	0.000716	0	0.000167	0	0	4.36×10^{-5}
NiO	0	0	0	0	0	0	0	0	0	0
P_2O_5	0	0	0	0	0	0	0	0	0	0
PbO	0	0	0	0	0	0	0	1.66×10^{-5}	0	0
SO_3	0	4.98×10^{-5}	0	0.0001	0.000266	0	0	0	0	0
SiO_2	0.406079	0	0.508207	0	0	0	0.996506	0	0.322526	2.77×10^{-5}
TiO_2	0.008769	0	0.0002	0	0	0	0.00015	0	0.001017	0
UO_3	0	0	0	0	0	0	0	0	0.00045	0
V_2O_5	0	0	0	0	0	0	0	0	0	0.994
ZnO	0	0	0	0	0	0	0	0.998145	0	0
ZrO_2	0	0	0	0	0	0	0	0	0.660036	0

Pacific Northwest National Laboratory

902 Battelle Boulevard
P.O. Box 999
Richland, WA 99354

1-888-375-PNNL (7665)

www.pnnl.gov